

University of Southern Queensland
Faculty of Engineering and Built Environment

**DYNAMIC RESPONSE TESTING METHOD OF DAMAGE DETECTION IN FIBRE
COMPOSITE STRUCTURES**

Dissertation By

James Kerr

u1004780

Supervised by

Dr Jayantha Epaarachchi

Project completed for fulfilment of courses
ENG4111 and 4112

Abstract

This dissertation analyses the practicality of the use of vibration signatures as a method to monitor structural health of a glass pultrusion square hollow section member and to detect the existence, magnitude and location of damage. 12 nodes spaced evenly along the 1m long beam were the test locations where an accelerometer was placed and an impact hammer was used to cause the forced oscillation. The data was collected using an LMS data acquisition system coupled with the LMS Xpress testware.

Two methods of identifying damage were applied. The empirical mode decomposition and the Hilbert-Huang transformation. The empirical mode decomposition proved inadequate at signifying damage, however, the Hilbert-Huang transformation showed clear indication of damage introduction. Figures of all numerical analysis and results are included. Also pictures to aid in understanding of the experiments are also included. A copy of the entire Matlab code used in the numerical analysis of the oscillatory signal.

Based on the results of the experiments and numerical analysis it is deemed that with further research it may be possible to build a industrially suitable dynamic testing method for a wide variety of complex materials that avoids the requirement of specialised technicians, abundant apparatus, lengthy time and costly processes.

University of Southern Queensland
Faculty of Health, Engineering and Sciences
ENG4111/ENG4112 Research Project

Limitations of Use

The Council of the University of Southern Queensland, its Faculty of Health, Engineering & Sciences, and the staff of the University of Southern Queensland, do not accept any responsibility for the truth, accuracy or completeness of material contained within or associated with this dissertation.

Persons using all or any part of this material do so at their own risk, and not at the risk of the Council of the University of Southern Queensland, its Faculty of Health, Engineering & Sciences or the staff of the University of Southern Queensland.

This dissertation reports an educational exercise and has no purpose or validity beyond this exercise. The sole purpose of the course pair entitled “Research Project” is to contribute to the overall education within the student’s chosen degree program. This document, the associated hardware, software, drawings, and other material set out in the associated appendices should not be used for any other purpose: if they are so used, it is entirely at the risk of the user.

Certification

I certify that the ideas, designs and experimental work, results, analyses and conclusions set out in this dissertation are entirely my own effort, except where otherwise indicated and acknowledged.

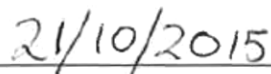
I further certify that the work is original and has not been previously submitted for assessment in any other course or institution, except where specifically stated.

James Lyle Kerr

0061004780



Signature



Date

Table of Contents

Abstract.....	2
Certification.....	4
Nomenclature	10
Chapter 1 Introduction.....	11
1.1 Background	12
1.2 Aims and Objectives.....	13
1.3 Project overview	14
1.3.1 Chapter 1 Introduction.....	14
1.3.2 Chapter 2 Literature	15
1.3.3 Chapter 3 Experimental methodology	15
1.3.4 Chapter 4 Data results and analysis	15
1.3.5 Chapter 5 Discussion	Error! Bookmark not defined.
Chapter 2 Literature.....	17
2.1 Existing conventional structural health monitoring methods	17
2.1.1 X-ray Tomography.....	17
2.1.2 Ultrasonic Tomography.....	18
2.1.3 Visual dye penetration inspection	18
2.1.4 Coin tap testing	19
2.1.5 Viability of methods discussed.....	19
2.2 Existing dynamic structural health monitoring methods	19
2.2.1 Changes in natural frequency	20
2.2.2 Changes in modal strain energy.....	21
2.2.3 Residual force/stress indicators.....	21
2.2.4 Neural Networks	22
2.2.5 Changes in damping ratios.....	22
2.2.6 Changes in mode shapes.....	22
2.2.7 Changes in frequency response functions	23
2.2.8 Change in mechanical impedance	24
2.2.9 Viability of methods discussed and method chosen	24
2.3 Composite materials	24
2.3.1 Glass fibre-reinforced polymers.....	25
2.3.2 Carbon fibre-reinforced polymers	26
2.3.3 Aramid fibre-reinforced polymers	27

2.3.4 Viability of composites discussed	28
2.4 Sensors for experimental data acquisition	28
2.5.1 Accelerometers	29
2.5.2 Fibre-optic Bragg Grating Sensors	29
2.5.3 Laser Doppler Vibrometers	30
2.5.5 Viability of Sensory Systems Discussed.....	31
2.5 Methods of Integration.....	31
2.5.1 Trapezoidal Rule.....	31
2.5.2 Midpoint Rule	32
2.5.3 Simpson’s Rule	33
2.6 Damage Indexing	33
2.7 Signal Transformation Method	34
2.7.1 Fast Fourier Transformation	34
2.7.2 Short-Time Fourier Transformation	35
2.7.3 Wavelet Shape Matching	35
2.7.4 Hilbert-Huang Transformation.....	37
Chapter 3 Project Specifics.....	45
3.1 Pertinent Resources.....	Error! Bookmark not defined.
3.1.1 Chosen Apparatus	45
3.1.2 Chosen Software	48
3.2 Dynamic Response Method Selection Criteria	49
3.3 Signal Specifics	Error! Bookmark not defined.
3.3.1 Signal production	41
3.3.2 Input Frequency	42
3.3.3 Filtering	43
3.3.4 Sampling Rate	44
3.3.5 Signal Transformation Technique	Error! Bookmark not defined.
3.4 Material Specifics.....	Error! Bookmark not defined.
3.5 Data acquisition System.....	53
3.6 Control Variables.....	Error! Bookmark not defined.
3.7 Induced Damage Method	55
3.8 Arithmetic Specifics.....	50
Chapter 4 Experimental Process Methodology	53
4.1 Project Methodology	Error! Bookmark not defined.

4.2 Experimental Methodology	54
4.3 Experimental Validation.....	Error! Bookmark not defined.
4.3.1 Literature	Error! Bookmark not defined.
4.3.2 Finite Element Analysis	Error! Bookmark not defined.
4.3.3 LMS Test Ware	Error! Bookmark not defined.
4.3.4 Supervisory Verification.....	Error! Bookmark not defined.
Chapter 5 Data Results and Analysis.....	57
5.1 Results from experiment	Error! Bookmark not defined.
Chapter 6 Discussion.....	Error! Bookmark not defined.
Chapter 7 Conclusion	73
References	74
Appendices.....	83
Appendix A Apparatus	83
Appendix A1: Fibre-optic Bragg grating sensor	106
Appendix A2: Power amplifier	106
Appendix A3: Signal generator	106
Appendix A4: Solenoidal Shaker	107
Appendix B Drawings.....	84
Appendix B1: Glass pultruded resign reinforced S.H.S beam	84

Table of figures

Figure 1: Low-frequency ultrasonic tomograph for concrete testing (BISHKO, SAMOKRUTOV et al. 2010)	18
Figure 2: Example of the application of visual die inspect of weld joints (Larson 2002).....	19
Figure 3: Corrugated resin reinforced glass fibre composite (Kittinger-Sereinig 2015)	25
Figure 4: Glass fibres (Jean-Pierre 2009)	25
Figure 5: Carbon fibre matting (Hadhuey 2005)	27
Figure 6: Aramid fibre matting (Jean-Pierre and Jaybear 2012).....	27
Figure 7: Accelerometer components diagram (Raki 2013)	29
Figure 8: Fibre-optic Bragg grating sensor optical function diagram (Rusaw 2010).....	30
Figure 9: LDV system diagram (Wang, Li et al. 2011)	30
Figure 10: Two data point example of the trapezoidal rule (Alexandrov 2007).....	31
Figure 11: Midpoint rule geometry example (Alexandrov 2007)	32
Figure 12: Graphical example of the Simpson's integration method (Alexandrov 2005)	33
Figure 13: Sinusoidal waveforms (Storr 2015).....	36
Figure 14: Square waveforms (Storr 2015).....	36
Figure 15: Triangular sawtooth waveforms (Storr 2015).....	37
Figure 16: Pulse waveforms (Storr 2015).....	37
Figure 17: Original signal to be analysed (UC-San_Diego 2014).....	39
Figure 18: IMF 1, Iteration 0 and 2 displaying residue (UC-San_Diego 2014)	39
Figure 19: USQ supplied accelerometer used for the experiments.....	46
Figure 20: USQ supplied instrumented force hammer	46
Figure 21: LMS VB8 data acquisition system	47
Figure 22: USQ supplied stands used to support beam during experiments	48
Figure 23: Graphical representation of the EMD process (Hassan 2005).....	51
Figure 24: Experimental Process and System Overview Diagram	54
Figure 25: Cross-sectional area	55
Figure 26: USQ supplied marked composite beam with accelerometer fixed in place.....	57
Figure 27: Raw imported data and calibration	58
Figure 28: Truncated acceleration data	59
Figure 29: Single and double pass filter examples.....	59
Figure 30: Velocity data	60
Figure 31: Deflection data.....	60
Figure 32: IMF stage 1, node 1.....	61
Figure 33: IMF stage 1, node 5.....	62
Figure 34: IMF stage 1, node 12.....	62
Figure 35: IMF stage 3, node 1.....	63
Figure 36: IMF stage 3, node 5.....	63
Figure 37: IMF stage 3, node 12.....	64
Figure 38: IMF stage 6, node 1.....	65
Figure 39: IMF stage 6, node 5.....	65
Figure 40: IMF stage 6, node 12.....	65
Figure 41: Instant. frequency and amplitude stage 1, node 1	67
Figure 42: Instant. frequency and amplitude stage 1, node 5	68
Figure 43: Instant. frequency and amplitude stage 1, node 12	68
Figure 44: Instant. frequency and amplitude stage 3, node 1	69
Figure 45: Instant. frequency and amplitude stage 3, node 5	69

Figure 46: Instant. frequency and amplitude stage 3, node 12.....	70
Figure 47: Instant. frequency and amplitude stage 6, node 1.....	70
Figure 48: Instant. frequency and amplitude stage 6, node 5.....	71
Figure 49: Instant. frequency and amplitude stage 6, node 12.....	71

List of tables

Table 1: Damage introduction scale	56
--	----

List of equations

Equation 1: Trapezoidal rule (Mathews and Fink 2004).....	32
Equation 2: Midpoint method of integration (Mathews and Fink 2004)	32
Equation 3: Simpson’s method of integration (Mathews and Fink 2004)	33
Equation 4: Short-time Fourier transformation (Barnhart 2011)	35
Equation 5: Refresh of Simpson’s method of integration (Mathews and Fink 2004)	50
Equation 6: Expression of the sifting process (Huang, Shen et al. 1998)	51
Equation 7: Hilbert transformation (Huang, Shen et al. 1998).....	52
Equation 8: Phase angle (Donnelly 2006)	52
Equation 9: Instantaneous frequency (Donnelly 2006)	52
Equation 10: Instantaneous amplitude (Donnelly 2006).....	52

Nomenclature

Abbreviations

HHT	Hilbert-Huang Transformation
FFT	Fast Fourier Transformation
EMD	Empirical Mode Decomposition
IMF	Intrinsic Mode Function
STFT	Short-Time Fourier Transformation
FRF	Frequency response function
FBG	Fibre-optic Bragg Grating Sensor
LDV	Laser Doppler Vibrometer
AC	Alternating current
DC	Direct current
PLM	Product lifecycle management
SHS	Square hollow section

Mathematical symbols

b	Location of second data point with regards to the x axis
a	Location of the first data point with regards to the x axis
$f(x)$	Function with regards to variable x
ω	Angular frequency (rad/s)
t	Global time (s)
τ	Local time (s)
h	Extraction step toward an IMF
$X(t)$	Signal X with respect to time
m	Maxima and Minima envelope mean
$H[h(t)]$	Hilbert transformation
PV	Cauchy principle
ϕ	Phase angle
f	Frequency
a	Amplitude
$\otimes A$	Cross sectional area

Chapter 1| Introduction

Monitoring structural health is of increasing interest and significance in the world of engineering as bigger and more complex projects go ahead in a time of great climactic uncertainty and with a vast and ageing established infrastructure. The need for cheap and accurate methods of monitoring and identifying structural damage is of increasing importance. Many of the current methods of damage detection are too slow, localised, costly and inaccurate to be practically applied to new complex materials and the pressure of the demand of the current infrastructure. Therefore the intention of the researcher is to assist in the promising expanse of the body of knowledge relating to the use of dynamic (vibrational) response in monitoring structural health. Specifically for monitoring the structural health of composite structures with and without damage.

There has been considerable development in the techniques used for dynamic response analysis and these techniques show great promise as a solution to the engineering problems ahead. Dynamic methods have a number of advantages over conventional methods as they are typically non-destructive, non-localised, and present the possibility of integrated real time application in the absence of an experienced technician. These methods also have the advantage of being capable of testing for a broad range of defects even below the surface of the material. These factors present the opportunity, given the necessary research, to develop cheaper and more effective means to monitor the safety of the structures we create. There are an increasing number of dynamic response analysis methods which will be briefly described in the literature review and compared to some traditional damage detection methods.

Composite materials were selected as the subject as they are becoming increasingly common in modern engineering applications due to their economic and mechanical advantages. However as these materials have such a brief phase between operation and catastrophic failure, careful analysis with practical methods are of great importance for maintaining acceptable levels of safety. Despite the promising theory and results produced in lab conditions, these techniques show limited practicality in real world applications due to the introduction of noise and the added requirements of apparatus.

The purpose of this project was to improve a novel dynamic structural health monitoring technique that could be applied at less cost, in real time, low cost of apparatus, and to exclude the requirement of skilled technicians while maintaining the ability to accurately describe structural damage severity and location. The primary focus was on investigating the feasibility of deflection signal processing using the *Hilbert-Huang transformation* (HHT) when compared to the effectiveness of other methods.

1.1 Background

Structural health testing is highly significant in engineering applications. As the complexity of structures and materials we used increases, so too does the need for more complex and effective monitoring methods. Parallel to these increases in complexity is an aging existing infrastructure (Doebling, Farrar et al. 1998) and high uncertainty with regards to changing climatic conditions. These factors indicate the urgent requirement for innovative and efficient methods for testing structural health.

Non-dynamic testing methods can be highly localised, slow, and costly and can require specialist operators leading to the pressure for innovation in this area. During the last few decades there has been a growing interest in the use of vibration for structural health tests and there have been a number of developments. It works by applying vibration to the structure and monitoring the response using sensory apparatus. The sensory apparatus monitors some kind of physical behaviour containing some kind of modal response. This response can be processed to find the natural frequency, modal shape, damping ratio, or frequency response function to name a few. These results can then be compared to some kind of undamaged index derived from historical measurements or FEA projections. As mentioned earlier, these methods show promise in lab conditions and theory, however, it is suggested by Doebling. et al. (1998) that the reason for such slow development in establishing a clear dynamic response testing method capable of industry practice is because of the several confounding factors involved in the application of vibration based methods of damage identification. These factors will be discussed in more detail in the literature review.

Due to availability accelerometers were used as the sensory apparatus which yielded acceleration data from various nodes spaced along the test subject. This was integrated using the *Simpson's method of integration* to double integrate the data giving the deflection signal. An impact hammer was used for excitation and was chosen as the weight of a solenoid would introduce a high degree of error into the data. The deflection data could then be transformed using the HHT giving instantaneous frequency information used to produce a beam stiffness matrix (Huang and Shen 2005). By introducing progressive stages of damage these compiled matrices were compared using a finite difference algorithm (Maia, Silva et al. 2003). These experimental results could then be assessed for feasibility for damage detection. Undamaged experimental results were validated using FEA results acquired using Abaqus (Simulia 2015).

The HHT is the combination of the *Empirical Mode Decomposition* (EMD) and the *Hilbert Spectral Analysis*. The Hilbert spectral analysis performs a Hilbert transform on a signal and computes the instantaneous frequency response. It was developed by David Hilbert in 1905 and is used to extend a signal from consisting of only real constituents to also containing complex constituents. The amplitude

and frequency can then be derived from this expression allowing for an AM/FM time modulated signal representation. The EMD was developed by Norden E. Huang and published in his paper entitled '*The empirical mode decomposition and the Hilbert spectrum for nonlinear and non-stationary time series analysis*' in 1998 (Huang, Shen et al. 1998). The EMD decomposes a signal into *Intrinsic Mode Functions* (IMFs). These IMFs are separate summative physical representations of the original signal and are complete and almost orthogonal to the original signal. These can be processed and reassembled by the Hilbert spectral analysis. This paper also discusses key aspects such as signal processing techniques and briefly touches on composite materials.

The discussed methods were chosen after extensive review of the existing literature which is included in the paper which can be referred to for the convenience of the reader.

1.2 Research Objectives

It was hypothesised that the use of the chosen methods would empirically justify the use of such methods in dynamic testing procedures and display the practicality of industry application. There are a number of kinds of degradation experienced by materials and the structures they form which typically require unique and specific testing procedures. These forms of degradation can occur due to wear from use, seismic activity, erosive atmospheric conditions and varying intensities of weather interaction to name a few. These events cause the lifespan of the material or structure to deviate from the expected lifespan. With the added uncertainty of the application of new innovative materials, it is important to monitor their structural integrity to establish revisions of forecasted lifespans. This is relevant to the economic management and functional capacity of the structure, and also to ensure the safety of those whom of which use the structure. For these reasons, research relating to innovative methods of structural health monitoring have become an area of growing interest in both industrial and academic communities. Innovation has resulted from such interest, however, some of the most promising techniques derived from theory and performed in lab experiments, such as dynamic response techniques, does not prove as effective when applied to real world scenarios.

The aim of this research task is to further develop some of the more innovative techniques used in the process of dynamic response testing in pursuit of damage severity and location. It is proposed that by first outlining the key areas in which these methods are encountering problems, followed by investigations into how such obstacles could be overcome. It is the intention of the researcher that by completing an extensive review and summary of the available literature on structural health monitoring, effective processes of applying innovative new techniques can be made to with respect to commercial applications.

The intention of the researcher was to achieve some small contribution in the way of developing such an approach to dynamic testing. Because of the short duration of this research project, a final aim of this research tasks is to produce some useful suggestions for future research that can be conducted to achieve the primary objective of the practical and widely applicable use of dynamic response testing.

The process undertaken to complete the research objectives is outlined in the following:

- Extensive review of existing literature conducted relating to methods of structural health testing, dynamic methods of structural health testing, composite material types, properties and behaviour, methods of integration, signal transformation methods, data acquisition systems and related apparatus, methods of damage indexing, and techniques for signal processing
- Formulation of investigation and methods pertinent to achieving the initial research objectives both empirically and within the expected time limitations
- Data acquisition of dynamic response of chosen composite structure when subjected to forced resonance
- Numerically solve experimental data to draw comparison and establish the effectiveness of chosen methods
- Evaluate and discuss the results and practicality of the chosen methods for identifying damage severity and location for industrial applications in a cheap, timely and accurate manner
- Reflect and discuss the pertinent findings of the research including anomalies, successfully achieved objectives and suggestions for further research

1.3 Project overview

This research project took place over the course of a year during 2015, ending on the 29th of October, 2015. During this time the following report was constructed. For the convenience of the reader, the researcher has included this section giving a brief outline of the report including relevant information, method of experimentation, results of experimental investigation, and conclusive remarks in reflection of the process.

1.3.1 Chapter 1| Introduction

Chapter 1 consists of a historical introduction to the testing structural health, a background of dynamic response analysis of structures, and the reasons why the research project is necessary. It also defines the objectives and scope of the project. The introduction includes a preliminary hypothesis in which the researcher discusses the expected outcomes of the research to be reflected upon in the results and discussion sections. The reference section and appendix was not included in this section however are referred to throughout the report.

1.3.2 Chapter 2| Literature

Chapter 2 consists of a review of all the research found pertinent to this project scope and its objectives. Other methods of structural health testing, dynamic methods of structural health testing, composite material properties and behaviour, sensor selection, methods of integration, signal processing methods, data acquisition systems, and other hardware and software selections relevant to this dissertation were extensively discussed and referenced. At the end of each topic, the viability of each topic is discussed with some preliminary remarks regarding what topic seems most applicable to the research objectives. The method chosen from such topic discussions is outlined clearly in Chapter 3.

1.3.3 Chapter 3| Project Specifics

The completion of this project involved the broad application of apparatus and methods of analysis. As such, it was deemed appropriate by the researcher to include a section dedicated to outlining the apparatus chosen and its relation to the system of experiments or analysis entailed. Chapter 3 includes a description of all the pertinent apparatus and software used in the project, including a description of the material that was used and the system of dynamic response testing applied. It also gives descriptions of the arithmetic used and how this arithmetic was logically translated into code usable by Matlab's numerical analysis and processing.

1.3.4 Chapter 4| Experimental process methodology

Chapter 4 outlines the procedure taken in completing the experiments involved, the data acquisition systems used, and numerical methods chosen. It has a full detailed explanation of steps and precautions taken to ensure correct scientific methods and has reference to related pictures and diagrams found in the appendix. For the preliminary report the safety procedures, inductions and timeline for important tasks are also included in this section. It also includes the resource requirements for the project. An important inclusion to the methodology section is a project system flowchart. This flowchart gives a clear and accurate description of the stages involved in the project, the systematic approach taken to completing them by the researcher, and the way in which each part of the project was related to each other with regards to analysis. This system flowchart can be found with description in Section 4.1 of Chapter 4.

1.3.5 Chapter 5| Discussion of Experimental Results

Chapter 5 was dedicated to the results in an easy to understand tabulated format and discussion of these results. The results are laid out in such a way that the results from each stage of experimental investigation and numerical analysis can be seen so that the process can be understood and the reader can properly understand the flow of the project that took place. The chapter includes some plotted examples of the raw dynamic response acquired from the LMS VB8 data acquisition system followed by the changes incurred by the inclusion of the chosen high pass filter mechanism. An example of the velocity data plot after the first stage of integration is displayed. This was then repeated showing

examples of the deformation achieved once the data had undergone the full double integration with all necessary applied filters. The interaction of the empirical mode decomposition was tabulated showing the results intrinsic mode functions. The instantaneous frequency of each node was then acquired by the Hilbert spectral analysis which were then assembled into a global stiffness matrix. The stiffness matrices are labelled corresponding to each particular stage of damage to which they are associated. Finally the results of the finite difference algorithm are shown and plotted. At the end of the chapter is an extensive comparison between the fast Fourier transformation results and the results of the Hilbert-Huang transformation. This comparison is presented in such a way that the physical characteristics of the response and the beam can be easily understood with brief discussions on the differences. These difference will be discussed in greater detail in Chapter 7. Each stage is briefly discussed with reference to its detailed description found in Chapter 4.

1.3.8 Chapter 6| Conclusion

The final Chapter of the paper was the conclusion where the most important findings and recommendations were briefly summarised. The most important findings include the comparison between the fast Fourier and Hilbert-Huang transformations and their expected accuracy in stationary signal analysis. It also includes some concluding statements regarding the practicality of the code produced in being used for real time analysis of structures. The Chapter is closed with a clear and brief recap on the recommended possible tasks for future researchers to making these methods a more practical option.

Chapter 2| Literature

Before experimental investigation could begin, it was important to clarify the existing literature to gain sound knowledge regarding the concepts and to ensure that the research completed was novel and unique. A review of the literature was therefore necessary and included number of different methods for structural health monitoring and the advantages and disadvantages with relation to vibration signature methods. An explanation of the different viable methods for dynamic response testing for structural health and their respective advantages and disadvantages with relation to the method chosen in this paper is included. A review of existing software and hardware including sensory mechanisms, methods of integration and signal processing, and a method for indexing the severity of damage with relation to pristine conditions is discussed. Finally the available signal processing techniques such as filtering and transformations are discussed. The literature formed the basis for this research and in turn guided the researcher to the decision of the project aims and scope. Dynamic response methods shows limited success in industrial applications but showed potential for use without skilled operators at low cost and time required.

2.1 Traditional structural health monitoring methods

There are a number of traditional testing methods that have been used frequently in the past with moderate success regarding composites. Some of these methods include X-ray tomography, Ultrasonic tomography, dye penetration visual inspection, and coin tap testing. The literature relating to these methods, their advantages and disadvantages, and why they were not pertinent to the research is explained in this section.

2.1.1 X-ray Tomography

X-ray tomography damage detection is a non-destructive test method in which an entire structure can be screened and inspected for damage (Kinney and Nichols 1992). It involves the use of X-ray two or three dimensional imaging of an object which can then be developed by computer tomography (Kinney and Nichols 1992). However a limiting factor of the size of an object that can be practically examined by the X-ray tomography method is that the spatial resolution be kept small with respect to the microstructural properties of the material being examined. X-ray tomography has limited capabilities with regards to image micro structures such as fibres in fibre composites (Kinney and Nichols 1992).

There are a number of promising developments in the area of X-ray tomography in industrial application however this method was not considered due to the high cost, requirement for specialist labour, insufficient ability to image fibres in composites, and the inability to find small damages in large structures.

2.1.2 Ultrasonic Tomography

Ultrasonic tomography is a local damage detection technique in which an ultrasonic signal is introduced to a structure. The signal is then monitored for deviations from the reference signal of an undamaged structure (Tsuda 2006). This technique uses similar principles to dynamic response techniques however the much higher frequency of ultrasonic signals (approx. 20-40 kHz according to HyperPhysics from Georgia State University) makes it only applicable for localised observation as the signal loses energy over a short distance. Once the ultrasonic signal from the object being tested is compared to the signal expected from an undamaged specimen, inconsistencies will display the nature of the damage. This technique is highly effective if prior knowledge of the location of damage is known. However this technique is not applicable for monitoring structural health of large civil structures and for the objective of this research.



Figure 1: Low-frequency ultrasonic tomograph for concrete testing (BISHKO, SAMOKRUTOV et al. 2010)

This technique has since been improved upon by (Dutta 2010). It was proposed that by the use of LAMB waves and modal data, or ultrasonic guided wave based techniques. This method was proposed to be a non-baseline technique capable of determining damage without comparison to an undamaged specimen. The data is gathered using piezoelectric wafer transducers and laser vibrometers. Vibrometers unfortunately are not applicable for the objectives of this project as it is restricted to monitoring the surface behaviour of an object. The analysis of the LAMB wave propagation is also deemed inappropriate for the objectives of this project as that testing equipment is quite costly and this method requires an experienced operator to determine the existence of damage.

2.1.3 Visual dye penetration inspection

Visual dye penetration inspection is one of the oldest and widely used non-destructive methods for testing structural health still being used today. It is used in a wide variety of tasks ranging from automobile spark plugs to critical engine components (Zuuk-International 2015). It works by applying a dye particular to the expected crack size and material being inspected so that the dye can penetrate the

crack. The surface dye can then be removed leave the dye that has entered the crack to stand out (Larson 2002).

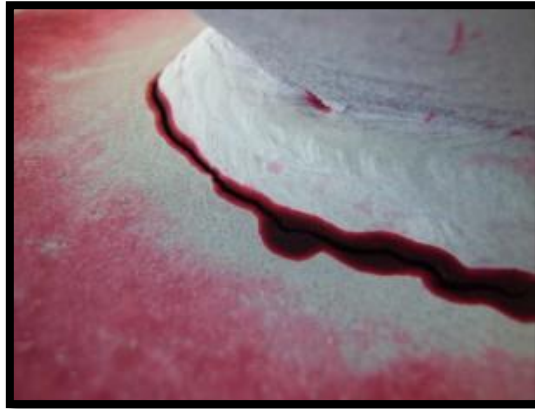


Figure 2: Example of the application of visual die inspect of weld joints (Larson 2002)

Unfortunately the dye penetration method can only be used to identify surface cracks therefore is inappropriate for a range of situations. It is also highly dependent on the types of chemicals and the operators attention to detail (Larson 2002).

2.1.4 Coin tap testing

The coin-tap test is one of the oldest methods of non-destructive testing and is commonly used for testing laminated structures (Kim 2008). This method requires an operator to tap each point of a structure with a coin or hammer listening for changes in sound radiated from the structure (Kim 2008). The characteristics of the impact are highly dependent on the impedance of the structure and on the hammer or coin used (Kim 2008). The effectiveness however is highly dependent on the skill of the operator. The method is low cost due to no complicated or expensive testing equipment however it can be wrought with human inaccuracy and is limited by the thickness of the test object that can be observed. As the scope of this project is with regards to testing civil composite structures of thickness greater than a laminate this method is not relevant and will not be considered.

2.1.5 Viability of methods discussed

All the non-dynamic structural health monitoring methods discussed in this section have proven insufficient for the objectives of this project. Restrictions such as localised testing, high costs, the requirement for specialised operators, and the inability to detect at a resolution for microstructural damages have ruled out all methods discussed.

2.2 Existing dynamic structural health monitoring methods

Dynamic methods of structural health monitoring or damage identification have undergone increasing levels of interest over the last thirty years. A number of different methods have been introduced to the body of literature and are discussed in this section. Some of the reasons for this method include the non-localised capabilities of dynamic methods and the applicability to various types of materials of dynamic

methods. Dynamic response methods can be used to determine the existence, location and severity of the damage with varying degrees of success in each. It should be noted that the sensor system, the method of integration and the method of signal processing make quite a difference in the effectiveness of each method and are discussed in greater detail in sections 2.4, 2.5 and 2.6 respectively of the literature review.

It may seem strange that such inconclusive methods for dynamic response testing have been produced for industry application but as discussed by Doebling et al. (1998), there are a confounding number of factors making dynamic methods of damage identification difficult to apply in the practical conditions experienced in most real engineering situations. Standard modal properties represent the compression of a large spectrum of data. Modal properties are typically estimated experimentally from measured response time histories. These histories may have over one thousand data points each and if measurements are made at 100 points, there are now 100,000 pieces of data to be considered. As more innovative processing techniques are developed the method becomes more applicable to industrial applications and is now used for various industry applications in civil, mechanical and aerospace engineering.

Dynamic methods are used to analyse changes with regards to fundamental modal parameters such as the changes in natural frequency, modal strain energy, residual stress or force indicators, frequency response functions, neural networks, damping ratios and/or mode shapes (Bisht 2005). Within each of these fundamental modal parameters, various methods of acquiring the data and analysing it have been created with varying degrees of accuracy and success. Only the most common and effective methods are discussed in this section. With some less effective methods briefly mentioned in a final section.

2.2.1 Changes in natural frequency

Over the lifespan of a structure it will experience degradation in which its material properties will change accordingly. One of these material properties is the natural frequency of the object. Dynamic response testing with regards to changes in natural frequency is the practice of comparing the natural frequency of the object of interest with the expected or known natural frequency of the object in undamaged conditions (Chen, Spyrakos et al. 1995).

In the experiments conducted by Chen et al. (1995) steel channel sections were subject to forced oscillations created by the release of a weight suspended of the test channel section. Some of the sections were damaged while others were kept in undamaged conditions. The locations of the damage were placed away from node points of low modes of vibration to ensure that the damage would influence the dynamic response. These signal of these oscillations were then interpreted by PCB accelerometers. The signals were analysed by a real-time spectrum analyser and numerical processing could be done on this

data. The power spectral density and magnitude of the frequency domain could be obtained by using the fast Fourier transformation. The data was then subject to linear regression to remove any noise and eradicate any baseline shift. This method concluded that an increase in damage typically decreased the expected frequency response. The location of the damage could be identified by noticing between which accelerometers showed varied frequency responses.

The accuracy of this method has been suggested that a 5% natural frequency change is the approximate requirement to be considered damage with a high reliability (Salawu 1997). However it is also mentioned that frequency changes can occur due to changes in ambient conditions. Salawu (1997) supplied notes that there have been occasions in which a 5% frequency shift has been tested conclusively when testing steel and concrete bridges in a single day.

2.2.2 Changes in modal strain energy

When a structure is subject to vibration there is strain as displacement occurs between modal nodes. Mode shapes can be recognised as the oscillating crests and troughs that form between the modal nodes. As this occurs the material experiences an increasing amount of strain on the outer minimum and maximums of the structure. Shi et al. (1998, 2000) presented a technique to identify the existence of damage by use of the mode shapes and elemental stiffness matrix. This technique requires no prior knowledge of the undamaged dynamic behaviour of the element which stands as a substantial advantage for this method. By monitoring the changes in the stiffness matrix between modal elements the location and severity of damage can be indicated. The limiting factor of this method is that the nodes of the structure being tested could introduce error in the response. The method requires a prevalent understanding of the modal nodes that is dependent on a number of factors. By analysing in a sub optimal location readings could give skewed data (Shi, Law et al. 1998, Shi, Law et al. 2000).

2.2.3 Residual force/stress indicators

Residual force indication utilises modal force vectors derived from a residual flexibility matrix to identify the existence of damage in structures (Ricles and Kosmatka 1992). The residual flexibility matrix can be found by measuring the contribution of the materials flexibility matrix from modes outside the measured bandwidth (Doebbling, Farrar et al. 1998). This method was developed to solve iteratively for optimisation problems using the Gauss-Newton method (Chen and Nagarajaiah 2007).

This method has been used by Reiter et al. to monitor the occurrence of ruptures in polymer films and showed practical use possibilities however for non-film materials this method proves to be less effective (Reiter, Hamieh et al. 2005). For this reason this method was not considered in the scope of experiments for this project.

2.2.4 Neural Networks

Neural networks, while in a primitive form, is a type of artificial intelligence. Digital computers operate in an entirely different manner than a natural brain however the function of a neural network is to create a systemic network connecting functions depending on events such as monitoring results data from sensory equipment and processing the data into a numerous amount of frequency response functions (Wu, Ghaboussi et al. 1992). This technique has been used by Castellini & Revel et al. (2000) involved the application of Laser Doppler Vibrometry as a sensory apparatus and the data was processed by the trained neural network. The sensory apparatus retrieved the vibration velocity spectra from a series of points on a test panel which could then be derived into displacement data by the neural network (Castellini and Revel 2000). The truly incredible thing about neural networks is the way in which it is trained. It becomes more functional by acquiring knowledge from its environment by use of learning algorithm which is capable of modifying synaptic pathways or synaptic weights (Haykin 2004).

This technique is highly promising and can be used to combine the advantages of multiple techniques to compile a more accurate hypothesis of the true nature and location of damage in a structure. However as such a technique requires much more time than available for the completion of this project this method was not chosen. It is however a desirable project in itself for further research and due to time constraints lies outside the scope of this project.

2.2.5 Changes in damping ratios

Damping is typically an irreversible process of converting mechanical vibration into heat as a result of motion (Rao 2005). It occurs due to friction factors internal or external of the material. Use of the change in damping ratio to analyse structural damage has been done by Abeykoon & Kawarai. et al. (2015) by decomposing modal damping ratios into mode-independent damping parameters of energy-dissipating sources in bridges (ABEYKOON, KAWARAI et al. 2015). Change in damping parameters can then be used to detect damaged structural components.

2.2.6 Changes in mode shapes

The mode shape analysis method of damage detection involves the analysis of the mode shape created during forced vibrational loading of a structure (Pandey, Biswas et al. 1991). Pandley & Biswas et al. (1991) analysed a cantilever and a simply supported beam for an analytical model and found that damage caused absolute changes in the curvature mode shape in the local region. There have since been developments to these methods with four different methods that can be utilised (Maia, Silva et al. 2003). These four methods include mode shape, mode shape curvature, mode shape curvature squared, and mode shape slope. These methods all involve analysis of the geometry of vibratory patterns exhibited by the structure.

This method has been effective at identifying the location of damage subjected to a structure however is less effective at indicating the severity of the damage (Doebeling, Farrar et al. 1998). This method has seen continual improvement. Such improvements include experiments by Kim & Stubbs (2002) in which have worked continually to improve the methods accuracy by removing erratic assumptions and limits existing in the related algorithms (Kim and Stubbs 2002).

This method was not considered viable for the project however as it has been noted by Maia & Silva et al. (2003) to be time consuming and fraught with numerous errors related to the curve fitting algorithms.

2.2.7 Changes in frequency response functions

There are several different definitions of frequency response functions. Frequency response functions (FRF) is a method similar to previously discussed methods in that it uses some combination of changes in natural frequency, damping and modal interaction (Lee and Shin 2002). however it involves the analysis of the structure at a range of different frequencies (Maia, Silva et al. 2003). Experiments completed by Maia & Silva et al. (2003) and Sampaio (1999) indicate that this method is much more accurate than the mode shape method. The FRF method works by collecting mode shape data at numerous standard frequencies for either a damaged and undamaged structure or section in order to detect local differences in the flexibility of the damaged and undamaged response. The four different types of analysis discussed in the mode shapes method being mode shape, mode shape curvature, mode shape curvature squared, and mode shape slope are the behaviours considered for analysis in this method also (Sampaio, Maia et al. 1999, Maia, Silva et al. 2003).

The FRF method works by analysis of several sets of deflection and oscillating force data. This data can then be used to construct a flexibility matrix. This matrix can then be analysed by use of a damage index algorithm. This method typically requires a lot of nodes as accuracy is lost with large nodal spacing (Fu and He 2001). FRF methods typically require smaller frequency ranges as higher frequency range bring about the inclusion of a large number of modal frequencies. Increased modal frequencies also require more intensive calculations (Sampaio, Maia et al. 1999, Fu and He 2001). This is because the FRF relies on higher stiffness changes which becomes less significant when compared to the amplitude difference of the frequency shift due to resonance (Sampaio, Maia et al. 1999, Fu and He 2001). For the FRF to be effectively applied, frequencies close to but before the first resonance or anti-resonance frequency is desirable.

Optimisation of the FRF has been done yielding much more conclusive results, however becomes far more computationally intensive (Schulz, Pai et al. 1996, Schulz, Pai et al. 1997). Experiments by Schulz et al. (1996) show that by “partitioning second-order matrix equations of motion into assigned and auxiliary degrees of freedom (DOF) and then optimizing elemental parameters to assign the measured

frequency response of the model” the location and extent of the damage can be identified to a high degree of accuracy (Schulz, Pai et al. 1996). This optimisation comes at a large increase in required computational capability.

2.2.8 Change in mechanical impedance

Impedance based structural health monitoring have been developed using the electromechanical coupling property of piezoelectric materials (Sun, Rogers et al. 1995). This is a non-destructive testing method that utilises the electromechanical coupling property of piezoelectric materials. Because structural mechanical impedance measurements are difficult to obtain, changes in electromechanical impedance reactions of piezoelectric sensory equipment is more effective. This sensory system is used to monitor changes in structural stiffness, damping and mass (Park and Inman 2005).

2.2.9 Viability of methods discussed and method chosen

The frequency response functions and changes mode shapes are both desirable methods for the purpose of this project according to the literature that has been reviewed. However, a decision between the two is highly dependent on the transform method chosen in further sections. The final decision on viable dynamic response method was to monitor the variations instantaneous frequency response functions. Changes in mode shapes was considered as a secondary tasks however was highly dependent on time as the project was conducted over only one year.

2.3 Composite materials

A composite material is required for vibration based structural health testing and the literature relating to composites is discussed in this section including a brief explanation of what constitutes a composite. There is also an explanation with regards to the viability of each composite type which said discussion indicates briefly the direction of thought involved in choosing the material used to collect experimental data.

A composite material consists of two or more individual materials in which the mechanical advantages of each complement the disadvantages of the other (William D. Callister and Rethwisch 2014). The purpose of composite materials is to achieve a specific combination of material properties that either aren't displayed by any single material, or to achieve similar material properties as another material at less cost of some sort (William D. Callister and Rethwisch 2014). Composites being most commonly a combination of Polymers, Ceramics and Metals, a large number of different material property variations can be found. Some of the popular characteristics of composite materials can be light weight while maintaining high strength, resistance to corrosion, electrically inert, durable and variably elastic and ductile.

This Section discusses some of the more common or advanced types of composites, their advantages and disadvantages and some practical applications for which they are used. It also outlines the feasibility of these materials with regards to the experimental investigation outlined in this report. While alloys can be considered a composite material, they lay outside the scope of this project as the purpose is to investigate the ability of structural health monitoring of a non-monolithic composite materials. Fibre composites are the focus and different kinds are discussed in this section as they present a difficult task to structural health monitoring. They do not consist of uniform material properties and are typically mechanically orthotropic. Other kinds of composites include Particle reinforced materials, nanomaterial reinforced materials and structural laminates or sandwich panel arrangements (William D. Callister and Rethwisch 2014). There are some less common composite materials that are not discussed in this section as they are not commonly used and these include boron, silicon, carbide and aluminium oxide and nanomaterial composites.

2.3.1 Glass fibre-reinforced polymers

Fibreglass is one of the most common and familiar composites (William D. Callister and Rethwisch 2014). It was one of the first clearly classified composites as the field was being established in the mid-20th century as it became highly applicable to the construction of boats and soon storage tanks, houses and plastic pipes to name a few of its applications. It consists of glass fibres, either in continuous or discontinuous arrangement, contained within a polymer matrix. This composite is the most vastly produced. Fibres are typically between 3 and 20 micrometres in diameter and are classified by either long or short length fibres (William D. Callister and Rethwisch 2014).

Figure 3: Corrugated resin reinforced glass fibre composite (Kittinger-Sereinig 2015)

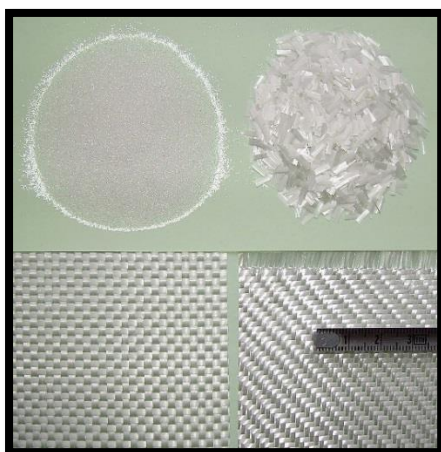


Figure 4: Glass fibres (Jean-Pierre 2009)



This is most popular or the fibre composites due to the following advantages:

- Easily manufactured by drawing into high strength fibres from molten state
- Low cost of manufacture compared to other fibre composites

- Applicable to multiple shapes and component functions
- Wide variety of manufacturing techniques
- Glass fibres are relatively strong and when embedded in a polymer matrix yields a very high specific strength
- Various polymer types can yield high chemical resistance making it ideal for corrosive environments
- Resistance to heat, fire and maintains dimensional stability in high temperature environments
- Electrically inert

There are challenges to this material however as interaction with another hard material can introduce surface flaws. Surface characteristics of glass fibre composites are very important and small defects can change the tensile properties by a great deal (William D. Callister and Rethwisch 2014). Some disadvantages of this material include:

- Specific applications to ensure no interaction at surface with other hard materials
- Low stiffness and rigidity
- Limited to applications below approximately 200 degrees Celsius depending on the polymer matrix used but can be extended as high as 350 degrees Celsius if cast in high purity infused silica
- There are possible health risks in handling if necessary safety precautions are not considered and met in practice
- Low Fatigue performance limits compared to other fibre composites

2.3.2 Carbon fibre-reinforced polymers

Carbon fibre is typically used in high performance material used in advanced polymer matrix composites. Some of the advantages of carbon fibre-reinforced polymers include:

- Carbon fibres have high specific moduli (elastic modulus per mass density) and high specific strength
- They retain high elasticity and strength at elevated temperatures however at high temperatures the carbon can becoming reactive with oxygen
- At room temperature carbon is unaffected by moisture or a wide variety of acids, solvents and bases
- Diverse range of desirable material properties therefore is applicable for a number of engineering applications
- Carbon fibre and composite manufacturing methods have been developed that are reasonably inexpensive and cost effective
- Good fatigue strength properties

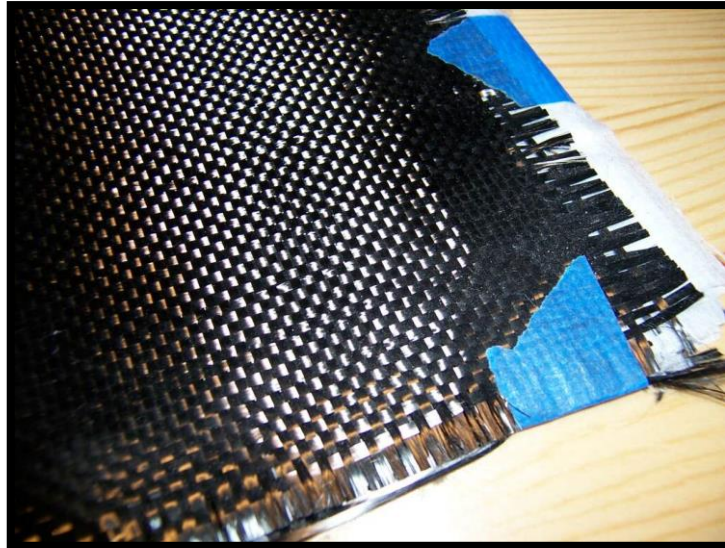


Figure 5: Carbon fibre matting (Hadhuey 2005)

While the price of manufacture has decreased considerably with modern techniques it is still high in comparison to other fibre composites which is one of the first disadvantages. This makes it for specific and advanced applications. The list of disadvantages experienced by this fibre composite are as follows:

- High cost of manufacture compared to other fibre composites
- Carbon fibres can have resin compatibility issues therefore epoxy resins are typically used which causes a further increased cost in finished products
- Carbon fibres is not as easily manufactured and the materials are not as readily available as other fibre materials

2.3.3 Aramid fibre-reinforced polymers

Aramid fibres are high strength and high modulus materials that are commonly used in aerospace and military applications. There are a number of different types however the most common types are made from Kevlar or Nomex. These fibre composite materials have superior strength to weight ratios than metals.



Figure 6: Aramid fibre matting (Jean-Pierre and Jaybear 2012)

The following section clearly outlines the advantages of the aramid fibre-reinforced polymers:

- High toughness, impact resistance, and resistance to creep and fatigue fracture
- High tensile strength
- Chemically resistant except by strong base or acid chemicals
- Even though they are thermoplastics they retain their mechanical properties from around -200 to 200 degrees Celsius

The disadvantages of aramid fibre-reinforced polymers are as follows:

- Poor compression strength due to micro buckling and poor performance when subject to traverse loading as bonding between fibres is typically weak
- Sensitive to ultraviolet radiation
- Absorbs moisture

2.3.4 Viability of composites discussed

Glass fibre-reinforced polymers were decided upon for the experimental analysis in this project for two reasons. Firstly because they are the most widely used in industrial applications, therefore increasing the body of knowledge surrounding this particular material will be widely beneficial to the engineering community. The second reason being that this material is cheap and readily available at the university as it is a common material made for other research here at USQ.

Glass fibre pultruded square hollow section beams are used as there are readily cast members available. Pultrusion is the process of pulling glass fibres of a spool through a polymer injection process. Long strands of glass fibre run right through the polymer giving high tensile strength in close to orthotropic uniformity.

2.4 Sensors for experimental data acquisition

Various data acquisition sensors are suitable for the analysis of dynamic response in structures. This section discusses the function, advantages and disadvantages of various sensors and the reason for the chosen sensor. As there are a number of dynamic response methods requiring different forms of data sensors are typically more suitable for certain methods therefore the type of sensor is primarily related to the chosen dynamic testing method chosen however as discussed in the following sections there are a number of suitable sensors for testing this projects chosen dynamic response method.

It is important that transducer's be placed either in places where modal nodes are known not to exist for the selected vibration frequency or set up at consistently at measurements at distances that are known to be prime numbers. As primes are multiples only of themselves, this method will ensure that even if some fall on a modal node, not all will be on a mode. In the event that an accelerometer gives no acceleration data it can be assumed to be either dysfunctional or on a modal node. Modal nodes are points in which no displacement occurs and stress is at a minimum (Salawu 1997).

2.5.1 Accelerometers

Accelerometers are micro electromechanical systems used to convert acceleration into electrical voltage signals. Accelerometers require calibration so that the voltage response responds to the correct acceleration. The calibration is typically the largest source for error however accelerometers are proven to provide highly accurate data (Kuehnel and Sherman 1994). Accelerometers involve micro electromechanical structures made from piezoelectric materials such as quartz.

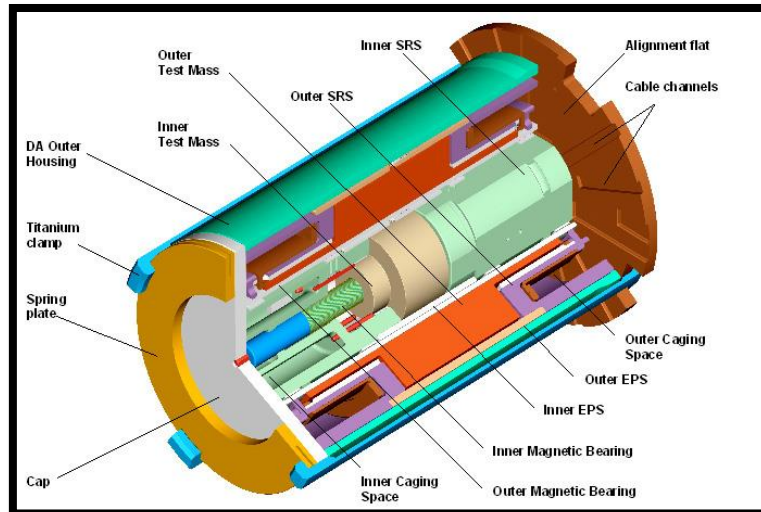


Figure 7: Accelerometer components diagram (Raki 2013)

Accelerometers are cheap components that are readily available at the university. Using this kind of sensory component would retrieve data in the form of acceleration therefore an effective integration method would be necessary to convert this data into displacement if this were to be chosen for experimental data acquisition.

2.5.2 Fibre-optic Bragg Grating Sensors

Fibre-optic Bragg grating (FBG) sensors utilise a type of distributed Bragg reflector in short segments of optical fibre. The function of the distributed Bragg grating (DBG) is to reflect particular wavelengths of light while transmitting other wavelengths (Morey, Meltz et al. 1990). Light is sent from a remote through the optical fibre and the signal response is determined by the return reflection from the FBG. These sensors are capable of monitoring changes in strain, temperature and pressure by means of monitoring phase shifts and time delays of the reflected light after these factor's effect material shape.

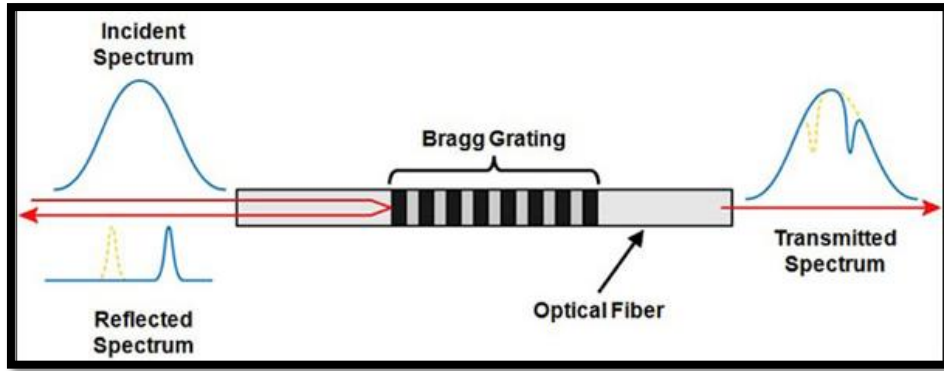


Figure 8: Fibre-optic Bragg grating sensor optical function diagram (Rusaw 2010)

Optical fibre sensors are immune to electromagnetic interference, light weight, small, have a high sensitivity, a large bandwidth and are easily implemented. While they have high sensitivity, their sensitivity to the specific application of sensing low amplitude vibrations is only of a moderate standard (Lee 2003). Spectral decoding methods cannot be utilised to detect high frequency signals due to the inherent low speed of the optical fibre sensing method (Wild and Hinckley 2010).

2.5.3 Laser Doppler Vibrometers

Laser Doppler Vibrometers (LDV) is a remote, non-destructive and high spatial recognition method of vibration based structural health monitoring. LDV has a high frequency bandwidth, up to 20 MHz, a velocity range of ± 30 m/s, resolution of about 8 nm and displacements of 0.5 $\mu\text{m/s}$ (Castellini, Martarelli et al. 2006). LDV's monitor instantaneous velocity data of objects subjected to oscillating loads. The LDV produces a laser directed at the surface of interest. Any vibratory behaviour will cause a Doppler shift in the reflected laser beam frequency (Castellini, Martarelli et al. 2006). The beams instantaneous frequency shifts can be translated to yield the instantaneous changes in velocity experienced at the surface.

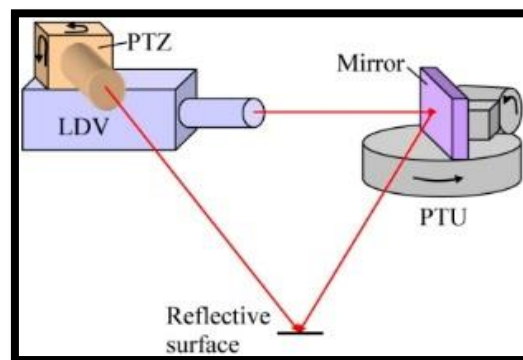


Figure 9: LDV system diagram (Wang, Li et al. 2011)

LDV structural health detection methods are highly accurate and would be an ideal tool for the purpose of this experiment. However, LDV technology is very expensive and is unavailable for use for this experiment. Therefore this sensory method was deemed outside the scope for the purpose of this experiment. It is however recommended as a desirable sensory system for use in future research.

2.5.5 Viability of Sensory Systems Discussed

Both FBG sensors and accelerometers are available for use in the present experimental facilities. However, as previously mentioned LDV systems are of high cost and unavailable for use in these experiments. A comparison made by reference to the literature suggests for detecting vibration in a solid object that the accelerometer will yield more accurate results. Therefore it was decided that the accelerometer would be the correct sensory apparatus for use in this projects experiments.

2.5 Methods of Integration

Using accelerometers to collect the dynamic response data, as suggested above, will lead to the acquired dynamic response consisting of acceleration data. It is required that acceleration be integrated twice in order to acquire the displacement data. Only then can the data be applied to a signal transformation and graphically represented for clear analysis. There are three suitable methods of integration that will be discussed and considered in this section (Heaton 2011).

Other important considerations are the sources of error in these methods and some of the proposed optimisation techniques that have surfaced in scientific literature. Noise is a major contributor to the error introduced to these techniques (Stiros 2008). Some unavoidable error can of course be contributed to the characteristic limitations of sensory apparatus, however, the majority of error during dynamic response tests will be attributed to the overwhelming effects of noise.

2.5.1 Trapezoidal Rule

The trapezoidal rule, or trapezium rule, is considered the simplest numerical methods for integrating. It works by breaking the function up by each of its data points and calculating each section based on strips where the data points are connected in a linear fashion (James 2008). The area of a series of trapezoids can be easily found therefore calculating the area under the curve is an easy tasks for numerical analysis. It should also be noted that the more dense the data points, the greater the accuracy of this method (James 2008). The area under a curve can be approximated by the trapezoidal rule which is expressed as the following:

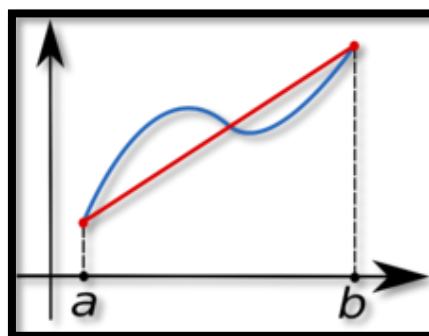


Figure 10: Two data point example of the trapezoidal rule (Alexandrov 2007)

Equation 1: Trapezoidal rule (Mathews and Fink 2004)

$$\int_a^b f(x)dx \approx (b-a) \left[\frac{f(a)+f(b)}{2} \right]$$

Where: b is the location of the second data point with regards to the 'x axis'
 a is the location of the first data point with regards to the 'x axis'

This formula can be applied to a function with 'n' number of data points 'n-1' times yielding the approximate area under the curve of a data set or signal. As the figure suggests, having more frequent data sets spaced more closely together yields a more accurate integration.

2.5.2 Midpoint Rule

The midpoint rule, or rectangle rule, is an integration technique used to integrate data in which two points are used as boundaries and an equation to find a suitable midpoint between the data points can be found (Burden and Faires 2011). This midpoint is then included as a data point and a typical integration method such as the Trapezoidal is used to integrate (Burden and Faires 2011).

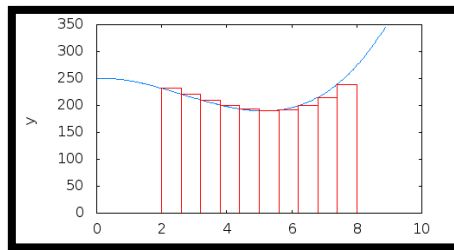


Figure 11: Midpoint rule geometry example (Alexandrov 2007)

This method can be considered an extension of another method to possibly increase the accuracy of the base method. This method was improved by Fink and Mathews et al. (2004) in which it was demonstrated how an error factor can be considered depending on the method and midpoint function used (Mathews and Fink 2004). The midpoint rule can be expressed as the following:

Equation 2: Midpoint method of integration (Mathews and Fink 2004)

$$\int_a^b f(x)dx \approx h \sum_{n=0}^{N-1} f(x_n)$$

$$h = (b-a) / N \quad x_n = a + nh$$

Where: b is the location of the second data point with regards to the 'x axis'
 a is the location of the first data point with regards to the 'x axis'
 N is the number of equally divided subintervals
 h is the length of subintervals
 x_n is the approximation of the left top corner to which subintervals are intersected

2.5.3 Simpson's Rule

This numerical method of integration is an approximation of definite integrals using quadratic and Lagrange polynomial interpolation between data points (James 2008). This method is said to be significantly superior in comparison to the midpoint and trapezoidal rule in almost all situations by a number of sources (Mathews and Fink 2004, James 2008, Burden and Faires 2011).

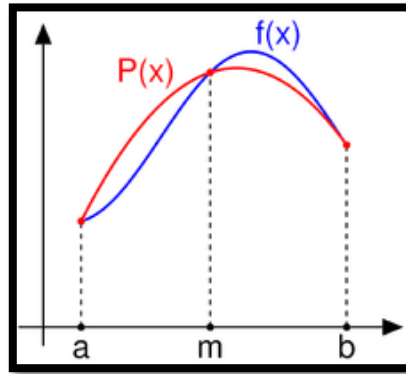


Figure 12: Graphical example of the Simpson's integration method (Alexandrov 2005)

One of the main advantages that the Simpson's rule has over other more conventional methods of integration is that it can be used to more accurately estimate the curve as the shape between data points can be estimated more accurately. Its advantage over the other methods becomes more apparent as the distance between data points increases. The equation used in this method corresponding to the figure above is shown below:

Equation 3: Simpson's method of integration (Mathews and Fink 2004)

$$\int_a^b f(x)dx \approx \frac{b-a}{6} \left[f(a) + 4f\left(\frac{a+b}{2}\right) + f(b) \right]$$

Where: b is the location of the second data point with regards to the 'x axis'
 a is the location of the first data point with regards to the 'x axis'

After the review of the literature numerous sources have pointed to the Simpson's method of integration as the most accurate. This is because it is best capable of fitting the curve between data points using both quadratic and Lagrange polynomials as a method of interpolation.

2.6 Damage Indexing

Damage indexing is a method used to numerically represent minute changes in a materials modal behaviour. Minute changes in such behaviour can represent the occurrence of serious damage. One method for indexing damage is the finite damage algorithm proposed by Maia, Sampaio and Silva et al. (1999). This finite difference approach yields a dimensionless number calculated using the changes in frequency response functions. Typically most research has utilised the node system to identify the location of damage. Experiments performed by Maia et al. (2003) found that by spacing data acquisition

sensors in multiple locations, the location in which the signal experienced an abnormal change could conclusively be determined to be near where the damage occurred (Maia, Silva et al. 2003). By identifying at exactly what location this abnormality occurred, it could be determined that the damage lie between that sensor and the sensor preceding it. This method requires closely localised sensory arrangements to be effective with current techniques making it slow and costly.

It may be possible to employ this technique in a more effective way by using it in cognition with a different transformation process. Research using the Hilbert-Huang technique of transformation has demonstrated the possibility of finding damage location based on a moving force generator, with known location related to time, with only one data acquisition node. The known force creation device, such as a car driving across a bridge monitored by one sensor location, is one such example of how this technique could be applied (Roveri and Carcaterra 2012). This works as the Hilbert-Huang transformation allows the user to analysis nonlinear and non-stationary signals. If the force creating apparatus moves the signal can still be analysed and a change can be noticed depending on at what position the apparatus is when a change of signal behaviour occurs. This method is highly dependent on the range of the sensor and with increasing distance, noise is to be expected. Over larger distances more sensors would still be required in order to establish effective dynamic response sensing.

Once the response has been translated into data by sensory apparatus, processing and indexing the location and severity of damage can be conducted. Indexing the damage severity can be done in a number of ways and is dependent on the dynamic or non-dynamical method chosen for damage detection. As only dynamic methods are to be considered in this research, they will be solely discussed.

2.7 Signal Transformation Method

Methods for signal transformation, also known as signal processing, are the possible ways of interpreting the results received by the data acquisition system. They work by converting the mechanical vibratory displacement signal into a series of fundamental signals used creating a series frequency dependant functions and possibly time-frequency dependant. These signals are more easily analysed for changes in behaviour once separated.

2.7.1 Fast Fourier Transformation

The fast Fourier transform (FFT) is a Fourier transformation with discrete boundaries which reduces the computations needed for N number of points from $2N^2$ to $2N * \log_2 N$ (Weisstein 2015). The FFT is used to convert a signal from its original domain, typically being time or space, into the frequency domain and can be used inversely to retrieve the original domain (Reddy 2000).

This transformation method proves problematic when the waveform deviates from sinusoidal and is for analysing stationary data. In typical structural health monitoring situations sinusoidal and stationary vibratory response may not be a practical or achievable outcome. While given that in the controlled circumstances of experiments this may be met, the purpose of this project is to optimise methods capable of practical application therefore this method was deemed inappropriate for the scope of this project.

2.7.2 Short-Time Fourier Transformation

The short-time Fourier transform (STFT) is a computationally simple method of estimating sinusoidal frequency and phase content of local sections of a signal. To compute the STFT a signal is divided into smaller sections that can then be separately analysed by use of the Fourier transform. A Fourier spectrum is then constructed out of the segments which can be plot as a function of time (Griffin and Lim 1984).

Equation 4: Short-time Fourier transformation (Barnhart 2011)

$$STFT(\omega, t) = \frac{1}{2\pi} \int_{-\infty}^{\infty} f(t)h(t - \tau)e^{-i\omega\tau} d\tau$$

Where: *STFT* is the short-time Fourier transformation (Hz)

h is the window function

t is the global time value (s)

τ is the local time value (s)

ω is frequency (rad/s)

This approach is typically optimised by use of the continuous-time STFT. This requires that the function is then multiplied by a window function, which performs a similar function to that of dividing the signal into smaller sections, however it operates on a continually repetitive basis. The Fourier transform is then taken as the window function continually isolates segments of the signal. The results from such an operation can then be used to construct a two-dimensional (time and frequency) representation of the data (Allen and Rabiner 1977).

There is considerable error introduced by the window function's refresh frequency. Many techniques using similar repetitive application methods similar to the window function all suffer from the same accumulative error (Kadambe and Boudreaux-Bartels 1992).

2.7.3 Wavelet Shape Matching

The method of wavelet shape matching involves measuring the similarity between the physical shapes of a signal and matching an appropriately shaped function to these reoccurring shapes (Veltkamp and Hagedoorn 2001). These functions are usually derived by computational analysis with regards to period,

frequency and amplitude, but with particular attention paid to the application of peak detection algorithms (Du, Kibbe et al. 2006). For such algorithms to function effectively, signals are typically subject to operations known as smoothing and baseline correction. This causes the shape of the signal function to substantially change in the case of complex signal responses (Belongie, Malik et al. 2002). Most peak detection algorithms simply identify peaks and amplitude while ignoring any additional information present in the signal. Belongie et al. (2002) produced a continuous wavelet transform based peak detection algorithm that identifies peaks at different scales and amplitudes (Belongie, Malik et al. 2002). While this innovative technique greatly increased the robustness of peak detection under a variety of conditions, the error introduced by the shape matching factor still proves to be of considerable magnitude. This technique becomes more effective as the signal approaches one of the shape of one of following waveforms:

1. **Sine waveform** – The sine waveform is the most common of all the electrical waveforms as it is the function explaining the behaviour of alternating current (AC). This is used for AC mains which is the form that current is transferred over distances (Storr 2015).

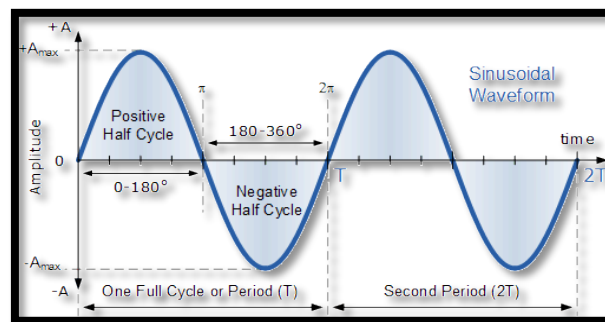


Figure 13: Sinusoidal waveforms (Storr 2015)

2. **Square-wave waveform** – These waveforms are used extensively in electronics for timing and control signals. These symmetrical square waveforms are of equal duration, each representing each half of a cycle and used in nearly all digital input and output logic gates.

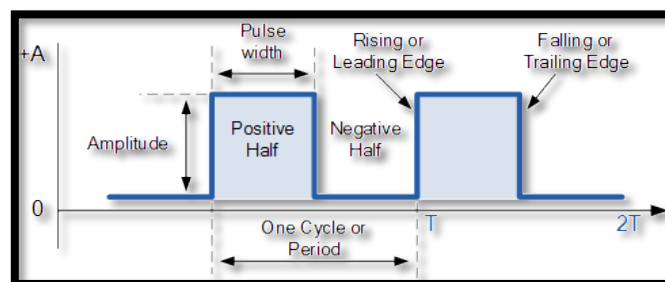


Figure 14: Square waveforms (Storr 2015)

There is a similar waveform to the square waveform known as a rectangular waveform which follows similar shape patterns but does not pertain to the symmetrical behaviour of the square wave.

3. **Triangular waveforms** – Triangular waveforms are bi-directional waveforms that oscillate between positive and negative peak values. Generally, the positive slopes and negative slopes have the same cycle time giving each triangle a 50% duty cycle. Triangle wave forms can also be used in an unsymmetrical form known as sawtooth waveforms. Saw-toothed waveform properties make them highly applicable to harmonics and is the wave form aimed to be produced in music synthesis.

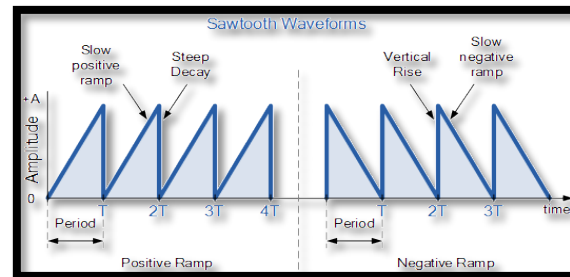


Figure 15: Triangular sawtooth waveforms (Storr 2015)

4. **Triggers or pulses** - The only difference between these two waveforms is that triggers can be positive or negative while pulses are only positive. Pulses and triggers are typically used to trigger something to begin such as an electromechanical system or event.

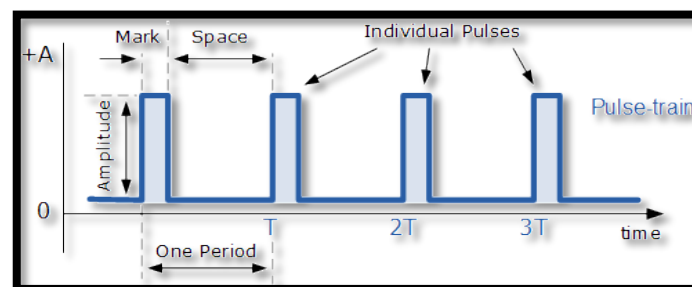


Figure 16: Pulse waveforms (Storr 2015)

This technique is highly sensitive to the amount of smoothing and baseline correction that the original signal is subject to and therefore introduces a great deal of error when analysing complex signal such as dynamic response of materials (Du, Kibbe et al. 2006). Even considering the optimisation conducted by Belongie et al. (2002) this method was deemed not accurate enough for application to the complex signal of fibre composite's dynamic behaviour.

2.7.4 Hilbert-Huang Transformation

Most transformations require that the time domain and the frequency domain be analysed separately or that the information for both is computed by a sliding window analysis of some sort. If a regular transformation is used, the information being analysed in the time domain lacks the frequency based resolution while if the signal is then transformed the frequency is known but no longer corresponds to any particular time. In the case of a sliding window function, the signal can be analysed in small sections. These sections can be reassembled in order giving the frequency in each window to an

accuracy of the time span of the window (Donnelly 2006). One other method used to analyse a signal with regards to frequency and time, is by employing pre-defined functions to match portions of the signal. This technique proves insufficient as the complexity of the response increases. This leaves the method in question. The largest advantage of the HHT over previously discussed methods is that the *Hilbert-Huang transformation* (HHT) (Huang, Shen et al. 1998) represent data in both the time and frequency domain simultaneously without a great burden on computational processing capabilities. The simplicity and robustness of the HHT are the main advantages of the technique but there are still sources of error inherent to this technique that will be discussed in detail further in this section.

After the Hilbert transform has been computed the arc tan of the real part divided by the complex part yields the phase. Unwrapping the phase causes the signal to increase monotonically. Finally the frequency is found as the derivative of the phase divided by 2π and the amplitude is determined as the vector magnitude of the real and complex components. The arithmetic pertaining to the discussed method can vary therefore only the most pertinent equation forms have been included. These equations after selection can be found in section 3.4.

By use of the HHT, the instantaneous change in frequency, or frequency response data is used to analyse structural damage and location to a high degree of accuracy depending on the influence of noise (Roveri and Carcaterra 2012). The use of this processing technique can also remove the requirement for prior knowledge regarding dynamic response of the beam and reduces the number of data acquisition points to one assuming within reasonable distance of the damage location and that the source of the dynamic signal is non-stationary (Roveri and Carcaterra 2012). The HHT method is more accurately known as a combination of two fundamental mathematical formulations, which includes the *empirical mode decomposition* (EMD) and the *Hilbert Spectral analysis* (Huang, Shen et al. 1998). The Hilbert spectral analysis can also be broken down into sub-fundamental mathematical formulations as it performs a spectral analysis of the signal using the Hilbert Transform followed by an instantaneous frequency computation.

The empirical mode decomposition

The function of the EMD is to identify proper time scales that reveal elements representing the physical characteristics of a signal. These elements are intrinsic to the signal function which are referred to as *Intrinsic Mode Functions* (IMF) (Huang, Shen et al. 1998, Zhang, Price et al. 2008). These IMFs must satisfy the two following basic conditions:

1. In the whole dataset of an IMF, the number of extrema and zero crossings must be equal or differ by at most one.
2. Secondly, at any point, the mean value of the envelope defined by maxima points and the mean value of the envelope defined by the minima points is equal to zero (Zhang, Price et al. 2008).

The EMD is an iteratively applied process that is continued until the above criteria are met. Suppose it is used to decompose the signal in the figure below.

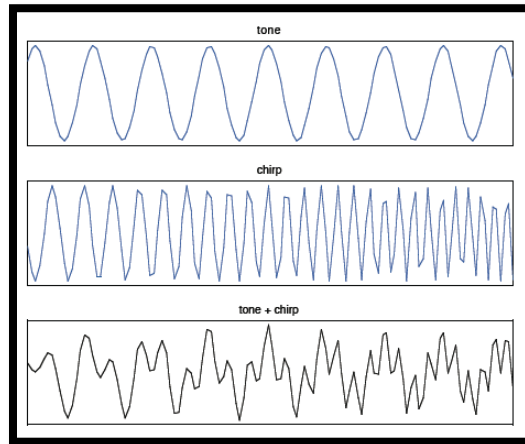


Figure 17: Original signal to be analysed (UC-San_Diego 2014)

The tone and the chirp make for a signal more complex than a simple sin wave. This prevents analysis by means of conventional arithmetic. Using a cubic spline, the maxima and minima can be interpolated creating what is known as *envelopes*. The mean value between these envelopes will follow a progression between these peaks resembling a low frequency component of the signal. The positive, negative and mean interpolations are displayed in the following figures as the red, blue and purple lines respectively.

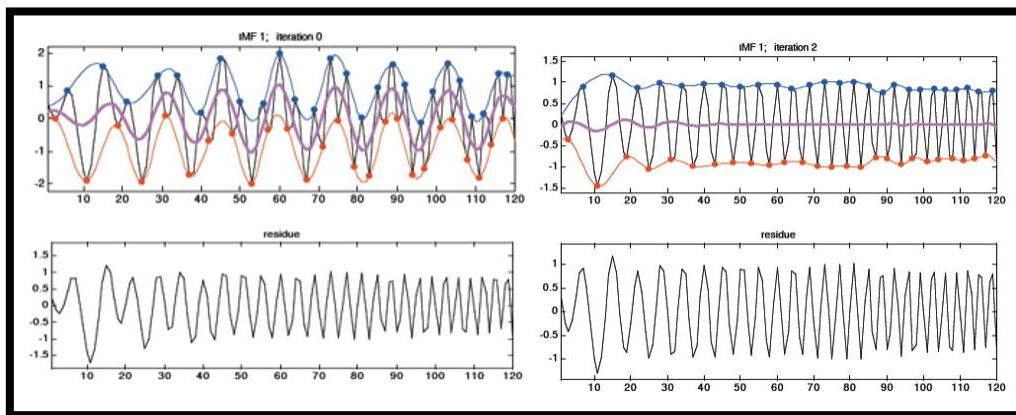


Figure 18: IMF 1, Iteration 0 and 2 displaying residue (UC-San_Diego 2014)

The signal represented by the mean can then be subtracted from the signal which leads to the flattening of the signal (Huang, Shen et al. 1998). This processes of interpolation and mean signal calculation and subtraction is performed iteratively and is commonly referred to as *sifting* as it resembles sifting contents in a pan to reveal the desired object. Sifting continues until the remaining signal is of zero mean. This result is then deemed an IMF. The IMF is subtracted from the original signal and the newly acquired signal is then decomposed again. This results in the signal being represented by its highest to lowest frequency contents separately. The EMD continues extracting IMFs until the stopping criteria is met. According to the literature, there are a number of suitable stopping criteria which include the following.

1. The absolute amplitude of the remaining signal is close to zero
2. The mean value of the envelope is close to zero
3. The cross-correlation coefficient between remaining signal and original signal is appropriate
4. The standard deviation (SD) between two consecutive results in the sifting is appropriately low. Process Experiments conducted by Zhang et al. (2008) show that reasonable values for the SD are between 0.25 and 0.3 for a stopping criteria.
5. Finally, the main stopping criteria is if the original signal has become monocomponent (only one extrema).

(Huang, Shen et al. 1999, Xu and Chen 2004, Yang, Lei et al. 2004, Zhang, Price et al. 2008)

The result of the EMD is that these IMFs are sums of zero-mean AM-FM modulated signal components (Rilling, Flandrin et al. 2003). This technique has been applied with a great deal of success in a number of areas of research including climate data analysis specifically analysis of the Pacific Decadal Oscillation, vibration response, cardiovascular behaviour and other rhythmic biological processes, stratospheric solar cycle analysis, digital signal processing and many more (Wu, Schnieder et al. 2001, Coughlin and Tung 2004, Flandrin, Rilling et al. 2004, Neto, Custaud et al. 2004). The following figures display the physical process that is the EMD through the example of a sample signal.

Although this algorithm has proved remarkably effective and widely applicable, it does still incur some degree of error tied with some of the assumptions needed. As such, optimisation has become an area of development (Rato, Ortigueira et al. 2008). The EMD algorithm depends on a number of options regarding to the application of the users intention. A basic operation of the EMD, as previously discussed, is the estimation of upper and lower envelopes as interpolated curves between extrema. Literature suggests that cubic splines are to be preferred for the interpolation method (Huang, Shen et al. 1998, Rilling, Flandrin et al. 2003). This interpolation is one of the sources of error even though other spline interpolation forms such as linear or polynomial consistently yield less accurate results. Another source of error is that the EMD operates on discrete time signals. This can cause the extrema to be hard to identify. The time interval must correspond to correctly identify the necessary extrema of the signal. In practice this source of error can be overcome by oversampling which thereby increases the time and computational power required to complete the analysis. Finally the third issue discussed in the literature is related to the established boundary conditions. As the EMD has finite observation lengths, error can be introduced and iteratively increase as it is reapplied to a signal if the boundary conditions are not correctly applied (Rilling, Flandrin et al. 2003).

Hilbert spectral analysis

The second stage of the HHT involves a spectral analysis. Once the necessary number of IMFs have been obtained, these can be subjected to a *discrete Fourier transform* yielding both real and imaginary

coefficients. These coefficients are necessary for then applying the Hilbert transform to the data. In a similar fashion the Hilbert transform yields a real and imaginary part corresponding to the IMF and its complex transform respectively. Instantaneous amplitude is expressed as the amplitude of the complex number while the instantaneous angular frequency is the derivative of the unwrapped phase. These act as the coefficients that are then used in using the *Hilbert transform*. The Hilbert transform produces the convolution of the IMF which emphasises the local properties of the signal preserving the local time structure of the signals amplitude and frequency (Huang, Shen et al. 1998, Huang and Shen 2005, Donnelly 2006). The phase can be calculated from the complex number and can then be unwrapped becoming a monotonic function. The frequency is determined through a phase derivative and the amplitude is determined using Pythagoras theorem.

In summation the main sources for error in this method have been identified as inherent miscalculations from the algorithm, incorrect stopping criterion, and the error introduced by the use of the mean envelope application (Rilling, Flandrin et al. 2003, Qin and Zhong 2006). Bearing these areas of error in mind, in almost all cases this method yields substantially less error than other transform methods. With the added advantage of maintaining both time and frequency resolution this method seems most desirable. However, there have been a number of flaws pointed out with regards to the HHT due to some drawbacks tied with some of the assumptions needed to implement the algorithm. Specifics pertaining to the arithmetic employed in this research project or of the HHT can be found in section 3.4

2.8 Signal processing

There are a number of variables that need to be considered to maintain empirical procedures in the entailed experiments. One such variable, the method of signal production, can substantially alter the type of data acquired and required to complete calculations while also altering the entire experimental method. This section also describes the methods for sampling and filtering to ensure that the signal being used is returning the necessary data with practical applications.

2.8.1 Signal production

In order to see how a material responds to vibration, the vibration must first be generated. There are two methods available for vibration generation which involve two different tools. A solenoidal shaker can be used which gives the benefit of greater control over force and frequency, or an impact hammer can be used. A solenoidal shaker can be mounted to the beam which when subject to a current, a vibratory load can be produced. In order to produce a reliable output frequency of vibration, an accurate input frequency must be applied. When using the impact hammer, the input force and output signal will be effected by human error as the same force cannot be produced accurately every repetition. However, the impact hammer is equipped with a force transducer that is rugged enough to withstand damage from

striking. This allows the force produced by the hammer to be recorded and included in the analysis of the signal.

The advantages of the solenoid also come with disadvantages. The solenoid also requires that a mounting apparatus be manufactured. This mounting apparatus must rigidly connect the solenoid to the beam so that the vibration produced by the oscillating force produced within the solenoid can be directly transferred into the beam. However, due to the large weight of the solenoid and the mounting device it requires, a great deal of error can be introduced by this secondary mass. As the dynamic response of an object is greatly affected by the mass and geometry of the object, the inclusion of this apparatus can greatly affect the results expected from the experiment, especially if the test member is light. The test member used in this project is in fact light with comparison to the weight of the shaker.

Another factor involved in the use of a shaker is its need for extra components for function. The solenoid would require the addition of a signal amplifier and signal generator. A signal generator is a device that simulates and creates a signal of the chosen frequency, waveform and sequence. This device however produces standalone very weak amplitudes. A signal amplifier would also be required to increase the power of the faint signal generated by the signal generator. It works by receiving power from an external power supply and then controlling the output to match the input signal shape but with a much larger amplitude.

For the reasons discussed above and to reduce the scope and complexity of the force creation procedure, it was decided that the force hammer would be most appropriately used. The main disadvantage of the force hammer, as mentioned earlier, is that it cannot produce a constant controlled force. However this disadvantage can be accounted for in the calculations that follow the procedure (PCB 2009). Another advantage of the impact hammer is that what is described as “a perfect impact” can be made. While the hammer does not truly produce a perfect impact, it’s strike does approach an infinitely small excitation duration which causes a constant amplitude response exciting all modes of vibration with equal energy (Champoux, Cotoni et al. 2003). For these reasons it was deemed necessary to use the instrumented impact hammer for force creation in the experiments.

2.8.2 Input Frequency

One of the factors that dynamic response tests are highly effected by is the frequency at which they are testing. There are three phenomena for consideration with regards to the frequency of vibration to be considered. The first being that when entering the higher natural frequencies of an object a greater amount of energy is required to produce the response. By attempting to keep the energy requirement low, one can keep the cost of components low thereby abiding by the attempt to reduce the cost of these methods. If less energy is required, smaller and cheaper oscillating force components can be used to

complete experiments. The second phenomena is the existence of modes, and the increase in the number of mode shapes as the frequency of oscillation increases. A larger number of mode shapes means there is a better chance of placing sensors above a stationary point which will fault the results to be expected. The final phenomena being that a frequency should be catered to the damage to be expected. As different shapes and severities of damage will respond differently to different bandwidth of vibration, varied frequencies may be necessary to illicit a readable response.

As the impact hammer was chosen for this experiment the input frequency will be dependent on the material and not regulated by the force creation device. When the beam is struck by the impact hammer, the impulse will create a signal in a number of frequencies expected to predominately be the modes of vibration of the beam. These expected frequencies are then those that are to be isolated by the filter mechanism as to reduce the error introduced by noise.

2.8.3 Filtering

Filtering is the processes of reducing the contributions of the environment to the signal data. Noise is substantially less influential in lab condition experiments conducted when compared to that expected in industrial environments. Noise is typically the result of peripheral components and any dynamic behaviour they are subject to as a result of their environment (Jones, Hamilton et al. 2002). Another major source of noise is the ambient noise generated by the sensory components themselves.

One method commonly used to remove noise from a signal is the high and low pass filter method. These methods involving removing a frequency response outside the expected limit of the expected frequency. For example, a high pass filter could be used to remove the contribution of ambient white noise from a sound recording device or the high pitch sound from a current travelling through a transformer. If only the signal of a person speaking was pertinent to the observer, one could perform a high pass filter to remove the high pitch tone experienced from a noise contributing transformer. It is important to remove the noise where possible before performing integration as the noise will be compounded with the information and will no longer be able to be differentiated from the signal itself.

As this research uses the empirical mode decomposition, it is possible to observe and discuss the necessary filter of signal responses by judging the returned IMF's. If an IMF is outside the expected frequency response, its origin can be discussed and if the source of the unexpected frequency response can be determined it may be necessary and empirically accurate to remove the IMF from the data set. It is also possible to set forth a criteria of the expected frequency bandwidths which all else can be numerically discarded in the signal processing stages. This however will not be used as it removes the possibility of anomaly discussion.

2.8.4 Sampling Rate

The sampling rate is the frequency in which samples are taken and therefore is a critical factor to consider for this experiment. If the sample rate is too low, the data acquired may not correctly represent the behaviour of the response. If the sample rate is too high, unnecessary numerical work will be taken. As the application for industrial purposes is a consideration, if an unnecessarily high sampling rate is chosen, the method may become completely impractical for real world use. For example, if the numerical processing time is two days, the results may be outside the limit of investigation and if the test has been conducted with some error the procedure must be completed again. This offers a great deal of impracticalities (Nise 2011).

Outlined in computer controlled systems is the standard criteria for signal processing with regards to sampling. It details the limits for which distortion occurs. According to Nise (2011) the sampling rate must be at least twice the bandwidth of the signal, or else distortion will occur (Nise 2011).

Chapter 3| Project Specifics

The purpose of this chapter is to outline the methods chosen based on the reviewed literature. It includes the resources required to complete all stages of the project with regards to both software and hardware. It also explains the dynamic response method selected and how it relates to the objects being tested.

3.1 Chosen Apparatus

The experiments required a small system of sensory apparatus, data acquisition hardware, a computer, and some secondary tools. As such, for the purpose of those whom of which may wish to recreate these experiments, the components of the experiments are briefly discussed including their relation to the experimental system. The following is a list of items used to perform the experiments.

- Glass fibre pultruded composite square hollow section beams
- Accelerometers
- Force hammer
- One LMS VB8 data acquisition system
- Stands

There were additional applicable apparatus and systems reviewed and considered that can be found outlined in the literature review and viewed in Appendix E.

3.1.1 Glass fibre pultruded composite square hollow section beam

The glass fibre pultrusion was luckily readily available in the correct dimensions after various demonstrations performed by the fibre composites centre. These beams are 50mmx50mmx5mm and the material properties are tabulated below.

Table of material properties

An important property of this material is its tendency to critically fail without showing visible signs of damage. Therefore advanced structural health testing procedures, such as the dynamic testing method of this project are desired.

3.1.2 Accelerometers

When deciding on sensory apparatus there were two applicable and readily available devices that could be used at USQ. These were accelerometers and FBG sensors. As outlined in Section 2.4, accelerometers are both simpler to use and yield more accurate results with respect to modal analysis applications. For this reason the sensory equipment chosen for dynamic response data acquisition were accelerometers.



Figure 19: USQ supplied accelerometer used for the experiments

USQ had only one applicable accelerometer available, therefore no further sensory equipment had to be purchased in order to conduct the necessary experiments. However, having only one accelerometer meant that the testing phases needed to be completed through iterative strategies in order to acquire the complete and necessary data. Distance from the force creation device and distance from the damage location were two variables considered in the research with regards to sensor application, which could not be demonstrated effectively with only one iteration and one accelerometer. After completing the multiple testing iterations the beam conditions could be changed with regards to damage or sensor location and the experiments could then be repeated.

The accelerometer used for the experiments is a cubic 10mm robust device used to record g-force reactions in only one direction within a range of $0 \pm 5000g$ which was well within the expected limits of the experiments. The accelerometer was orientated such that the axis in which acceleration could be monitored was normal to the surface of the beam.

3.1.3 Force hammer

While the Solenoidal shaker was most desirable for the experiments, the apparatus used to mount the device to a beam was made for a larger beam specimen. As this research was largely focused on investigating the practicality of new and innovative transformation methods available, the manufacture of a new mounting device was deemed an unnecessary task for the scope of the project. Instead the use of a force hammer, also known as an impact hammer, was employed. Instrumented force hammers include a rugged force sensor that is integrated with the hammer's striking surface (PCB 2009).



Figure 20: USQ supplied instrumented force hammer

While a force hammer does not have the ability for modulated constant force similar to a solenoidal shaker, the integrated force sensor allows the user to include the force data into the data analysis. The researcher was able to use reasonably similar force in each iteration to reduce the variation in force data, however, human error is unavoidable while using such a device. As the force data can be included in the numerical stiffness analysis mitigates the problem of such human errors.

3.1.4 LMS VB8 data acquisition system

The LMS VB8 data acquisition system is a product designed and manufactured by Siemens Inc. PLM and LMS testing solutions (Siemens 2015). The system is necessary in translating the physical response of the sensory apparatus into data sets usable in numerical analysis. The software packages associated with the LMS VB8 data acquisition system was used in conjunction with its software package which allowed the results of the numerical analysis to be verified as the system has inbuilt signal analysis capabilities that perform the fast Fourier transformation. This will be discussed further in the chosen software section.



Figure 21: LMS VB8 data acquisition system

The researcher experienced problems in using this device as it was damaged and experiencing technical difficulties to do with charging, however, apart from this the system was very effective and simple to use in acquiring the necessary data. The serial number of the data acquisition apparatus was the LMS SCM05 Serial 46080207. This unit allowed the processing of up to 16 sensors at one time and had the capability to boost these signals individually as it has an internal amplification unit. The amplification unit reduced the effect of noise on the signal. The experiments only required the use of two sensors ports only. These were connected to the accelerometer and the impact hammer.

3.1.5 Stands

In order to test the dynamic response effectively, the peripheral damping needed to be minimised. To achieve this the test beam needed to be suspended off the ground as the ground would be a major source of damping. By placing the stands at 0.8m from each other the beam could be simply supported at each end with 0.1m of the beam on each stand. The stands are made from heavy steel and can be adjusted for different heights by the twist adjustment tops.



Figure 22: USQ supplied stands used to support beam during experiments

3.2 Chosen Software

Similarly to the instance of the hardware, software played an essential role in the development of this project. It was used for a number of tasks including gaining access to the necessary literature, developing a report, acquisition of experimental results, the analysis of said results, and the tabulation and demonstration of results. This section outlines the software involved in such tasks and the method in which they were used to develop this project.

- Matlab
- Microsoft Office
- LMS SCADAS Test.Xpress Software
- Creo Parametric 3.0

Much like the chosen hardware, the researcher was fortunate enough to source all these resources at USQ incurring no cost on behalf of the researcher

3.2.1 Matlab

Matlab is described by its makers as a high level language used by scientists and engineers to visualise ideas relating to signal and image processing, communications, control systems and computational finance (Mathworks 2015). It was used by the researchers to perform a series of tasks requiring numerical brute force. Screenshots of the Matlab code can be found in Appendix C. The code to perform the double Simpson's integration, the HHT, the assembly of a global stiffness matrix, and the calculation of the finite differences are all separated into separate appendix sections, however, the code was compiled into one so that only one step was involved in data analysis which returned all the pertinent results, tabulated them in the command window and displayed all necessary plots.

3.2.2 Microsoft office

The Microsoft Office package was used to type the report, create all property tables and to tabulate the results produced from the Matlab code. Microsoft PowerPoint. Microsoft Project was used to develop an estimated timeframe for the research proposal and preliminary report.

3.2.3 LMS SCADAS Test.Xpress Software

LMS SCADAS Test.Xpress Software is the software facet of Siemens LMS product lifecycle management (PLM) tool (Siemens 2015). The LMS software is used in conjunction with the LMS VB8 data acquisition system, providing it with a friendly user interface and easy or automated calibration tools. The software made the experiments time efficient, the data easy to display, tabulate and even, to a limited extent, process. It was pertinent to translating the physical acceleration behaviour experienced by the sensory apparatus and the force data experienced by the force hammers integrated force transducer into data plots usable by the researcher in numerical analysis software. The LMS Express vibration signal processing software was available on the P2 laboratory computer.

3.2.4 Creo Parametric 3.0

The final software package used by the researcher was Creo Parametric 3.0. This program is typically used for finite element analysis, however, for this project it was used for the purpose of making part drawings as it is an easy to use piece of software that produces well-presented images. The drawings produced are as follows:

- Glass fibre resin reinforced pultruded SHS beam
- Single axis piezoelectric accelerometer

These drawings can be found in Appendix B giving the reader a clear image of dimensions of the apparatus that was used in this project.

3.3 Dynamic Response Method Selection Criteria

An extensive review of the literature relating to dynamic response health monitoring was completed in order to establish a method practical to achieving the aims of this project. After a broad review it was found that while great promise to dynamic methods of health monitoring had been expected and good lab results had been produced, effective industry application was limited by a number of factors. These factors typically were the following:

- Low economic feasibility
- Highly effected by typical noise interference
- High levels of error from traditional signal processing techniques
- Requires a great deal of time for apparatus set up and data processing
- Requires specialist technicians or engineers to interpret test results

Development of dynamic methods of monitoring structural health remains the focus of this research task because of the inability of non-dynamic methods to be effectively applied to fibre composites. So the interest of the research became to optimise dynamic response techniques with regards to their

weaknesses expressed above. The methods chosen and the proposed adaption to these factors are discussed in more depth in Chapter 4.

3.4 Arithmetic Specifics

All arithmetic was conducted using Matlab. By completing the arithmetic on Matlab, the time taken to complete iterations of the simple arithmetic was greatly reduced to the benefit of the researcher and to those whom of which should choose to use these methods, or code directly, to repeat similar investigations in the future. It was essential to the application of the HHT due to the numerical software's brute force in iterative analysis. Finally it serves to possibly be a foundation for a user friendly tool utilising these numerical and dynamic analysis methods for anyone to monitor a structures health with ease and little cost.

There are a number of available variations of the mathematical concepts used, however, these in specific were chosen for the purpose of these experiments. The function, relation and justification of using these specific formulations is discussed.

3.4.1 Method of Integration

As previously discussed the chosen method of integration is the Simpson's method. The data acquired from experiments is in the form of acceleration which will need to be converted to deflection prior to the use of signal processing techniques. The researcher used the Simpson's rule to double integrate the acquired data which is represented below once again.

Equation 5: Refresh of Simpson's method of integration (Mathews and Fink 2004)

$$\int_a^b f(x)dx \approx \frac{b-a}{6} \left[f(a) + 4f\left(\frac{a+b}{2}\right) + f(b) \right]$$

This function was built as a function handle to be used in the Matlab code (Mathworks 2015). All Matlab codes can be found in appendix C.

3.4.2 Empirical Mode Decomposition

The EMD extracts information from the original signal reducing it into a number of functions of progressively decreasing frequency previously mentioned to be IMFs which when reassembled become to original signal. It works through a series of steps and operates using certain conditions. Let the signal being analysed be known as $x(t)$. The steps taken to perform the EMD are as follows.

- The original signal $x(t)$ has at each local section a series of minima and maxima. These will be used as points for interpolation. With regards to local consideration it is important to notice this will be the highest frequency contents therefore it is essential to first remove noise from the signal.

- Once an envelope has been created connecting the local extrema and encompassing the entire signal 'x(t)', assuming the criteria for the envelope has been met, the mean of these signal can be drawn. The criteria for envelopes are:
 - The number of maxima or minima must be equal to the number of zero crossings; or differ by no more than one
 - Error is introduced depending on factors such as sample rate, interpolation factors, local peak finding factors, signal complexity, etc.
- The mean of these envelopes can then be subtracted from x(t) possibly leaving an IMF. The process up until now can be seen in the figure below in example (a), the original signal, and example (b), the envelopes and mean. To be sure that what has been extracted is an IMF, the following criteria must be met:
 - Similar to envelopes only one extreme between zero crossings
 - Has a mean value of zero

The mean value of this signal is iteratively taken away until h meets the criteria for an IMF. This is represented in the expressions below. Once an IMF has been found it is subtracted from the original signal and the decomposition can be done again to find another IMF.

Equation 6: Expression of the sifting process (Huang, Shen et al. 1998)

$$X(t) - m_1 = h_1$$

- In the figure below the original signal was made from only 2 sinusoids, however, the processes can retrieve many. Examples (c) and (d) show the two intrinsic mode functions found.

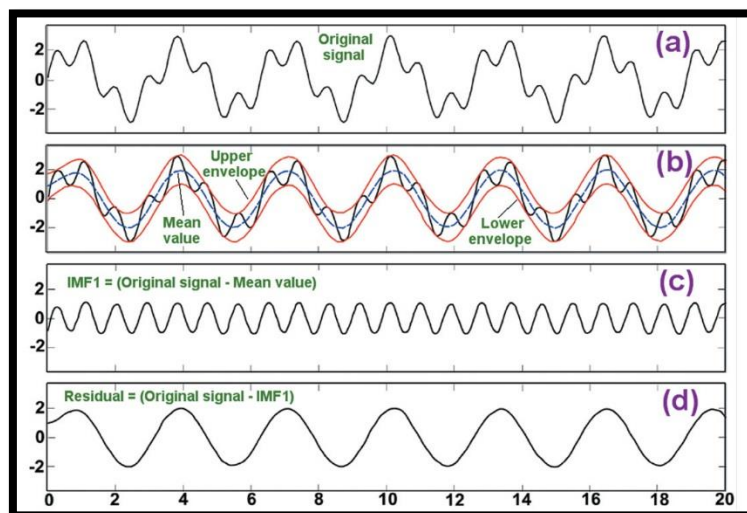


Figure 23: Graphical representation of the EMD process (Hassan 2005)

The IMFs can then be used to perform the Hilbert spectral analysis.

3.4.3 Hilbert Spectral Analysis

The Hilbert spectral analysis performs two functions under the guise of one heading. It performs both the Hilbert transformation followed by an instantaneous frequency computation. The Hilbert transformation produces a convolution of the original signal into real and imaginary parts. It is done so through the following expression:

Equation 7: Hilbert transformation (Huang, Shen et al. 1998)

$$H[h(t)] = \frac{1}{\pi} PV \left(\sum \int_{-\infty}^{\infty} \frac{h(t) dt}{t - h} \right)$$

Where PV is the Cauchy principal value and h is the IMF derived from the EMD. Using the complex 'iy' and real 'x' parts of this the rest of the necessary information can be found. The phase is found by:

Equation 8: Phase angle (Donnelly 2006)

$$\phi = \tan^{-1} \frac{y}{x}$$

It is then necessary to unwrap the phase making it a monotonically increasing function. The instantaneous frequency is calculated by taking the derivative of the phase times the inverse of 2π :

Equation 9: Instantaneous frequency (Donnelly 2006)

$$f = (2\pi)^{-1} \cdot \frac{d\phi}{dt}$$

Finally the amplitude is the magnitude of the real and complex parts:

Equation 10: Instantaneous amplitude (Donnelly 2006)

$$a = \sqrt{x^2 + y^2}$$

These calculations were used in the formulation of the Matlab code which can be found included in Appendix C.

Chapter 4| Experimental Process Methodology

This research task included a number of processes to achieve both the necessary level of safety and an empirically accurate conclusion. The literature reviewed was used to produce a practical method of analysis of the structural health of fibre composite beam structures using an equally practical dynamic response monitoring technique. This chapter explains in detail all processes undertaken by the researcher in order to complete the project as a whole with special focus on the experimental procedures undertaken as to ensure that the experiments can be reused, should someone wish to test similar or related phenomena. It also details the way in which the described resources and software were applied to the experiments and their role experimental process to ensure completeness of description.

The project as a whole involved a series of tasks essential to establishing empirical results. The tasks have been broken down into the most pertinent milestones and are outlined in the following points:

- Build Matlab code to perform double integration using Simpson's method of integration on the acceleration data acquired from experiments to convert it to displacement data
- Build Matlab code to perform the empirical mode decomposition and Hilbert spectral analysis on the displacement and time data acquired from experiments and integration
- Build Matlab code to perform finite difference comparison's on all final assembled stiffness matrices
- Perform dynamic response experiments on the undamaged glass pultrusion members acquiring the acceleration data
- Processing of the acceleration data using Matlab code and assembly of response into the stiffness matrices to verify the accuracy of the method by comparing the achieved mode shapes
- Perform iterative dynamic response experiments on the damaged glass pultrusion members acquiring the acceleration data for each iteration
- Processing of the acquired acceleration data sets using Matlab code to acquire displacement
- Process the experimental signal data using Matlab to acquire the time-frequency response of the beam and comparison between the numerically processed HHT response
- Plot and tabulate results to identify changes in response patterns

4.1 Experimental System Overview

The experiment can be considered a system with a number of distinguishable sub systems and interactions. To make the stages of the experiment easier to visualise the researcher has presented each stage in a systems analysis diagram which includes the data acquisition system, the numerical evaluation of acquired data, and the post processing tasks. These sub systems were then used to create a system consisting of three parts which were the following:

- Stage 1: Lab experiments
- Stage 2: Numerical analysis
- Stage 3: Post processing

The following diagram is an illustration on how each piece of apparatus and software is applied with relation to the systematic process of experimental investigation:

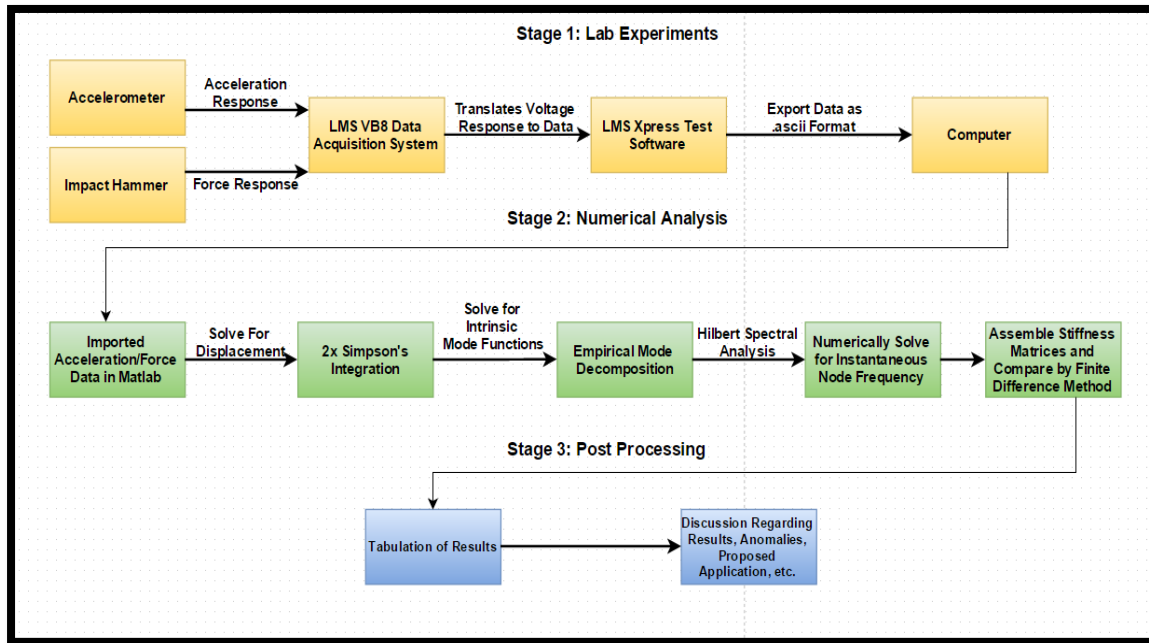


Figure 24: Experimental Process and System Overview Diagram

Tasks of Stage 1, 2, and 3 can be identified by the grey, green, and blue box colours respectively. This was the process reflects the actual steps taken to complete the research project.

4.2 Experimental Methodology

As the purpose of the experiment was to establish if damage could be detected using the apparatus and processing techniques outlined above, damage was introduced sequentially and testing was conducted between each interval. As discussed in section 3.6 damage was introduced as a 1mm wide cut at increasing depths removing a percentage of the active cross sectional area at the damage location. Two test beams were tested in which cuts were introduced in different locations. The

The procedure taken to complete the dynamic response testing was as follows:

1. The two stands placed with the support edges 0.8m apart as to leave 0.1m of the glass fibre resin reinforced pultruded SHS (beam) simply supported at each end

2. The beam is placed as to allocate 0.1m at each end as to be simply supported by the platform
3. An accelerometer was wired to communicate with the data acquisition system and then fixed to the beam by a small portion of bee wax at node 1
4. The impact hammer was then connected to the data acquisition system which is connected to the computer
5. LMS data acquisition software is then calibrated as necessary to record sensory response of impact hammer and accelerometer
6. The beam is then struck at the strike location inducing dynamic excitation
7. The data relating to the force, acceleration, time, and conditions are then saved for numerical analysis
8. The control variables are then changed firstly with regards to accelerometer distance from damage location and then by introducing damage
9. The data compiled from all experiments could then be analysed by numerical methods using the Matlab code produced
10. The results and anomalies were then analysed and discussed

4.3 Control variables

The control variables to be tested are the induced damage severity, distance between the sensor and the damage and excitation location and how the chosen transformations perform at identifying the damage. These objectives relate to establishing the effective application of the method in real world situations. The damage severity and sensory location are the control variables that are part of the experimental procedure.

4.3.1 Induced damage

Damage was introduced in intervals to the beam in a controlled way as to maintain a strict empirical method. Literature suggested a method of inducing damage relating to the cross sectional area at the damage location thereby changing the moment of inertia (Heaton 2011). Experiments by Heaton (2011) were conducted in such a way that the level of damage was measured by the percentage of cross-sectional area removed by a hacksaw. It was decided that this method would be adopted and a damage scale was produced specifically for the beam type being tested. The cross sectional area of this particular beam was calculated to be 900 squared millimetres using the following equation:

$$\otimes A = O \otimes -I \otimes$$

Figure 25: Cross-sectional area

$$\begin{aligned} \otimes A &= (50\text{mm})^2 - (40\text{mm})^2 \\ &= 900\text{mm}^2 = 0.0009\text{m}^2 \end{aligned}$$

Where: $\otimes A$ is the cross-sectional area of the actual beam (m^2)

$O \otimes$ is the cross-sectional area without the hollow section (m^2)

$I \otimes$ is the cross-sectional area of the hollow section (m^2)

This area was then used to calculate the necessary cut depths to achieve a practical damage introduction method. The following tabulation demonstrates the 6 stage damage scale to be implemented in the experiments.

Table 1: Damage introduction scale

Stage	Damage percentage (%)	Cross sectional area removed (mm^2)	Cut depth (mm)
1	0	0	0
2	15	135	2.7
3	30	270	7
4	45	405	20.5
5	60	540	34
6	75	675	40

4.3.2 Node spacing

The distance between nodes was a crucial variable as it was used to identify the range at which dynamic response testing could be considered effective. A greater effective range would mean that a greater area of material could be tested at once having the potential to substantially reduce testing time. The distance between nodes can be compared to the distance between nodes of a mesh when performing finite element analysis. Closely spaced nodes have a higher accuracy, however, greatly increase the time required in experiments and numerical analysis. If the nodes are spaced too far apart, the results will be less accurate and also run the risk of having incomplete data due to sensors being located on a zero deformation node. The advantage of greater distances between nodes is that experiments and numerical analysis will be performed faster. It may seem intuitive to then do tests with the closest reasonable distances between nodes, however, as outlined in section 1.2, one of the objectives of this research is to further the development of dynamic methods for real world applications.



Figure 26: USQ supplied marked composite beam with accelerometer fixed in place

Node spacings of 0.06m were used for the purpose of experiments with a total of 10 nodes distributed across the beam. As the beam was 1m long with 0.1m simply supported at each end, only 0.8m was deemed capable for testing. The noise expected from the nodes closer to the stands was also a factor to be considered. The force created in the beam upon being struck was expected to cause the beam vibrate against the stand causing a greater amount of noise.

4.3.3 Transformation performance comparison

The two chosen transformation methods for comparison are the fast Fourier transformation and the Hilbert-Huang transformation. The conditions in which they will be tested does not highlight the major advantage of the Hilbert-Huang transformation but will give an indication of the expected effectiveness of the method for dynamic response testing. The Hilbert-Huang is a desirable method for many reasons including the ability to monitor non-stationary signal sources, possibly reducing the number of required sensors to one, and the ability to maintain both the signal frequency and time resolution. The FFT was chosen as the comparison as it is the most commonly used transformation method for dynamic response applications. This became evident during the review of the dynamic response literature.

The HHT was performed using the Matlab code and was the primary focus of the project. Once the results of the HHT were produced they could immediately be compared to those results produced by the LMS Xpress test ware's inbuilt FFT capabilities. These two transformations are very different in nature therefore different filtering, sampling and analysis techniques must be employed.

Chapter 5| Discussion of Experimental Results

The results obtained involved a series of processes to acquire the necessary data. This chapter is discussed in two primary parts. Firstly the results from the process steps are discussed with reference to the numerical methods applied to achieve these results. This includes plots and comparisons. As there was a great deal of data obtained, 3 stages of damage and 3 nodes will be compared and discussed in this section. The second part of this section will include the primary results to be discussed. This section includes the results obtained from the EMD and from the completion of the full HHT as these methods are hypothesised to be applicable in mitigating the disadvantages commonly experienced in dynamics response methods for industrial applications.

5.1 Secondary Numerical Results

Results due to calibration, SI unit correction, data truncation, signal filtering, and data integration will be displayed and discussed in this section. As these are not primary results, data obtained from only one node during undamaged conditions will suffice in the explanation.

5.1.1 Raw data import and calibration

The first step after performing the experimental analysis was to import the data. Upon doing so it was found during initial numerical analysis that the sensory apparatus was not fully calibrated, therefore, it was necessary to correct the mean shifted data. As can be seen in the figure below, the accelerometer was accurately calibrated for. However, the researcher experienced difficulty in calibrating the LMS system with regards to the impact hammer. To fix this the mean force per signal was subtracted from the original signal. The raw data (red) was then shifted to a zero mean signal (blue).

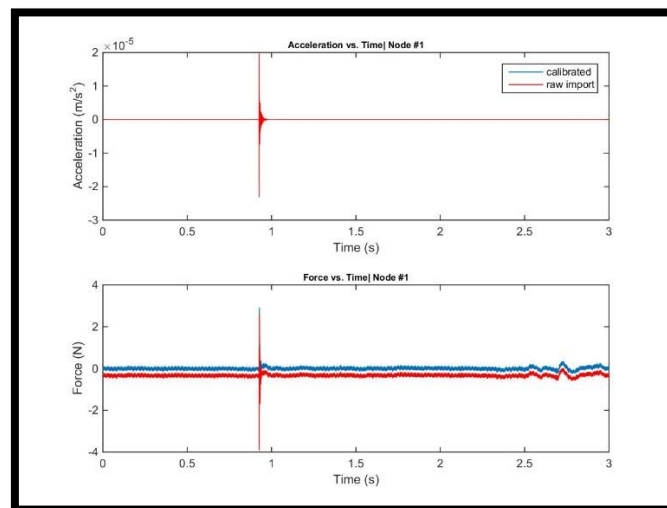


Figure 27: Raw imported data and calibration

5.1.2 SI unit conversion and data truncation

As the LMS system acquired acceleration in gravity it was first appropriate to convert the units to SI to avoid confusion. Next was to isolate the pertinent data. By observing figure 27 from the section above,

it can be easily seen that the majority of the data is not relevant. In order to reduce processing time the data was truncated to decrease the data to be analysed. This was completed by finding the maximum experienced acceleration and windowing a certain number of steps either side of this maximum value.

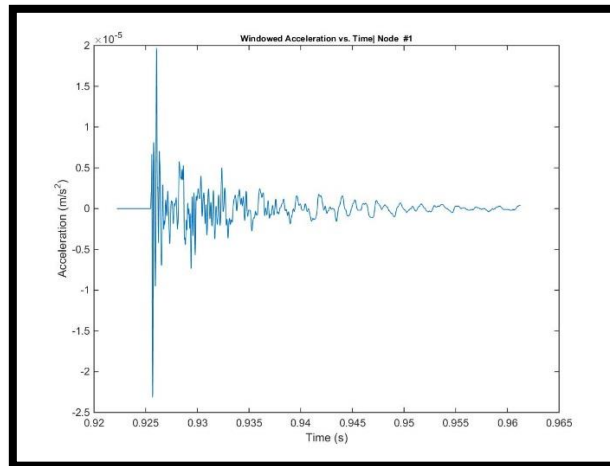


Figure 28: Truncated acceleration data

The number of data points in the acceleration signal was then reduced from 153600 to 2001 which greatly reduced the memory and time required in the analysis of this data. The figure above also shows how, for purely observational purposes, greater resolution is achieved from this process.

5.1.3 Signal filtering

According to the literature reviewed, noise was to be expected. For this purpose, both single and double pass filters were tested using the coefficients derived from a Butterworth filter analysis. It was found that the double pass filter caused a slight phase shift in the positive time direction. For this reason the single pass filter was employed to remove the high frequency noise.

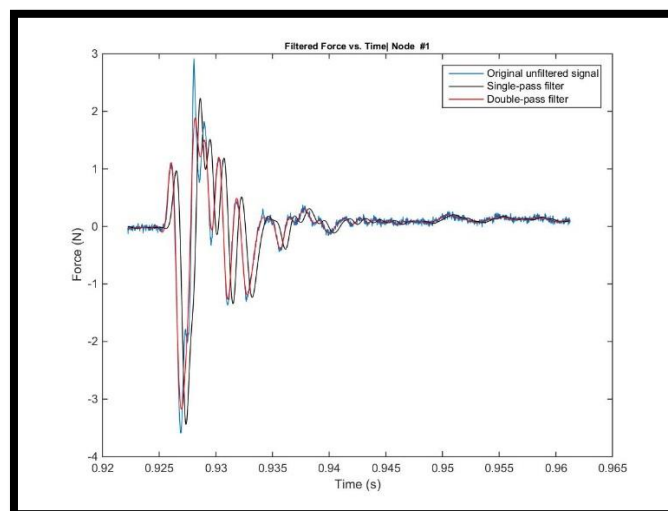


Figure 29: Single and double pass filter examples

5.1.4 Integration

Accelerometers were used in as sensory apparatus which acquires acceleration data. Before analysing the signal this needed to be integrated twice into deflection. The plotted results for both velocity and deflection are shown below.

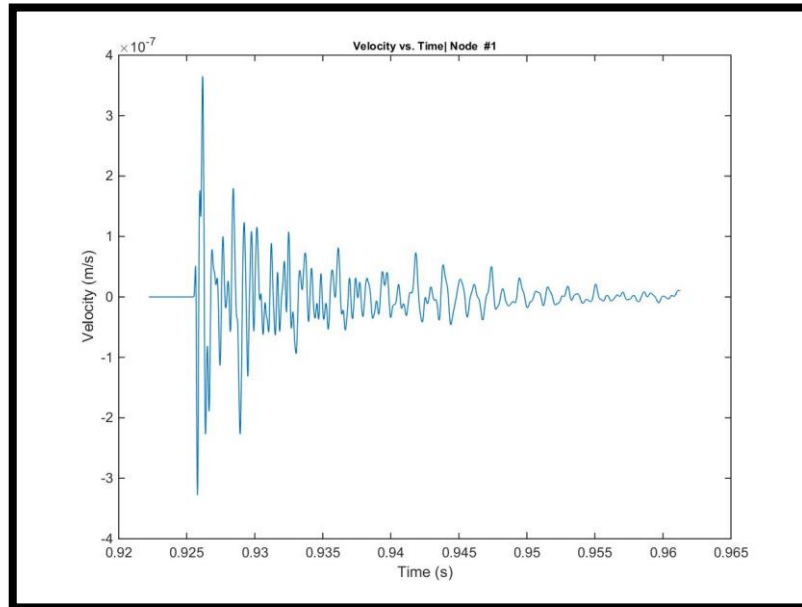


Figure 30: Velocity data

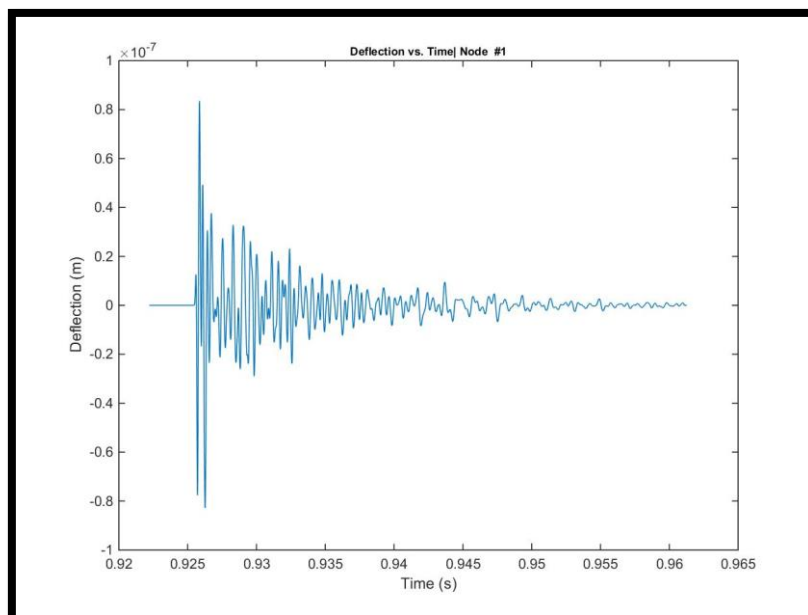


Figure 31: Deflection data

This is the final stage of the secondary results. Each of these stages was looped and repeated for each node and stage of damage.

5.2 Primary Numerical Results

As mentioned in previous chapters the EMD decomposes the signal into a series of signals of descending frequency known as IMFs. These IMFs somewhat resemble the separated natural modes of vibration. These are presented in this section to investigate the applicability they may offer in identifying crack severity as higher frequency are more sensitive to small changes in geometry. The second data set presented is the instantaneous-frequency and amplitude calculated with respect to time. Data from stages 1, 3, and 6 are presented in this section from nodes 1, 5, and 12. The order data is displayed is sorted by stage and each stage is sorted by node. All data analysed in this section is a 0.039062754 second recording.

5.2.1 Empirical mode decomposition

The EMD derives each signals inherent IMFs which is typically a step in a larger process, being the HHT. They have been presented for analysis in this section for the purpose of inspection and discussion with regards to the possibility of identifying damage using the IMFs.

IMF for Stage 1 - Node 1

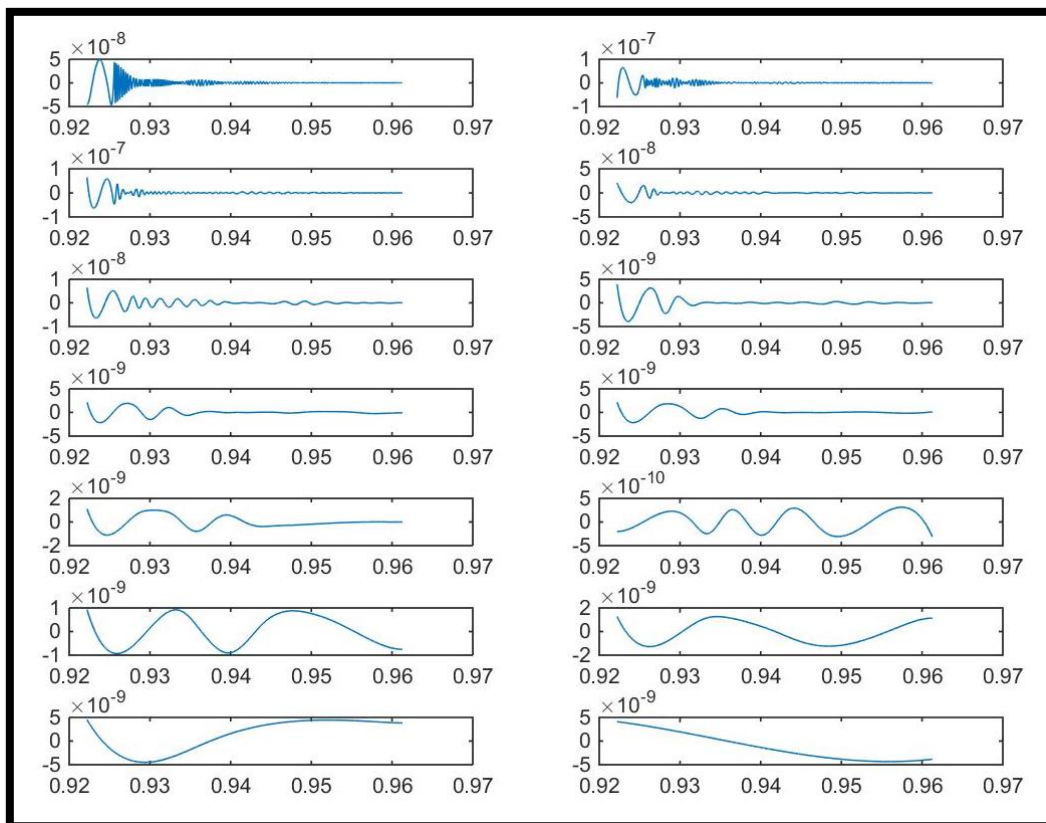


Figure 32: IMF stage 1, node 1

IMF for Stage 1 - Node 5

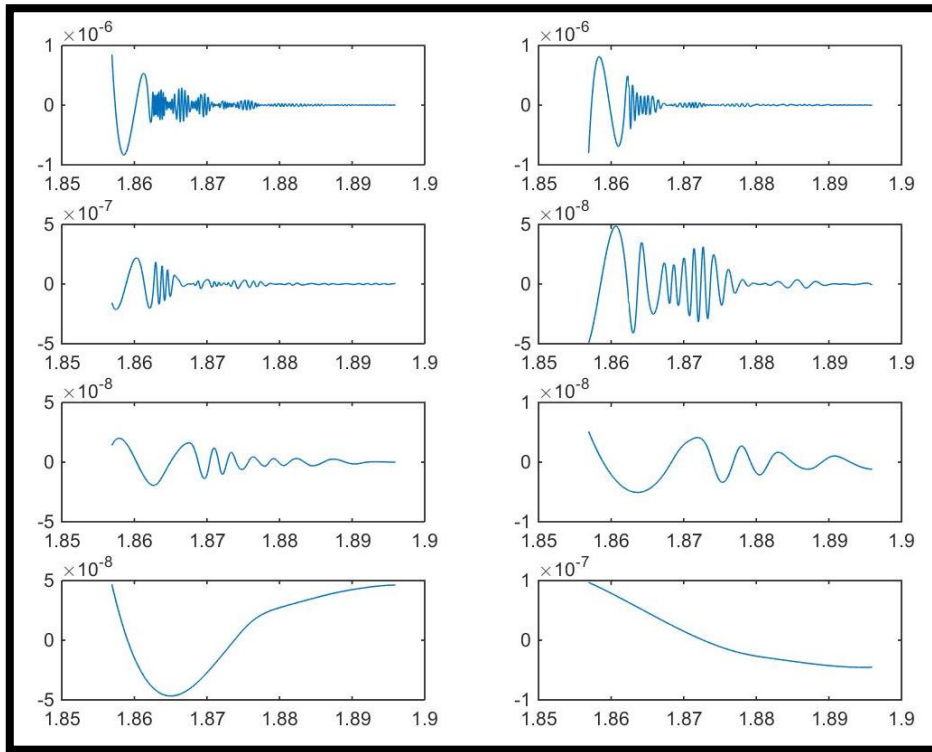


Figure 33: IMF stage 1, node 5

IMF for Stage 1 - Node 12

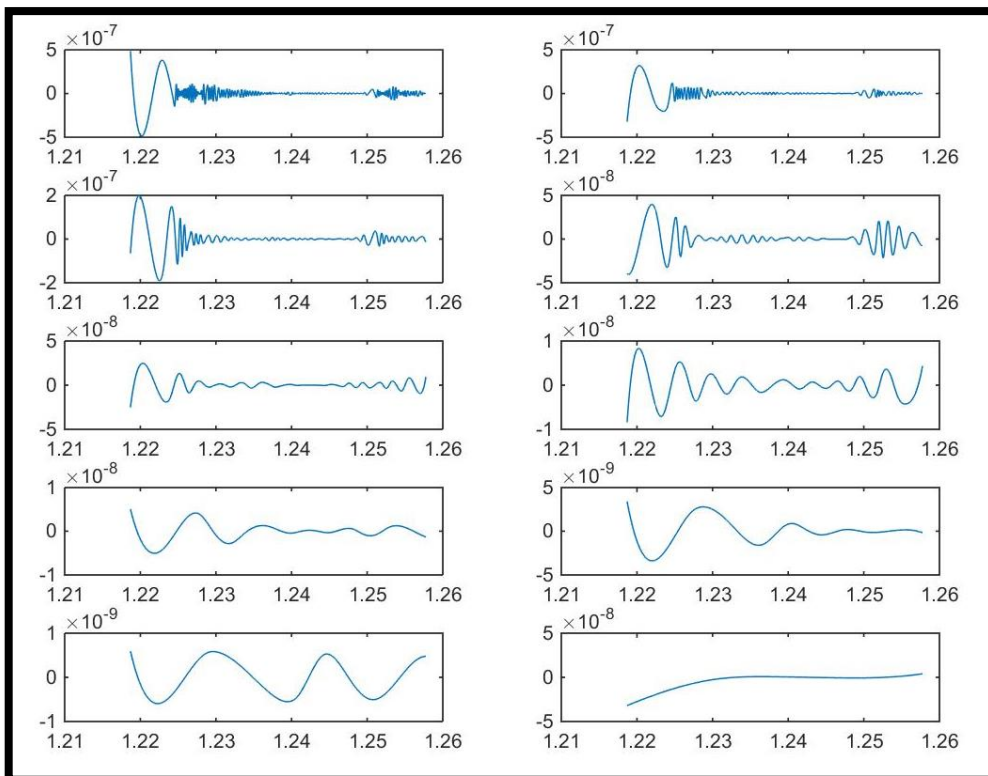


Figure 34: IMF stage 1, node 12

IMF for Stage 3 - Node 1

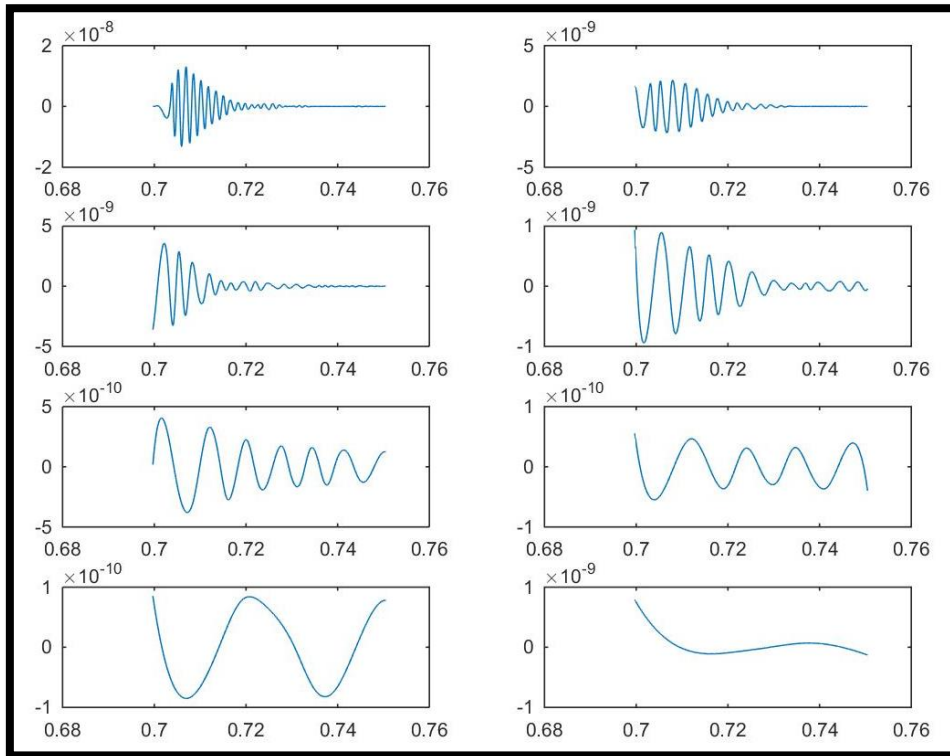


Figure 35: IMF stage 3, node 1

IMF for Stage 3 - Node 5

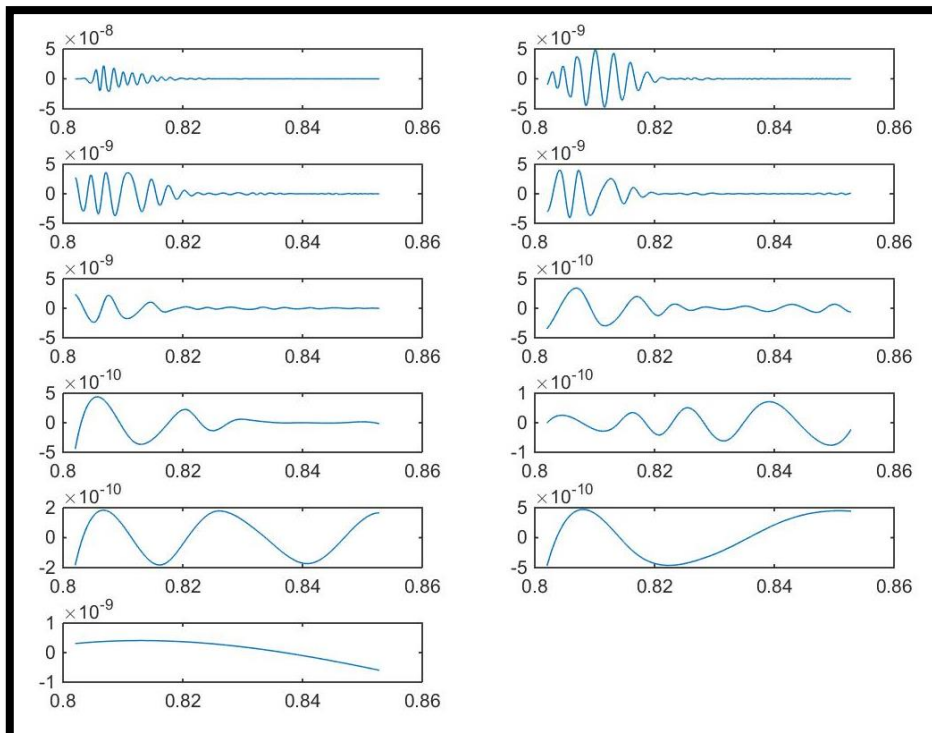


Figure 36: IMF stage 3, node 5

IMF for Stage 3 - Node 12

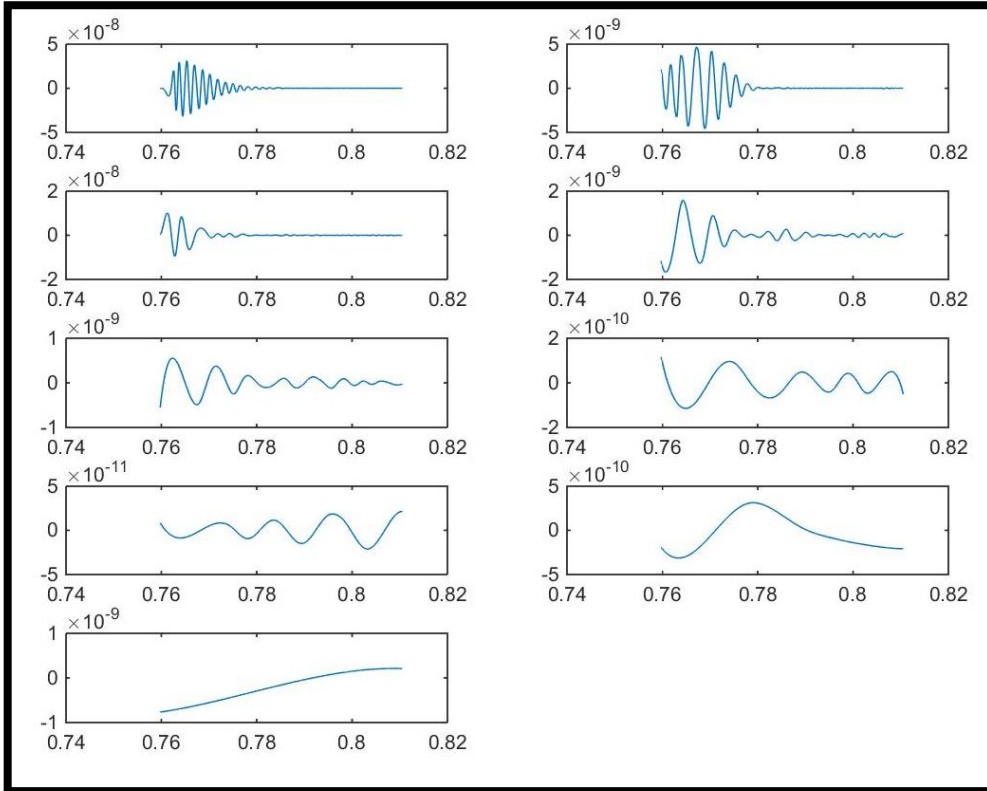


Figure 37: IMF stage 3, node 12

IMF for Stage 6 - Node 1

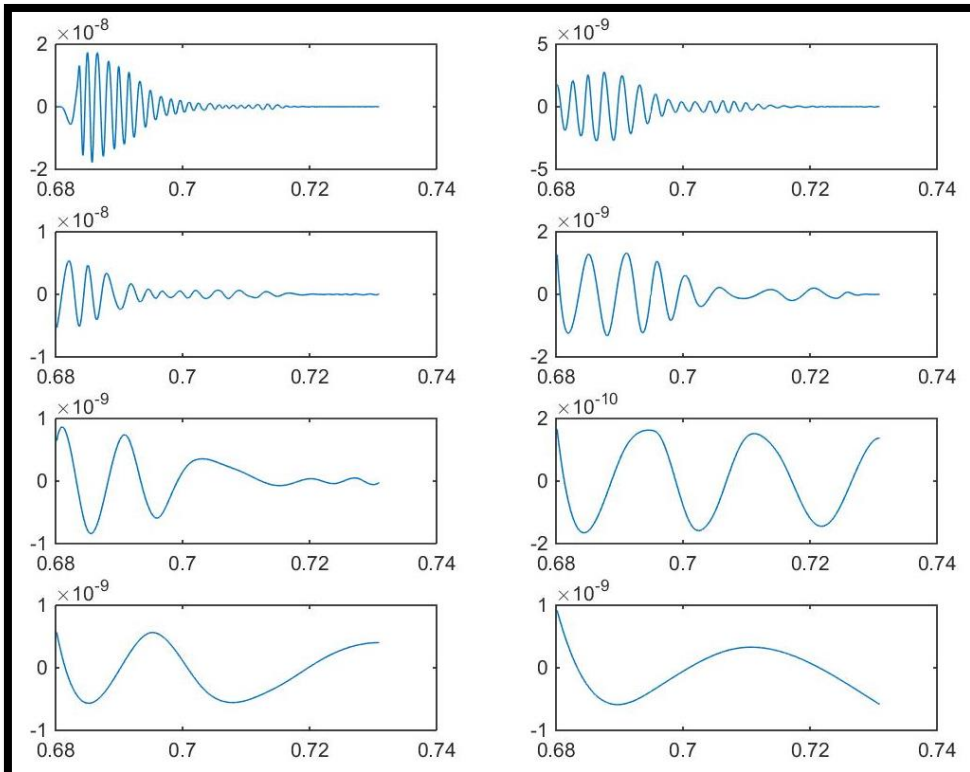


Figure 38: IMF stage 6, node 1

IMF for Stage 6 - Node 5

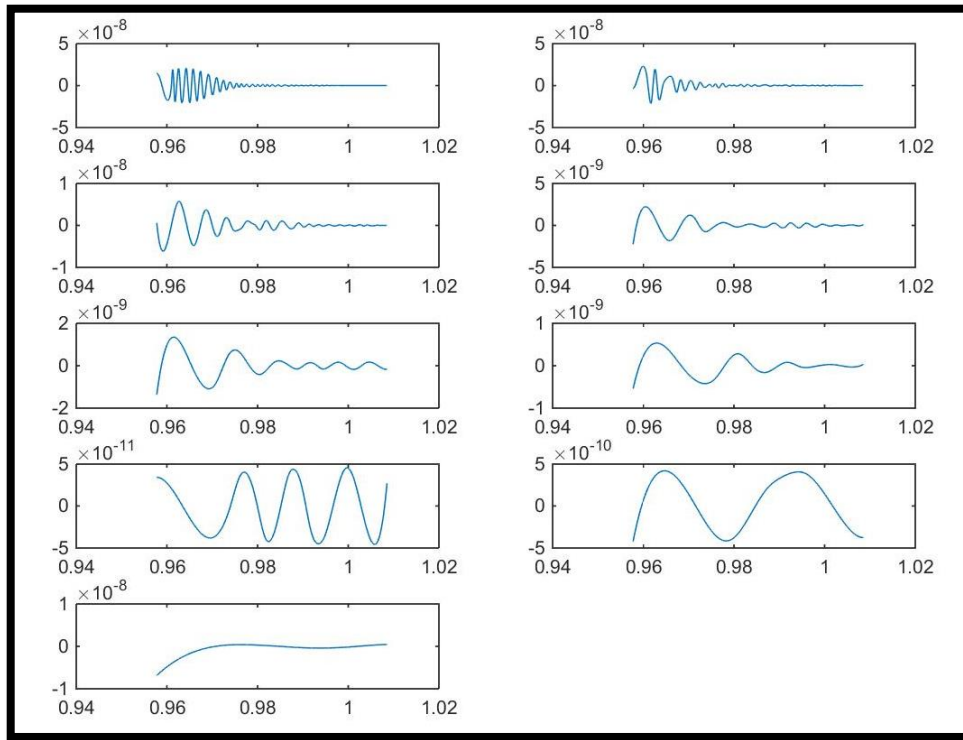


Figure 39: IMF stage 6, node 5

IMF for Stage 6 - Node 12

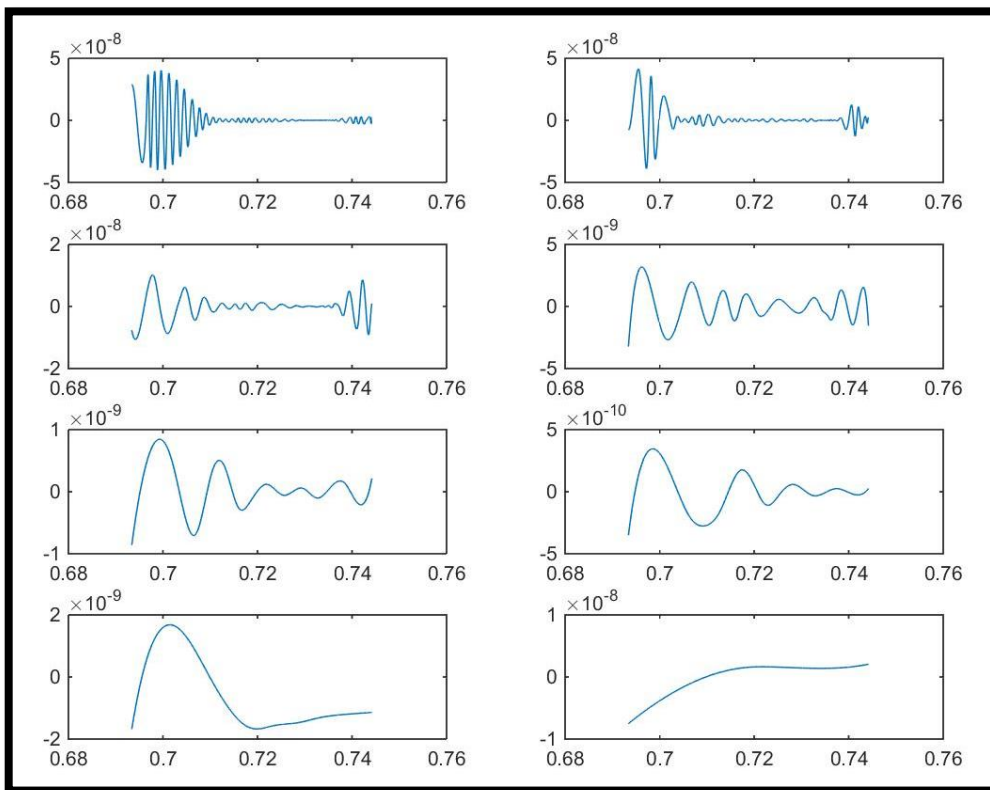


Figure 40: IMF stage 6, node 12

By observation there seems to be little significant correlation between the shape or magnitude of an IMF and damage to a structure leading to a possibly disproved hypothesis. There are number of possible reasons for the large fluctuations in the data. For instance with respect to the lack of consistency with regards to tests at different nodes in the same stage, a large source of error could be to do with modes. A problem can arise when node spacings are placed far enough apart. This means that the sensor could be placed close to an anti-mode in some cases, where it would experience very little deflection, and at other times be unknowingly placed at the maximum deflection point.

As for the counter-intuitive inconsistency between stages of damage, it may be caused simply by simple code errors in one of the many stages of numerical analysis. Signal processing with regards to filtering, sample rate etc. were areas that due to time constraints could only be briefly visited. A great deal of the inconsistencies in the data could be contributed to inadequate signal processing parameters.

5.2.2 Hilbert spectral analysis

After completion of the EMD, the IMFs were analysed using the Hilbert spectral method. This involves computing the Hilbert transform of the signal resulting in real and complex coefficients. These coefficients are necessary in calculating both the instantaneous frequency and amplitude data with respect to time.

Instantaneous-frequency and amplitude for Stage 1 - Node 1

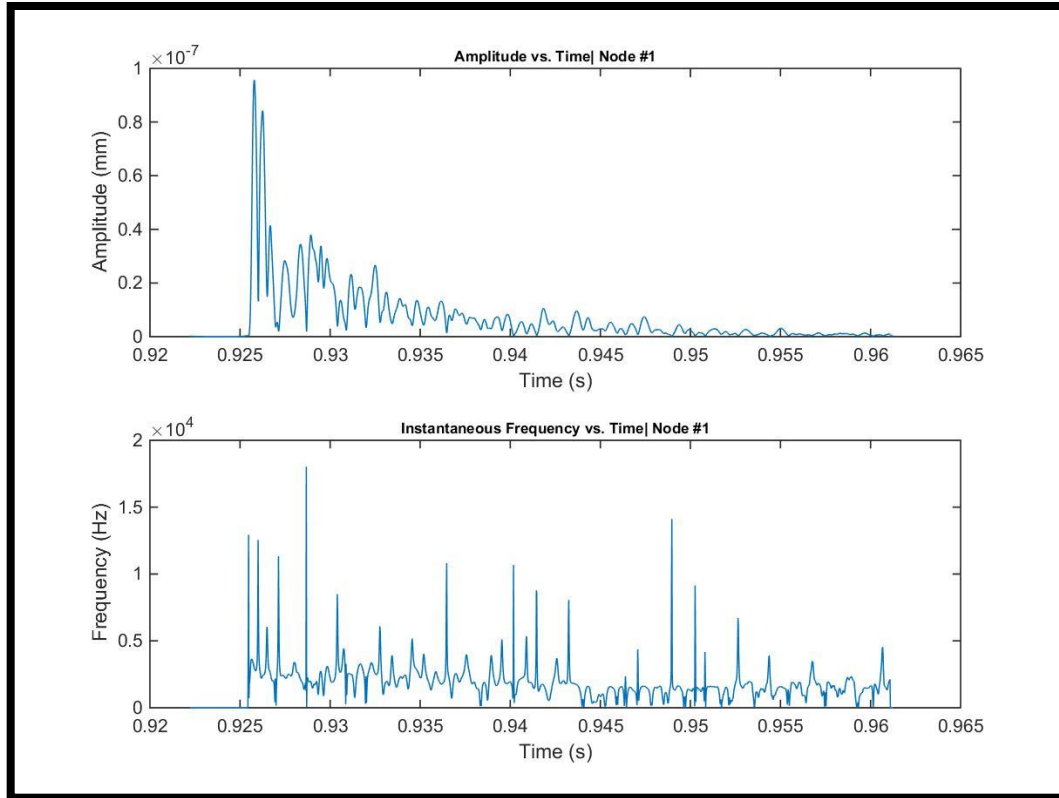


Figure 41: Instant. frequency and amplitude stage 1, node 1

Instantaneous-frequency and amplitude for Stage 1 - Node 5

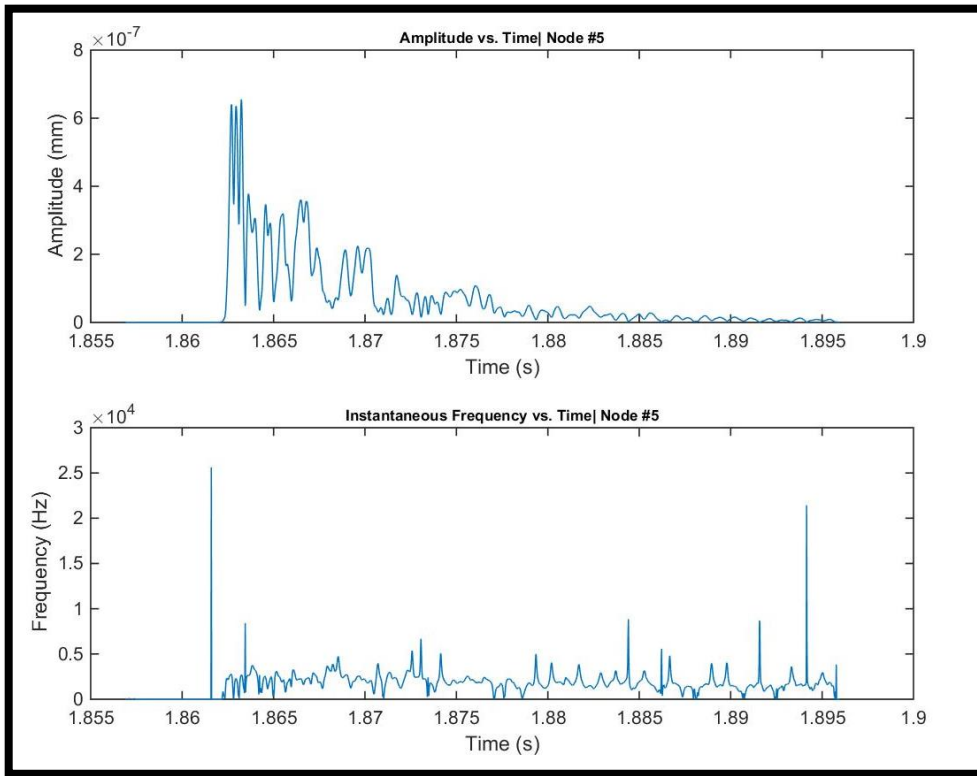


Figure 42: Instant. frequency and amplitude stage 1, node 5

Instantaneous-frequency and amplitude for Stage 1 - Node 12

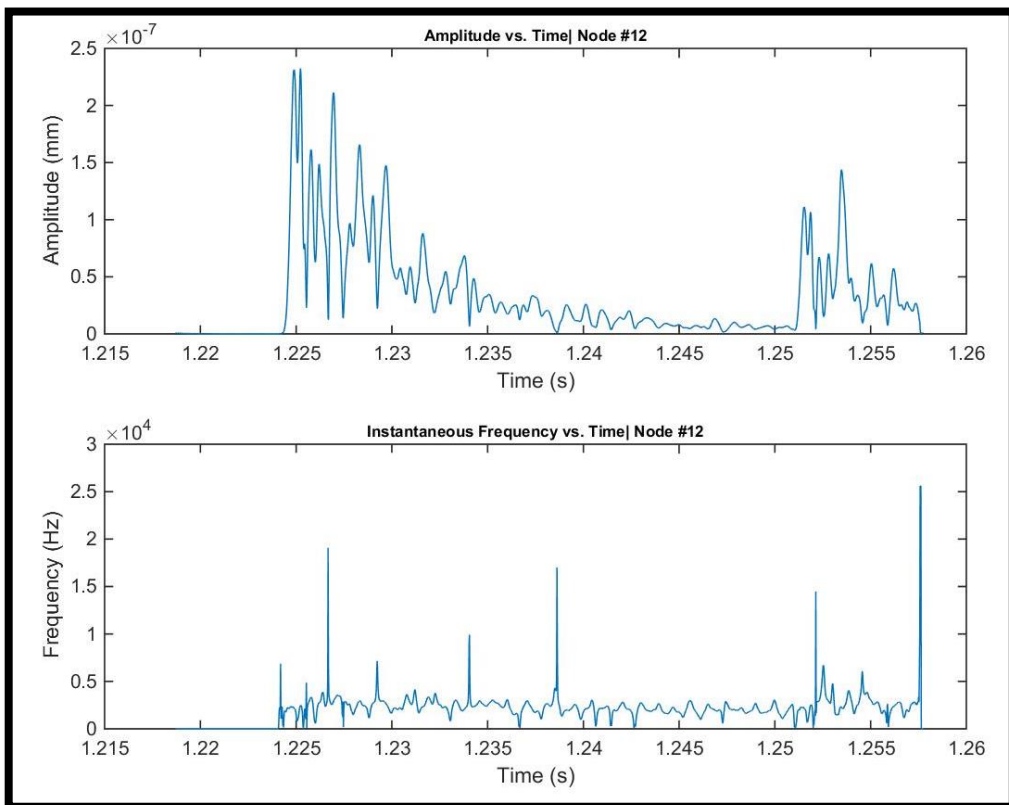


Figure 43: Instant. frequency and amplitude stage 1, node 12

Instantaneous-frequency and amplitude for Stage 3 - Node 1

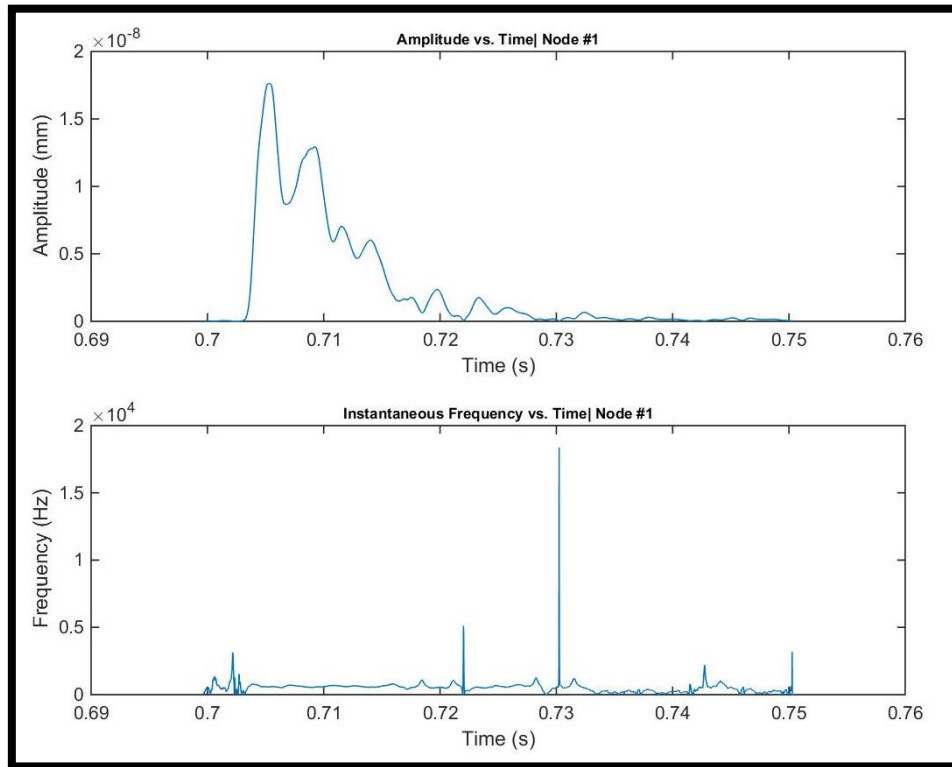


Figure 44: Instant. frequency and amplitude stage 3, node 1

Instantaneous-frequency and amplitude for Stage 3 - Node 5

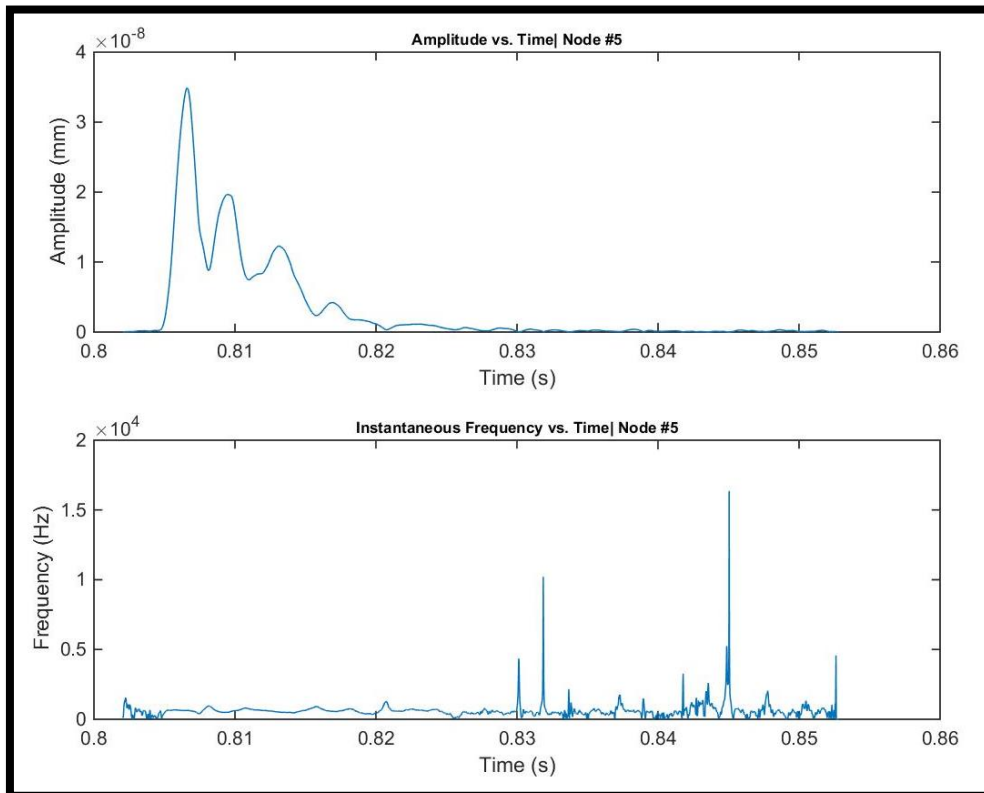


Figure 45: Instant. frequency and amplitude stage 3, node 5

Instantaneous-frequency and amplitude for Stage 3 - Node 12

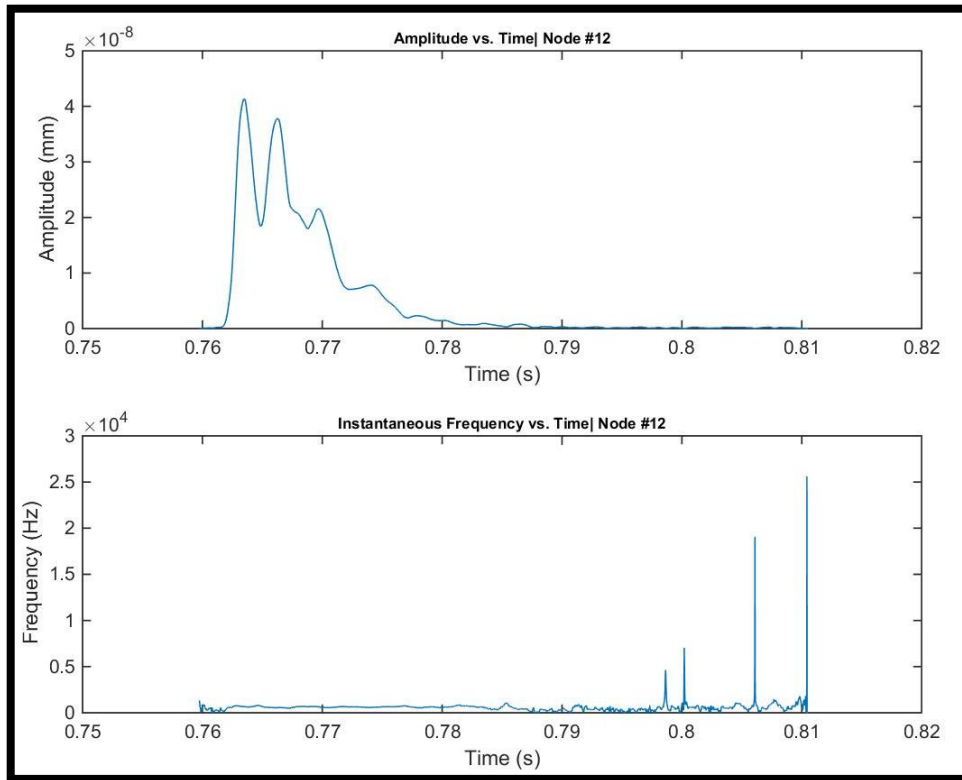


Figure 46: Instant. frequency and amplitude stage 3, node 12

Instantaneous-frequency and amplitude for Stage 6 - Node 1

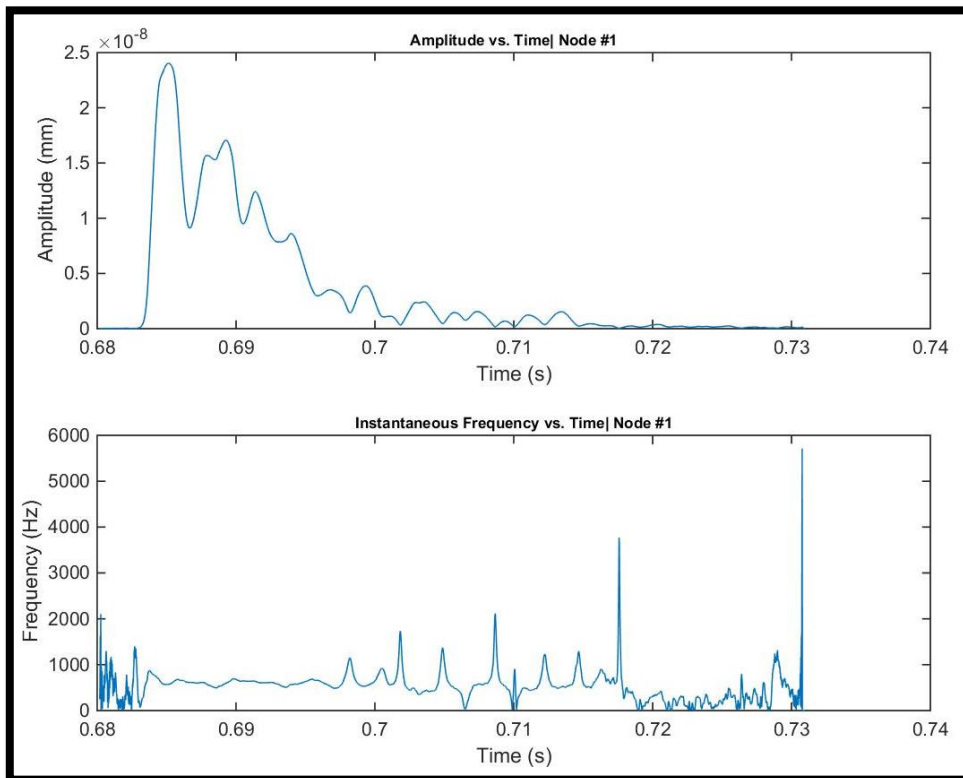


Figure 47: Instant. frequency and amplitude stage 6, node 1

Instantaneous-frequency and amplitude for Stage 6 - Node 5

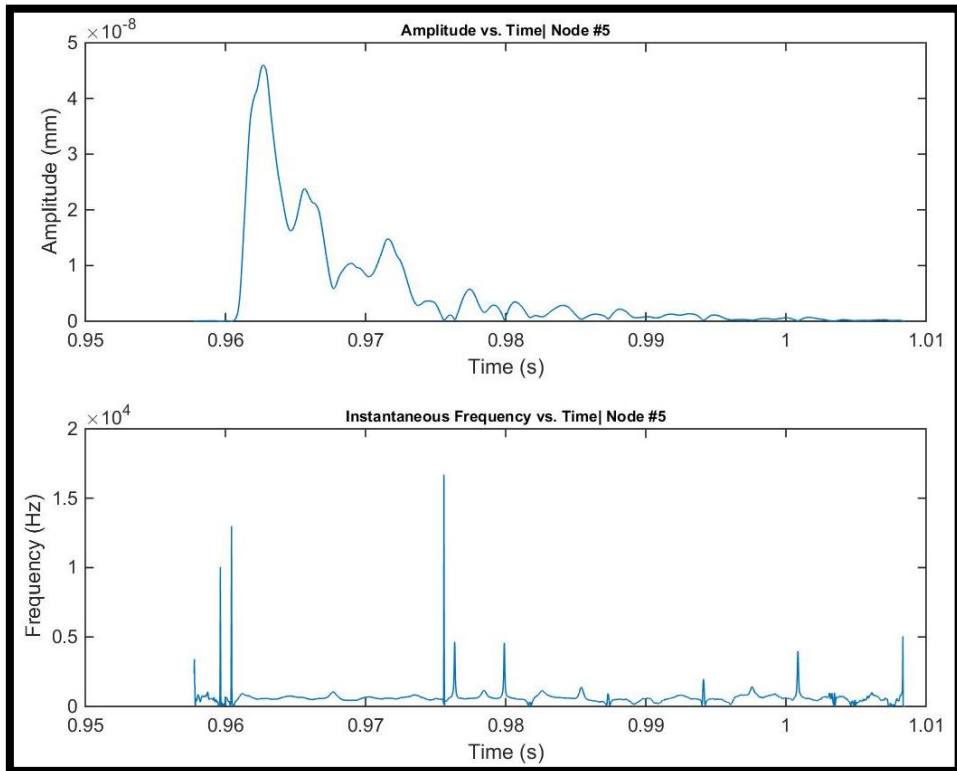


Figure 48: Instant. frequency and amplitude stage 6, node 5

Instantaneous-frequency and amplitude for Stage 6 - Node 12

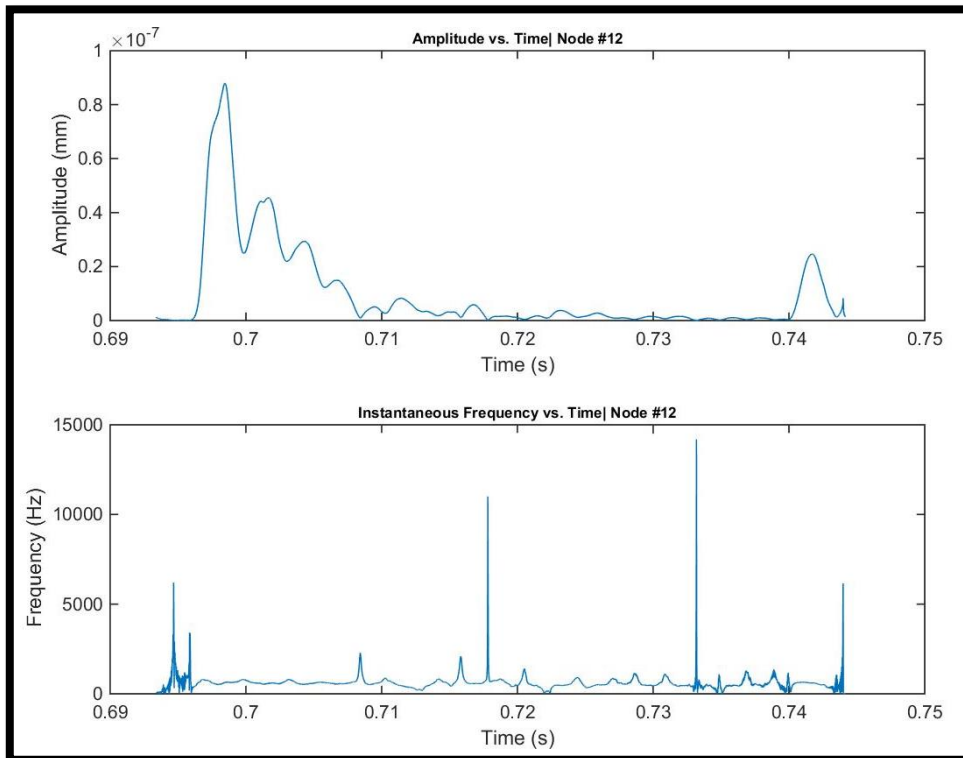


Figure 49: Instant. frequency and amplitude stage 6, node 12

The results from the HHT show far more promising results. The progressive addition of damage stages effected the instantaneous frequencies by orders of magnitude. Stage one was experiencing frequencies as high as $3 \cdot 10^4$. Stage 3 showed peak frequencies around half that of the undamaged section and stage 6 showed 15,000 and 6000. These are substantial changes. Another interesting feature is the change in behaviour of the amplitude. This can be attributed to the cancellation of frequencies. As the frequency of oscillation decreases, the rapid change in amplitude also decreases. This part of the analysis seems to be quite successful.

Chapter 6| Conclusion

Reflecting on the results of the experiments produced some positive results. While the EMD doesn't prove to distinguish damage clearly, the HHT showed clear changes based on what stage of damage had been reached. Both the amplitude and frequency reflected the damage clearly. As mentioned in section 1.2 the objectives of this research was to improve the practicality of dynamic testing methods, making it more practical for real world applications with regards to the following factors:

- Low economic feasibility
- Highly effected by typical noise interference
- High levels of error from signal processing techniques
- Requires a great deal of time for apparatus set up and data processing
- Requires specialised technicians to interpret test results

After completing testing it was apparent that due to the broad range of components required to complete the dynamic response testing, viability would come through the manufacture of a mobile apparatus including a battery of sufficient power and storage for the expected workload, the data acquisition system, a computer to perform the numerical analysis, and a display to express the response in one package. The sensory apparatus and impact hammer would still remain separate, however, by centralising this unit, increasing the mobility, and innovating the design to reduce the weight, the design would then become a more practical tool for commercial use. The purpose of such a design would be to decrease the time for apparatus set up and data processing.

As the numerical calculations could be conducted leaving finally the results of the Hilbert spectral analysis, assuming the necessary computational power could be equipped to the compact device, it would be possible to manufacture and install user friendly software capable of simplifying the analysis process thereby enabling the use by personal with little to no training. The results have shown to be effective therefore the functionality wouldn't be a problem.

Further research suggestions

- Use of LDV to reduce error incurred by double integration.
- Optimisation of the signal processing code.
- Application to a mobile apparatus.

Upon reflection the researcher has realised that it is necessary to have much closer node spacings as to avoid the effect of modes on the data. It also seems necessary that if research is to continue in this area, careful attention must be paid to the signal processing techniques. Filtering played a much more demanding role in the effectiveness of these experiments

References

ABEYKOON, D., et al. (2015). "EXPERIMENTAL-ANALYTICAL FRAMEWORK FOR DAMPING CHANGE-BASED STRUCTURAL HEALTH MONITORING OF BRIDGES."

Adams, R. D. and P. Cawley (1988). "A review of defect types and nondestructive testing techniques for composites and bonded joints." NDT International **21**(4): 208-222.

Alexandrov, O. (2005). Simpsons method illustration - Simpson's rule can be derived by approximating the integrand $f(x)$ (in blue) by the quadratic interpolant $P(x)$ (in red). Wikimedia Commons, Wikipedia.

Alexandrov, O. (2007). Trapezoidal rule illustration - The function $f(x)$ (in blue) is approximated by a linear function (in red). T. r. illustration.png. Wikimedia Commons, Wikipedia.

Allen, J. B. and L. R. Rabiner (1977). "A unified approach to short-time Fourier analysis and synthesis." Proceedings of the IEEE **65**(11): 1558-1564.

Arangio, S. and F. Bontempi (2008). Inference model for structural systems integrity monitoring: Neural networks and Bayesian enhancements, Ph. D. thesis on Structural Engineering, University of Rome "La Sapienza."

Autodesk, I. (2015). "Finite element analysis." from <http://www.autodesk.com/solutions/finite-element-analysis>.

Barnhart, B. L. (2011). "The Hilbert-Huang transform: theory, applications, development."

Belongie, S., et al. (2002). "Shape matching and object recognition using shape contexts." Pattern Analysis and Machine Intelligence, IEEE Transactions on **24**(4): 509-522.

BISHKO, A. V., et al. (2010). "ULTRASONIC ECHO-PULSE TOMOGRAPHY OF CONCRETE USING SHEAR WAVES LOW-FREQUENCY PHASED ANTENNA ARRAYS."

Bisht, S. (2005). "Methods for structural health monitoring and damage detection of civil and mechanical systems."

Bommer, J. J., et al. (2000). Compatible acceleration and displacement spectra for seismic design codes. Proceedings of the 12th World Conference on Earthquake Engineering, Citeseer.

Burden, R. L. and J. D. Faires (2011). Numerical Analysis. 20 Channel Center Street, Boston, MA 02210, USA, Cengage Learning.

Castellini, P., et al. (2006). "Laser Doppler Vibrometry: Development of advanced solutions answering to technology's needs." Mechanical Systems and Signal Processing **20**(6): 1265-1285.

Castellini, P. and G. M. Revel (2000). "An Experimental Technique for Structural Diagnostic Based on Laser Vibrometry and Neural Networks." Shock and Vibration **7**(6).

Cerri, M. N. and F. Vestroni (2003). "Use of frequency change for damage identification in reinforced concrete beams." Journal of Vibration and Control **9**(3-4): 475-491.

Champoux, Y., et al. (2003). "Moment excitation of structures using two synchronized impact hammers." Journal of Sound and Vibration **263**(3): 515-533.

Chen, B. and S. Nagarajaiah (2007). Flexibility-based structural damage identification using Gauss-Newton method.

Chen, H., et al. (1995). "Evaluating structural deterioration by dynamic response." Journal of Structural Engineering **121**(8): 1197-1204.

Chen, R. H. L., et al. (1997). Nondestructive Evaluation of Ceramic Candle Filters Using Vibration Response.

Coughlin, K. and K.-K. Tung (2004). "11-year solar cycle in the stratosphere extracted by the empirical mode decomposition method." Advances in space research **34**(2): 323-329.

Doebling, S. W., et al. (1998). "A summary review of vibration-based damage identification methods." Shock and vibration digest **30**(2): 91-105.

Donnelly, D. (2006). The fast Fourier and Hilbert-Huang transforms: a comparison. Computational Engineering in Systems Applications, IMACS Multiconference on, IEEE.

Du, P., et al. (2006). "Improved peak detection in mass spectrum by incorporating continuous wavelet transform-based pattern matching." Bioinformatics **22**(17): 2059-2065.

Dutta, D. (2010). "Ultrasonic Techniques for Baseline-Free Damage Detection in Structures."

Esposito, E. (2008). "Laser Doppler Vibrometry." Handbook of the Use of Lasers in Conservation and Conservation Science.

- Flandrin, P., et al. (2004). "Empirical mode decomposition as a filter bank." Signal Processing Letters, IEEE **11**(2): 112-114.
- Fu, Z.-F. and J. He (2001). Modal analysis, Butterworth-Heinemann.
- Gittes, F. and C. F. Schmidt (1998). "Signals and noise in micromechanical measurements." Methods in cell biology **55**: 129-156.
- Griffin, D. W. and J. S. Lim (1984). "Signal estimation from modified short-time Fourier transform." Acoustics, Speech and Signal Processing, IEEE Transactions on **32**(2): 236-243.
- Grossmann, A. and J. Morlet (1984). "Decomposition of Hardy functions into square integrable wavelets of constant shape." SIAM journal on mathematical analysis **15**(4): 723-736.
- Hadhuey (2005). A cloth of woven carbon filaments. Kohlenstofffasermatte. German Wikipedia, Wikimedia Commons.
- Hartman, W., et al. (2010). Non destructive integrity testing of rock reinforcement elements in Australian mines. Coal Operators' Conference.
- Hassan, H. H. (2005). Empirical mode decomposition (EMD) of potential field data: airborne gravity data as an example. 2005 SEG Annual Meeting, Society of Exploration Geophysicists.
- Haykin, S. (2004). "Neural Networks: A comprehensive foundation." Neural Networks **2**(2004).
- Hearn, G. and R. B. Testa (1991). "Modal analysis for damage detection in structures." Journal of Structural Engineering **117**(10): 3042-3063.
- Heaton, E. (2011). "Use of vibration signature in structural health monitoring (composite/internal damages).".
- Huang, N. E. and S. S. Shen (2005). Hilbert-Huang transform and its applications, World Scientific.
- Huang, N. E., et al. (1999). "A new view of nonlinear water waves: The Hilbert Spectrum 1." Annual review of fluid mechanics **31**(1): 417-457.
- Huang, N. E., et al. (1998). The empirical mode decomposition and the Hilbert spectrum for nonlinear and non-stationary time series analysis. Proceedings of the Royal Society of London A: Mathematical, Physical and Engineering Sciences, The Royal Society.

Huang, N. E., et al. (2009). "On instantaneous frequency." Advances in adaptive data analysis **1**(02): 177-229.

James, G. (2008). Modern Engineering Mathematics. Edinburgh Gate, Harlow, Essex, England, Pearson Education Limited.

Jean-Pierre, C. (2009). Glass reinforcements used for fiberglass are supplied in different physical forms, microspheres, chopped or woven., Wikimedia Commons.

Jean-Pierre, C. and Jaybear (2012). Glass-aramid-hybrid Fabric (for high tension and compression). Glass-aramid-hybrid-area_used-for-reinforced-plastics.jpg. Dortmund, Germany, Wikimedia Commons.

Jones, K. E., et al. (2002). "Sources of Signal-Dependent Noise During Isometric Force Production." Journal of Neurophysiology **88**(3): 1533-1544.

Kadambe, S. and G. F. Boudreaux-Bartels (1992). "A comparison of the existence of cross terms' in the Wigner distribution and the squared magnitude of the wavelet transform and the short-time Fourier transform." Signal Processing, IEEE Transactions on **40**(10): 2498-2517.

Kim, J.-T. and N. Stubbs (2002). "Improved damage identification method based on modal information." Journal of Sound and Vibration **252**(2): 223-238.

Kim, S. J. (2008). "Damage detection in composite laminates using coin-tap method." Journal of the Acoustical Society of America **123**(5): 3064.

Kinney, J. H. and M. C. Nichols (1992). "X-ray tomographic microscopy (XTM) using synchrotron radiation." Annual review of materials science **22**(1): 121-152.

Kittinger-Sereinig, R. (2015). Corrugated fibre-glass reinforced resin sheets. Graz, Österreich, Pixabay.

Kuehnel, W. and S. Sherman (1994). "A surface micromachined silicon accelerometer with on-chip detection circuitry." Sensors and Actuators A: Physical **45**(1): 7-16.

Larson, B. (2002). Study of the factors affecting the sensitivity of liquid penetrant inspections: review of literature published from 1970 to 1998, DTIC Document.

Lee, B. (2003). "Review of the present status of optical fiber sensors." Optical Fiber Technology **9**(2): 57-79.

Lee, U. and J. Shin (2002). "A frequency response function-based structural damage identification method." Computers & structures **80**(2): 117-132.

Leonard, K. R., et al. (2002). "Ultrasonic Lamb wave tomography." Inverse problems **18**(6): 1795.

Liu, D., et al. (2004). Assessment of structural integrity through coupled vibration. Structural Integrity and Fracture International Conference (SIF'04), Australian Fracture Group.

Maia, N., et al. (2003). "Damage detection in structures: from mode shape to frequency response function methods." Mechanical Systems and Signal Processing **17**(3): 489-498.

Malyarenko, E. V. and M. K. Hinders (2001). "Ultrasonic Lamb wave diffraction tomography." Ultrasonics **39**(4): 269-281.

Mathews, J. H. and K. D. Fink (2004). Numerical Methods using Matlab. Upper Saddle Ribber, Pearson Education.

Mathworks (2015). "MATLAB: The Language of Technical Computing." from <http://au.mathworks.com/products/matlab/>.

Montalvao, D., et al. (2006). "A review of vibration-based structural health monitoring with special emphasis on composite materials." Shock and vibration digest **38**(4): 295-326.

Morassi, A. and F. Vestroni (2008). Dynamic methods for damage detection in structures, Springer.

Morey, W. W., et al. (1990). Fiber optic Bragg grating sensors. OE/FIBERS'89, International Society for Optics and Photonics.

Neto, E. S., et al. (2004). "Assessment of cardiovascular autonomic control by the empirical mode decomposition." Methods of information in medicine **43**(1): 60-65.

Nise, N. S. (2011). Control Systems Engineering, Wiley Inc.

Norton, M. P. and D. G. Karczub. (2003). Fundamentals of Noise and Vibration Analysis for Engineers, Cambridge University Press.

O'Connor, J. J. and E. F. Robertson (2000). "Biography: Richard Courant." from <http://www-history.mcs.st-andrews.ac.uk/Biographies/Courant.html>.

Ojalvo, I. and D. Pilon (1988). Diagnostics for geometrically locating structural math model errors from modal test data. Proceedings of the 29th AIAA Structures, Structural Dynamics and Materials Conference, Williamsburg, VA.

Okasha, S. (2002). Philosophy of Science: A very short introduction, Oxford University Press Inc.

Ono, T. (2015). An investigation of the vibration testing method for small diameter endmills. Key Engineering Materials. **625**: 134-139.

Orfanidis, S. J. (1995). Introduction to signal processing, Prentice-Hall, Inc.

Ortiz, J., et al. (1997). Damage detection from vibration measurements using neural network technology. Artificial Neural Networks for Civil Engineers@ sFundamentals and Applications, ASCE.

Pandey, A. K., et al. (1991). "Damage detection from changes in curvature mode shapes." Journal of Sound and Vibration **145**(2): 321-332.

Park, G. and D. J. Inman (2005). "Impedance-based structural health monitoring." Damage prognosis for aerospace, civil and mechanical systems: 275-292.

PCB (2009). "Impact Hammers." from <http://www.pcb.com/testmeasurement/impacthammers.aspx>.

PCB (2009). "Introduction to Piezoelectric Accelerometers." from https://www.pcb.com/techsupport/tech_accel.aspx.

Qi, H. J. (2006). "Finite Element Analysis." from http://www.colorado.edu/MCEN/MCEN4173/chap_01.pdf.

Qin, S. and Y. M. Zhong (2006). "A new envelope algorithm of Hilbert–Huang transform." Mechanical Systems and Signal Processing **20**(8): 1941-1952.

Raki (2013). Accelerometers. Accelerometer_2.jpg, Daily Technology Updates.

Rao, S. S. (2005). Mechanical Vibrations. Prentice Hall, 1 Lake Street, Upper Saddle River, Pearson Education Inc.

Rato, R. T., et al. (2008). "On the HHT, its problems, and some solutions." Mechanical Systems and Signal Processing **22**(6): 1374-1394.

Reddy, V. U. (2000). "On Fast Fourier Transform: A Popular Tool for Spectrum Analysis ".

Reiter, G., et al. (2005). "Residual stresses in thin polymer films cause rupture and dominate early stages of dewetting." Nat Mater **4**(10): 754-758.

Ricles, J. and J. Kosmatka (1992). "Damage detection in elastic structures using vibratory residual forces and weighted sensitivity." AIAA Journal **30**(9): 2310-2316.

Rilling, G., et al. (2003). On empirical mode decomposition and its algorithms.

Roveri, N. and A. Carcaterra (2012). "Damage detection in structures under traveling loads by Hilbert–Huang transform." Mechanical Systems and Signal Processing **28**(0): 128-144.

Rusaw, R. (2010). Fiber Bragg grating-based sensor. Diagram_02.jpg, Electric power research institute.

Sakata, S., et al. (2012). "A microscopic failure probability analysis of a unidirectional fiber reinforced composite material via a multiscale stochastic stress analysis for a microscopic random variation of an elastic property." Computational Materials Science **62**: 35-46.

Salawu, O. S. (1997). "Detection of structural damage through changes in frequency: a review." Engineering Structures **19**(9): 718-723.

Sampaio, R., et al. (1999). "Damage detection using the frequency-response-function curvature method." Journal of Sound and Vibration **226**(5): 1029-1042.

Scharf, L. L. (1991). Statistical signal processing, Addison-Wesley Reading, MA.

Schulz, M. J., et al. (1997). "FREQUENCY RESPONSE FUNCTION ASSIGNMENT TECHNIQUE FOR STRUCTURAL DAMAGE IDENTIFICATION."

Schulz, M. J., et al. (1996). Structural damage diagnosis by frequency response function optimization. AIAA Dynamics Specialists Conference, April.

Shi, Z., et al. (2000). "Structural Damage Detection from Modal Strain Energy Change." Journal of Engineering Mechanics **126**(12): 1216-1223.

Shi, Z. Y., et al. (1998). "STRUCTURAL DAMAGE LOCALIZATION FROM MODAL STRAIN ENERGY CHANGE." Journal of Sound and Vibration **218**(5): 825-844.

Siemens (2015). Siemens PLM Software: LMS SCADAS. S. Inc. Siemens Aktiengesellschaft, Wittelsbacherplatz 2, 80333 Munich, Germany, Siemens PLM software and LMS testing.

Signell, S. and T. Schier (2001). Signal transformation method and apparatus, Google Patents.

Simulia (2015). "ABAQUS UNIFIED FEA: COMPLETE SOLUTIONS FOR REALISTIC SIMULATION.". from <http://www.3ds.com/products-services/simulia/products/abaqus/latest-release/>.

Stanbridge, A. and D. Ewins (1999). "Modal testing using a scanning laser Doppler vibrometer." Mechanical Systems and Signal Processing **13**(2): 255-270.

Stiros, S. C. (2008). "Errors in velocities and displacements deduced from accelerographs: An approach based on the theory of error propagation." Soil Dynamics and Earthquake Engineering **28**(5): 415-420.

Storr, W. (2015). "Electronics tutorials." from <http://www.electronics-tutorials.ws/waveforms/waveforms.html>.

Sun, F., et al. (1995). Structural frequency response function acquisition via electric impedance measurement of surface-bonded piezoelectric sensor/actuator. Proceedings of 36th AIAA/ASME/ASCE/AHS/ASC Structures, Structural Dynamics, and Materials Conference.

Szabo, B. A. and I. Babuška (1991). Finite element analysis, John Wiley & Sons.

Tsuda, H. (2006). "Ultrasound and damage detection in CFRP using fiber Bragg grating sensors." Composites Science and Technology **66**(5): 676-683.

UC-San_Diego (2014). HHT Full Lecture. San Diego, UC San Diego: Jacobs School of Engineering.

Van Loan, C. (1992). Computational frameworks for the fast Fourier transform, Siam.

Veltkamp, R. and M. Hagedoorn (2001). "State of the art in shape matching." Principles of visual information retrieval: 87.

Wang, T., et al. (2011). Active stereo vision for improving long range hearing using a laser Doppler vibrometer. Applications of Computer Vision (WACV), 2011 IEEE Workshop on, IEEE.

Weisstein, E. W. (2015). "Fast fourier transform."

Widas, P. (1997). "Introduction to Finite Element Analysis." from http://www.sv.vt.edu/classes/MSE2094_NoteBook/97ClassProj/num/widas/history.html.

Wild, G. and S. Hinckley (2010). Optical fibre Bragg gratings for acoustic sensors. Proc. 20th International Congress on Acoustics.

William D. Callister, J. and D. G. Rethwisch (2014). Materials Science and Engineering: An Introduction. 111 River Street, Hoboken, New Jersey, USA, John Wiley & Sons, Inc.

Wu, X., et al. (1992). "Use of neural networks in detection of structural damage." Computers & structures **42**(4): 649-659.

Wu, Z., et al. (2001). The impact of global warming on ENSO variability in climate records, Center for Ocean-Land-Atmosphere Studies.

Xu, Y. and J. Chen (2004). "Structural damage detection using empirical mode decomposition: experimental investigation." Journal of Engineering Mechanics **130**(11): 1279-1288.

Yang, J., et al. (2006). "A simple approach to integration of acceleration data for dynamic soil-structure interaction analysis." Soil Dynamics and Earthquake Engineering **26**(8): 725-734.

Yang, J. N., et al. (2004). "Hilbert-Huang based approach for structural damage detection." Journal of Engineering Mechanics **130**(1): 85-95.

Zhang, J. Z., et al. (2008). Detection of involuntary human hand motions using Empirical Mode Decomposition and Hilbert-Huang Transform. Proceedings of the IEEE International 51st Midwest Symposium on Circuits and Systems.

Zuuk-International (2015). "Liquid Dye Penetrant Testing." from <http://www.zuukinspection.com/services/liquid-dye-penetrant-testing/>.

Appendices

Appendix A| Project Specifications

University of Southern Queensland
Faculty of Engineering and Built Environment

ENG4111/4112 Research Project
Project Specification

FOR: James L. KERR

TOPIC: THE USE OF DYNAMIC RESPONSE IN TESTING THE STRUCTUREAL
HEALTH OF FIBRE COMPOSITE S.H.S.

SUPERVISOR: Dr Jayantha Epaarachchi

ENROLMENT: ENG4111 – S1, 2015

ENG4112 – S2, 2015

PROJECT AIM: The aim of this project is to investigate the possibility of accurate vibration testing of fibre composites to determine faulty mechanical properties, breaks, or other structural defaults and if these methods are feasible over classical testing methods.

PROGRAMME:

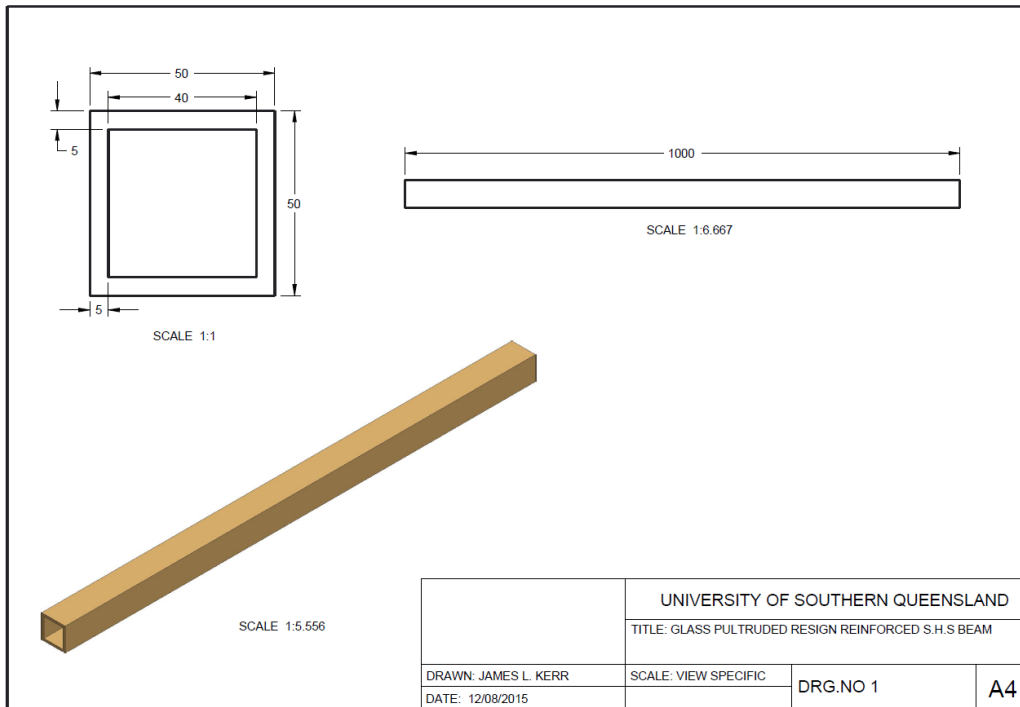
1. Research literature regarding dynamic response/vibration testing for structural health and fibre composite material properties
2. Perform vibration testing on a pultruded composite beam and analyse mode shapes
3. Identify changes in modal geometry and dynamic response/vibration signature with the inclusion of structural defects
4. Perform FEA analysis of the beam vibration/dynamic response using Abaqus FEA software and correlate FEA results with experimental data.
5. Predict modal change and change of vibration signature using correlated FEA model and validate with experimental data
6. Present preliminary research and prepare and submit final dissertation.

As time permits:

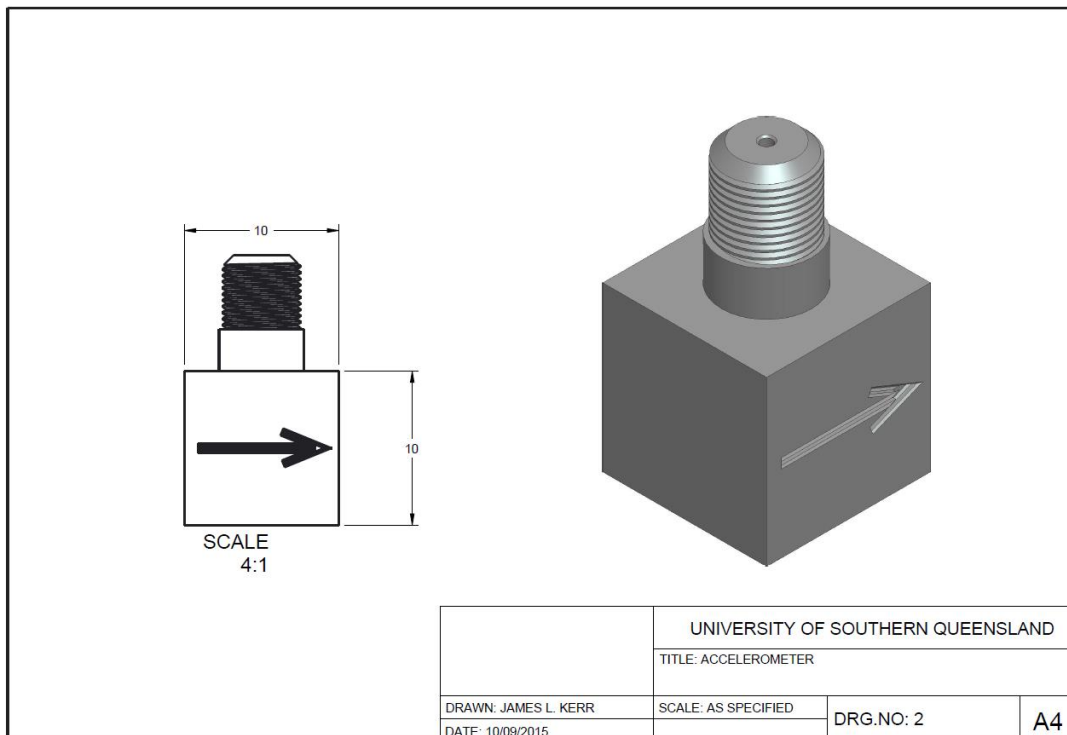
7. Use embedded FBG sensor to measure vibration signature of a pultruded beam

Appendix B| Drawings

Appendix B1: Glass pultruded resin reinforced S.H.S beam



Appendix B2: Single axis piezoelectric accelerometer



Appendix C| Matlab Code

Appendix C1: Main Code stage 1

```
% This program performs a series of steps according to the paper named:
%
% "COMPARISON OF THE HILBERT-HAUNG AND FAST FOURIER TRANSFORMS FOR DYNAMIC
%     RESPONSE TESTING OF DAMAGE IN FIBRE COMPOSITE S.H.S."
%
%     Author/Code Developer: James Kerr
%
%-----
%
% This program was created to complete the following steps:
%
% 1) Import the acceleration data files created by experimental
%     investigations for each node for particular damage stage
% 2) Apply low/high pass filters to pertinent truncated window of data
% 3) Plots all necessary stages and saves data sets for later reflection
% 4) Performs Simpson's integration on acceleration data by referring to
%     external function script
% 5) Decompose the deflection signal by empirical mode decomposition (EMD)
%     until the stopping criteria is met
% 3) Plots the intrinsic mode functions (IMF) yielded by the EMDs
% 4) Computes the discrete fourier transform (DFT) of each IMF
% 5) Computes the summative Hilbert transform of the acquired IMFs
% 6) Computes phase from real & complex components of the Hilbert
%     transform
% 7) Computes and plots instantaneous frequency and amplitude with respect
%     to time
%
%=====
close all; clear; format long; clc;
%% =====Damage: Stage 1=====

%% S1.Initial parameters/Import and organise data
disp('Data Processing of Stage 1: Undamaged Beam, 12 nodes')
%-----
node = (1:12);           %Number of nodes per stage
dist = 0.06;            %Distance between nodes
rawD = cell(zeros(1,12)); %Padding

% Import data as cell per node (excludes trash lines)
for k = node
    rawD{k} = dlmread(fullfile('E:\James_KERR Semester 2 2015\Research Project\data\Stage1' ...
        ,sprintf('Stage1_%d.txt',k)),',';',11,1);
        %^11 lines of trash from LMS
end

% Organise data
rd = cell2mat(rawD);      %Removes cell format making large matrix
ai = rd(:,(2:4:end));    %Retrieve acceleration data
fi = rd(:,(4:4:end));    %Retrieves force data

% Retrieves time array and gives all unique values
ti = (0:max(rd(:,1))/(length(rd(:,1))-1):max(rd(:,1)))';

%-----
```

```

%% S1.Conversion to SI units/Calibration/Plots
%-----
amean = mean(ai);           %Mean acceleration per node
fmean = mean(fi);           %Mean force per node
at = zeros(size(ai)); ft = at; %Padding

% Zero mean calibration
for k = node
    at(:,k) = ai(:,k)-amean(k); %Acceleration correction
    ft(:,k) = fi(:,k)-fmean(k); %Force correction
end

% SI unit conversion (m/s^2)
ai = (ai.*9.80655)./1000000; %Conversion of pre calibrated acc.
ac = (at.*9.80655)./1000000; %Conversion of post calibrated acc.
h = zeros(1:12);           %Padding

%=====
%% S1.Establish window parameters/Truncate dynamic response data
%-----
% Magnitude and location of maximum force per node
[~,floc] = max(ft); %Used as location for data truncation

% Window parameters [-200 to 2400 = 2601 steps or aprx. 0.05 seconds]
stepb = 300; %Step back - Window start parameter
stepf = 1700; %Step forward - Window end parameter
wb = floc-stepb; %Location of window start per node
wf = floc+stepf; %Location of window end per node

% Time matrix - Max force occurs at unique time per node
tmat = repmat(ti,1,length(node));

%=====

```

```

%% S1.Data windowing/Window plot
%-----
aw = zeros(stepb+stepf+1,length(node)); %Padding
tw = aw; fw = aw; %Padding

% Truncation of data followed by optional plots
for k = node

    %Application of window parameters to data sets
    aw(:,k) = ac(wb(k):wf(k),k); %Windowed acceleration
    fw(:,k) = ft(wb(k):wf(k),k); %Windowed force
    tw(:,k) = tmat(wb(k):wf(k),k); %Corresponding time windows

    %*****optional task*****
    %Windowed force data plot
    h(k) = figure(k);
    plot(tw(:,k),fw(:,k))
    caption = sprintf('Windowed Force vs. Time| Node #d',k);
    title(caption,'FontSize',8);
    xlabel('Time (s)');
    ylabel('Force (N)');
    baseFileName = sprintf('Windowed_Force_%d.jpg',k);
    fullFileName = fullfile('E:\James_KERR Semester 2 2015\Research Project\data\Stage1\Windowed',baseF:
    saveas(h(k),fullFileName);
    %Windowed acceleration data plot
    h(k+12) = figure(k+12);
    plot(tw(:,k),aw(:,k))
    caption = sprintf('Windowed Acceleration vs. Time| Node #d',k);
    title(caption,'FontSize',8);
    xlabel('Time (s)');
    ylabel('Acceleration (m/s^2)');
    baseFileName = sprintf('Windowed_Acceleration_%d.jpg',k);
    fullFileName = fullfile('E:\James_KERR Semester 2 2015\Research Project\data\Stage1\Windowed',baseF:
    saveas(h(k+12),fullFileName);

end
close all;
%*****

%Correct for varried force
for k = node

    aw(:,k) = aw(:,k)/max(fw(:,k)); %Force correction

end

%=====

```

```

%% S1.High pass filter pre-integration
%-----
% Integrating will amplify the Low frequency components of noise therefore
% filtering is necessary.

fs = length(aw)/(mean(max(tw))-mean(min(tw))); %Sample frequency
[b,a] = butter(4,2000/(fs/2)); %Butterworth coefficients (600Hz)
[bb,aa] = butter(4,1000/(fs/2)); %Butterworth coefficients (1600Hz)

af1 = zeros(size(aw)); %Padding
af2 = af1; ff1 = af1; ff2 = af1; %Padding

% Single/double pass filter comparison using butterworth coefficients
for k = node

    af1(:,k) = filter(b,a,aw(:,k)); % Single-pass filter acceleration
    af2(:,k) = filtfilt(b,a,aw(:,k)); % Double-pass filter acceleration
    ff1(:,k) = filter(bb,aa,aw(:,k)); % Single-pass filter force
    ff2(:,k) = filtfilt(bb,aa,aw(:,k)); % Double-pass filter force

%*****optional task*****
% Plotting of filter mechanisms for comparison of accuracy
h(k) = figure(k);
plot(tw(:,k),aw(:,k))
hold on
plot(tw(:,k),af2(:,k),'r-')
plot(tw(:,k),af1(:,k),'k-')
legend('Original unfiltered signal','Single-pass filter','Double-pass filter')
xlabel('Time (s)');
ylabel('Acceleration (m/s^2)');
caption = sprintf('Filtered Acceleration vs. Time| Node %d',k);
title(caption,'FontSize',8);
hold off
baseFileName = sprintf('Acceleration_Filter_Examples_%d.jpg',k);
fullFileName = fullfile('E:\James_KERR Semester 2 2015\Research Project\data\Stage1\Acceleration_Fil
saveas(h(k),fullFileName);
h(k+12) = figure(k+12);
plot(tw(:,k),fw(:,k))
hold on
plot(tw(:,k),ff1(:,k),'k-')
plot(tw(:,k),ff2(:,k),'r-')
legend('Original unfiltered signal','Single-pass filter','Double-pass filter')
xlabel('Time (s)');
ylabel('Force (N)');
caption = sprintf('Filtered Force vs. Time| Node %d',k);
title(caption,'FontSize',8);
hold off
baseFileName = sprintf('Acceleration_Filter_Examples_%d.jpg',k);
fullFileName = fullfile('E:\James_KERR Semester 2 2015\Research Project\data\Stage1\Acceleration_Fil
saveas(h(k+12),fullFileName);

end
close all;
%*****
%=====

```



```

%% S1.Integrates the windowed & filtered acceleration data to acquire velocity
%-----
vw = zeros(size(af1)); %Padding

% Simpsons integration of discrete acceleration data (External function file)
for k = node

    vw(:,k) = Simpson(af1(:,k),tw(:,k));

%*****optional task*****
    h(k) = figure(k);
    plot(tw(:,k),vw(:,k));
    xlabel('Time (s)');
    ylabel('Velocity (m/s)');
    caption = sprintf('Velocity vs. Time| Node %#d',k);
    title(caption,'FontSize',8);
    baseFileName = sprintf('Velocity_after_Simpsons_integration_%d.jpg',k);
    fullFileName = fullfile('E:\James_KERR Semester 2 2015\Research Project\data\Stage1\Velocity',baseFi
    saveas(h(k),fullFileName);

end
close all;
%*****

%-----

%% S1.Integrates the windowed velocity data to acquire deflection
%-----
dw = zeros(size(vw)); %Padding

% Simpsons integration of discrete velocity data (External function file)
for k = node

    dw(:,k) = Simpson(vw(:,k),tw(:,k));

%*****optional task*****
    h(k) = figure(k);
    plot(tw(:,k),dw(:,k));
    xlabel('Time (s)');
    ylabel('Deflection (m)');
    caption = sprintf('Deflection vs. Time| Node %#d',k);
    title(caption,'FontSize',8);
    baseFileName = sprintf('Deflection_after_Simpsons_integration_%d.jpg',k);
    fullFileName = fullfile('E:\James_KERR Semester 2 2015\Research Project\data\Stage1\Deflection',base
    saveas(h(k),fullFileName);

end
close all;
%*****

%-----

```

```

%% S1.Performs Empirical Mode Decomposition
%-----
% EMD variables
r1 = 44;
r2 = 44;
EMD1 = cell(12,1); %Padding
w = zeros(12,1); b = zeros(12,1); %Padding

% Creates plots and cell array to store IMF's for each node IMF{k}(:,j)
for k = node

    EMD1{k} = (ParabEmd(dw(:,k),r1,r2,1));
    [w(k,1),b(k,1)] = size(EMD1{k});

    %*****optional task*****
    h(k) = figure(k);
    for j = 1:b(k)
        if b(k) > 5
            if ceil(b(k)/2) == floor(b(k)/2)

                subplot((b(k))/2,2,j);
                plot(tw(:,k),EMD1{k}(:,j))
            else

                subplot((b(k))/2+0.5,2,j);
                plot(tw(:,k),EMD1{k}(:,j))
            end
        else

            subplot(b(k),1,j);
            plot(tw(:,k),EMD1{k}(:,j))
        end
    end

    baseFileName = sprintf('Intrinsic_Mode_Function_Node_%d.jpg',k);
    fullFileName = fullfile('E:\James_KERR Semester 2 2015\Research Project\data\Stage1\IMF',baseFileNam
    saveas(h(k),fullFileName);

end
close all;
%*****

%=====

%% S1.Calculates the HT/phase/frequency/amplitude of each IMF
%-----
dt = diff(tw(1:2,1));
EMD1 = EMD1';
rr = zeros(length(tw(:,1)),length(node)); %Padding
phase = rr; mono = rr; xr = rr; xi = rr; %Padding
amp = rr; fr = cell(1,12); %Padding
time = tw(1:end-1,:);

for k = node

    rr(:,k) = sum(hilbert(EMD1{k},length(tw(:,k))),2);
    phase(:,k) = angle(rr(:,k));
    mono(:,k) = unwrap(phase(:,k));
    fr{k} = abs(diff(mono(:,k))./(dt*2*pi));
    xr(:,k) = real(rr(:,k));
    xi(:,k) = imag(rr(:,k));
    amp(:,k) = (xr(:,k).^2 + xi(:,k).^2).^(1/2);

end

%=====

```

```
%% S1.Plot displaying changes in amplitude and frequency with respect to time
%-----
for k = node

    h(k) = figure(k);
    subplot(2,1,1)
    plot(time(:,k),amp(1:end-1,k))
    caption = sprintf('Amplitude vs. Time| Node #%d',k);
    title(caption, 'FontSize', 8);
    xlabel('Time (s)');
    ylabel('Amplitude (mm)');
    subplot(2,1,2)
    plot(time(:,k),fr{k})
    caption = sprintf('Instantaneous Frequency vs. Time| Node #%d',k);
    title(caption, 'FontSize', 8);
    xlabel('Time (s)');
    ylabel('Frequency (Hz)');
    baseFileName = sprintf('Amplitude-Time_&_Frequency-Time_Node %d.jpg',k);
    fullFileName = fullfile('E:\James_KERR Semester 2 2015\Research Project\data\Stage1\AM_FM_time',base
    saveas(h(k),fullFileName);

end
%-----
```

Appendix C2: Simpson's Integration

```

function a = Simpson(t,da)
i = 1;
a = zeros(size(da));

while i <= length(da)-9

    dai = da(i); daf = da(i+1); %Position/motion step for interp
    ti = t(i); tf = t(i+1); %Time steps for interp

    % Interpolation between 10 points maximum per computation
    daw = [da(i) da(i+1) da(i+2) da(i+3) da(i+4) da(i+5) da(i+6) da(i+7) da(i+8) da(i+9)];
    dae = interp(daw,100);

    if i>1
        a(i) = ((tf-ti)/6)*(dai+4*(dae((1/20)*length(dae)))+daf);
    else
        a(i) = ((tf-ti)/6)*(dai+4*(dae((1/20)*length(dae)))+daf);
    end

    i = i+1;
end

while i <= length(da)-9
    if i >= length(da)-9

        daw = [da(length(da)-9) da(length(da)-8) da(length(da)-7) da(length(da)-6) ...
                da(length(da)-5) da(length(da)-4) da(length(da)-3) da(length(da)-2) ...
                da(length(da)-1) da(length(da))];

        dae = interp(daw,1000);

        a(i) = ((tf-ti)/6)*(dai+4*(dae((1/20)*length(dae)))+daf);

        i = i+1;

    end
end

while i <= length(da)-8
    if i >= length(da)-9

        daw = [da(length(da)-9) da(length(da)-8) da(length(da)-7) da(length(da)-6) ...
                da(length(da)-5) da(length(da)-4) da(length(da)-3) da(length(da)-2) ...
                da(length(da)-1) da(length(da))];

        dae = interp(daw,1000);
    end
end

```

```

        i = i+1;

    end
end
-
 while i <= length(da)-7
    if i >= length(da)-9

        daw = [da(length(da)-9) da(length(da)-8) da(length(da)-7) da(length(da)-6) ...
                da(length(da)-5) da(length(da)-4) da(length(da)-3) da(length(da)-2) ...
                da(length(da)-1) da(length(da))];

        dae = interp(daw,1000);

        a(i) = ((tf-ti)/6)*(dai+4*(dae((1/20)*length(dae)))+daf);

        i = i+1;

    end
end
-
 while i <= length(da)-6
    if i >= length(da)-9

        daw = [da(length(da)-9) da(length(da)-8) da(length(da)-7) da(length(da)-6) ...
                da(length(da)-5) da(length(da)-4) da(length(da)-3) da(length(da)-2) ...
                da(length(da)-1) da(length(da))];

        dae = interp(daw,1000);

        a(i) = ((tf-ti)/6)*(dai+4*(dae((1/20)*length(dae)))+daf);

        i = i+1;

    end
end
-
 while i <= length(da)-5
    if i >= length(da)-9

        daw = [da(length(da)-9) da(length(da)-8) da(length(da)-7) da(length(da)-6) ...
                da(length(da)-5) da(length(da)-4) da(length(da)-3) da(length(da)-2) ...
                da(length(da)-1) da(length(da))];

        dae = interp(daw,1000);

```

```

        a(i) = ((tf-ti)/6)*(dai+4*(dae((1/20)*length(dae)))+daf);

        i = i+1;

    end
end
while i <= length(da)-4
    if i >= length(da)-9

        daw = [da(length(da)-9) da(length(da)-8) da(length(da)-7) da(length(da)-6) ...
                da(length(da)-5) da(length(da)-4) da(length(da)-3) da(length(da)-2) ...
                da(length(da)-1) da(length(da))];

        dae = interp(daw,1000);

        a(i) = ((tf-ti)/6)*(dai+4*(dae((1/20)*length(dae)))+daf);

        i = i+1;

    end
end
while i <= length(da)-3
    if i >= length(da)-9

        daw = [da(length(da)-9) da(length(da)-8) da(length(da)-7) da(length(da)-6) ...
                da(length(da)-5) da(length(da)-4) da(length(da)-3) da(length(da)-2) ...
                da(length(da)-1) da(length(da))];

        dae = interp(daw,1000);

        a(i) = ((tf-ti)/6)*(dai+4*(dae((1/20)*length(dae)))+daf);

        i = i+1;

    end
end
while i <= length(da)-2
    if i >= length(da)-9

        daw = [da(length(da)-9) da(length(da)-8) da(length(da)-7) da(length(da)-6) ...
                da(length(da)-5) da(length(da)-4) da(length(da)-3) da(length(da)-2) ...
                da(length(da)-1) da(length(da))];

        dae = interp(daw,1000);

```

```

        a(i) = ((tf-ti)/6)*(dai+4*(dae((1/20)*length(dae)))+daf);

        i = i+1;

    end
end
while i <= length(da)-1
    if i >= length(da)-9

        daw = [da(length(da)-9) da(length(da)-8) da(length(da)-7) da(length(da)-6) ...
                da(length(da)-5) da(length(da)-4) da(length(da)-3) da(length(da)-2) ...
                da(length(da)-1) da(length(da))];

        dae = interp(daw,1000);

        a(i) = ((tf-ti)/6)*(dai+4*(dae((1/20)*length(dae)))+daf);

        i = i+1;

    end
end
while i <= length(da)
    if i >= length(da)-9

        daw = [da(length(da)-9) da(length(da)-8) da(length(da)-7) da(length(da)-6) ...
                da(length(da)-5) da(length(da)-4) da(length(da)-3) da(length(da)-2) ...
                da(length(da)-1) da(length(da))];

        dae = interp(daw,1000);

        a(i) = ((tf-ti)/6)*(dai+4*(dae((1/20)*length(dae)))+daf);

        i = i+1;

    end
end
end

```


Appendix C3: Empirical Mode Decomposition

```
%% EMD code
%-----
% This function performs the Empirical Mode Decomposition intended for the
% application of the Hilbert-Huang transformation.
%
% x - must be a vector (Vector array of original signal)
%
%-----
%% Signal Decomposition - Main Loop
function IMFbank = EMDf(sig)
%-----

% Initial variables - can be changed for accuracy or time
rsl = 44;          %Resolution [DBs: 10*log(SignalEnergy/BiasEnergy)]
rsd = 44;          %Residual energy [DBs: 10*log (SignalEnergy/ResidualEnergy)]
Gs = 1;           %Gradient step

% Signal parameters
ic = sig(:);      %Copy input signal for manipulation
ie = ic'*ic;      %Original signal energy
Lic = length(ic); %Length of vector

%-----

IMFbank = [];    %Padding for IMF vectors
EMDno = 0;
rsdE = 0;
Ino = Isc(ic);

while ((rsdE < rsd) && (Ino > 2))

    IMFs = ic;          %IMFs is initial signal
    Irx = MAXpl(IMFs);  %Peak signal maxima
    Irn = MINpl(IMFs);  %Peak signal minima
    MAXr = MAXextr(Irx, Irn, Lic); %Upper envelope extrapolation
    MINr = MINextr(Irx, Irn, Lic); %Lower envelope extrapolation

    Uenv = spline(MAXr(:,1), MAXr(:,2), 1:Lic); %Upper envelope interp
    Lenv = spline(MINr(:,1), MINr(:,2), 1:Lic); %Lower envelope interp
    err = (Uenv+Lenv)/2; %Estimate of bias error

    %Identifies IMF
    while true(1)
        IMFE = IMFs'*IMFs; %IMF energy
        Berr = err*err'; %Bias error energy
```

```

    %Resolves primary requirements for IMF
    if Berr > 0
        resolve = 10*log10(IMFE/Berr);
    else
        resolve= Inf;
    end

    if (resolve>rs1)
        break
    end

    %Resolves secondary requirements for IMF
    IMFf = IMFf-Gs*err';
    Irx= MAXpl(IMFf);
    Irr= MINpl(IMFf);
    MAXr= MAXextr(Irx, Irr, Lic);
    MINr= MINextr(Irx, Irr, Lic);
    Uenv= spline(MAXr(:,1), MAXr(:,2), 1:Lic);%Upper envelope interp #2
    Lenv= spline(MINr(:,1), MINr(:,2), 1:Lic);%Lower envelope interp #2
    err= (Uenv+Lenv)/2; %Bias error energy #2
end

IMFbank = [IMFbank;IMFf'];
ic = ic - IMFf;
Ino = Isc(ic);
EMDno=EMDno+1;

if (ic'*ic)>0
    rsdE = 10*log10(ie/(ic'*ic));
else
    rsdE = Inf;
end
end

% If residual it is stored as final IMF
if ((ic'*ic)/ie) > (10^-12)
    IMFbank=[IMFbank; ic'];
    EMDno=EMDno+1;
    NumOscqResiduals= Isc(ic);
end
IMFbank= IMFbank';
end

=====
%% Oscillation count - Secondary loops
function Nosc = Isc(x)
%-----

```

```

j = 0;
qisTop = false;
qisDown = false;

for i=2:(length(x)-1)
    %Maximum
    if ((x(i-1)) < (x(i))) && ((x(i+1)) < (x(i)))
        j = j+1;
    end
    %Minimum
    if ((x(i-1)) > (x(i))) && ((x(i+1)) > (x(i)))
        j = j+1;
    end

    %Upper
    %Positive slope
    if ((x(i-1)) < (x(i))) && ((x(i+1)) == (x(i)))
        qisTop = true;
        qisDown = false;
    end
    %Negative slope
    if ((x(i-1)) == (x(i))) && ((x(i+1)) < (x(i)))

        if qisTop
            j = j+1;
        end
        qisTop = false;
    end

    %Lower
    %Negative slope
    if ((x(i-1)) > (x(i))) && ((x(i+1)) == (x(i)))
        qisTop = false;
        qisDown = true;
    end
    %Positive slope
    if ((x(i-1)) == (x(i))) && ((x(i+1)) > (x(i)))

        if qisDown
            j = j+1;
        end
        qisDown = false;
    end
end
end

```

```

Nosc = j;
end
%End of function
%=====
%% Envelope Extrema Maxima - Secondary loops
%-----

```

```

function MAXextrap = MAXextr(MAXr,MINr,Lic)

MAXr= sortrows(MAXr);
MINr= sortrows(MINr);
T1 = MAXr(:,1);
T2 = MINr(:,1);
V1 = MAXr(:,2);
V2 = MINr(:,2);

% Extrapolate begining
if ((T1(1) > 1) || (T2(1) > 1))
    T1=[2-T2(1); T1];      %New first Top at the (one based) specular Min
    V1=[V1(1); V1];      %Same Val as old first Top
end

% Extrapolate ending
if ((T1(end) < Lic) || (T2(end) < Lic))
    T1=[T1; (2*Lic - T2(end))]; % New last Top at the specular Min
    V1=[ V1; V1(end)];      % Same Val as old last Top
end

MAXextrap = sortrows([T1, V1]);
end
%End of function
%=====
%% Envelope Extrema Maxima - Secondary loops
%-----

```

```

function MINextrap = MINextr(MAXr,MINr,Lic)

MAXr= sortrows(MAXr);
MINr= sortrows(MINr);
T1 = MAXr(:,1);
T2 = MINr(:,1);
V1 = MAXr(:,2);
V2 = MINr(:,2);

% Extrapolate begining

```

```

if ((T1(1) > 1) || (T2(1) > 1))
    T2=[2-T1(1); T2];      % New first Dwn at the (one based) specular Max
    V2=[V2(1); V2];      % Same Val as old first Dwn
end

% Extrapolate ending
if ((T1(end) < Lic) || (T2(end) < Lic))
    T2=[T2; (2*Lic - T1(end))];      % New last Dwn at the specular Max
    V2=[ V2; V2(end)];      % Same Val as old last Dwn
end

MINextrap= sortrows([T2, V2]);
end

%End of function
=====
%% Exclude Maxima Plateaus - Secondary loops
%-----
function Irx = MAXpl(IMFs)

nMAX = 0;      %Stores length
ij = IMFs(:);
Lj = length(ij);

% Padding
MAXv = [];      %Maxima values
MAXi = [];      %Maxima indices
MAXt = [];      %Maxima time values
MAXp = [];      %Maxima parabola values

% Maxima Value Loop
if (Lj>2)
    %Find Maxima
    for i = 2:(Lj-1)
        if (((ij(i) > ij(i+1))) && ((ij(i) >= ij(i-1))) || ...
            ((ij(i) >= ij(i+1))) && ((ij(i) > ij(i-1))))

            nMAX = nMAX+1;
            MAXi = [MAXi;i];
            MAXv = [MAXv;ij(i)];
        end
    end
end

% Input Variables
MAXg = max(ij)-min(ij);

```

```

Px = -(Inf);
Py = -(Inf);

% Parabola Maxima Loop
for jj = 1:nMAX

    v1 = ij(MAXi(jj)-1); %Prior point
    v2 = ij(MAXi(jj));   %Central point
    v3 = ij(MAXi(jj)+1); %Following point

    D = (-4*v2+2*v1+2*v3);
    if (D == 0)
        xx = MAXi(jj);

    else

        xx = MAXi(jj)+(v1-v3)/D;
    end

    D = (-16*v2+8*v1+8*v3);
    if (D == 0)

        vv = v2;
    else

        vv = v2+(2*v3*v1-v1*v1-v3*v3)/D;
    end

    % Ensure no repetition of maxima
    if ((xx == Px) || (abs(vv-Py)/abs(xx-Px)) > (2*MAXg))

        xx = (xx+Px)/2;
        vv = max(vv,Py);
        MAXt(length(MAXt)) = xx;
        MAXp(length(MAXp)) = vv;
    else
        MAXt = [MAXt;xx];
        MAXp = [MAXp;vv];
    end

    Px = xx;
    Py = vv;
end

```

```

if nMAX > 0

    %Consider starts and finishes as maxima
    if (ij(1) >= MAXp(1))

        MAXt = [1;MAXt];
        MAXp = [ij(1);MAXp];
    end

    if (ij(end) >= MAXp(end))

        MAXt = [MAXt;Lj];
        MAXp = [MAXp;ij(end)];
    end
end

if nMAX == 0
    if (ij(1) > ij(2))

        MAXt = [1;MAXt];
        MAXp = [ij(1);MAXp ];
    end

    if (ij(end) > ij(end-1))

        MAXt = [MAXt;Lj];
        MAXp = [MAXp;ij(end)];
    end
end

Irx = sortrows([MAXt,MAXp]);
end

```

%End of function

=====

%% Exclude Maxima Plateaus - Secondary loops

function Irn = MINp1(IMFs)

```

nMIN = 0;           %Stores length
ij = IMFs(:);
Lj = length(ij);

% Padding
MINv = [];         %Maxima values
MINi = [];         %Maxima indices
MINt = [];         %Maxima time values
MINp = [];         %Maxima parabola values

```

```

% Minima Value Loop
if (Lj>2)
    %Find Minima
    for i = 2:(Lj-1) %search the Mins
        if (((ij(i) < ij(i+1))) && ((ij(i) <= ij(i-1))) || ...
            ((ij(i) <= ij(i+1))) && ((ij(i) < ij(i-1))))

            nMIN = nMIN+1;
            MINi = [MINi;i];
            MINv = [MINv;ij(i)];
        end
    end
end

% Input Variables
MAXg= max(ij)-min(ij); %Largest gap
Px = -Inf;
Py = -Inf;

% Parabola Minima Loop
for jj = 1:nMIN

    v1 = ij(MINi(jj)-1); %Prior point
    v2 = ij(MINi(jj)); %Central point
    v3 = ij(MINi(jj)+1); %Following point

    D = (-4*v2+2*v1+2*v3);
    if (D==0)

        xx = MINi(jj);
    else

        xx = MINi(jj)+(v1-v3)/D;
    end

    D = (-16*v2+8*v1+8*v3);
    if (D == 0)

        vv = v2;
    else

        vv = v2+(2*v3*v1-v1*v1-v3*v3)/D;
    end

    % Ensure no repetition of minima
    if ((xx == Px) || (abs(vv-Py)/abs(xx-Px)) > (2*MAXg))

```



```

    xx = (xx+Px)/2;
    vv = min(vv,Py);
    MINt(length(MINt)) = xx;
    MINp(length(MINp)) = vv;
else
    MINt = [MINt; xx];
    MINp = [MINp; vv];
end

Px = xx;
Py = vv;
end

if nMIN > 0

    %Consider starts and finishes as maxima
    if (ij(1) <= MINp(1))

        MINt = [1;MINt];
        MINp = [ij(1);MINp];
    end

    if (ij(end) <= MINp(end))

        MINt = [MINt;Lj];
        MINp = [MINp;ij(end)];
    end
end

if nMIN==0
    if ( ij(1) < ij(2) )

        MINt = [1;MINt];
        MINp = [ij(1);MINp];
    end

    if (ij(end) < ij(end-1))

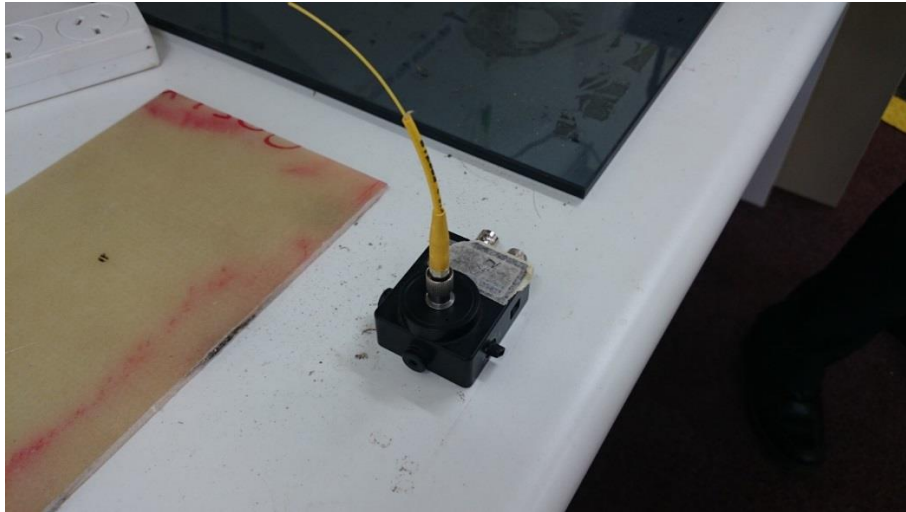
        MINt = [MINt;Lj];
        MINp = [MINp;ij(end)];
    end
end

Irn = sortrows([MINt, MINp]);
end
=====

```

Appendix D| Apparatus

Appendix D1: Fibre-optic Bragg grating sensor



Appendix D2: Power amplifier



Appendix D3: Signal generator



Appendix D4: Solenoidal Shaker

